Einfluss von ZNS-Verletzung auf die m-RNA-Expression der Protease-Aktivierenden Rezeptoren (PARs) und Identifizierung eines Interaktionspartners für PAR-2 in Retina

Dissertation

Zur Erlangung des akademischen Grades

doctor rerum naturalium
(Dr. rer. nat.),

genehmigt durch
die Fakultät für Naturwissenschaften
der Otto-von-Guericke Universität Magdeburg

von Diplom-Biologin Tanuja Rohatgi

geb. am. 1 September 1973 in Delhi, India

Gutachter:
Prof. Dr. Georg Reiser
Prof. Dr. V. Höllt
PD Dr. Thomas Schmitt-John

Eingereicht am:
29th October 2003

Verteidigung am:
30th March 2004

Effect of CNS injury on expression of protease- activated receptors (PARs) in brain and identification of a putative PAR-2- interacting protein in retina

Dissertation

To the acquisition of the academic degree

Doctor rerum naturalium
(Dr. rer. nat.),

Approved by
The Faculty of Natural Science
Otto-von-Guericke Universität Magdeburg

From Master of Science Tanuja Rohatgi

Born on 1 September 1973, in Delhi, India

Reviewers:
Prof. Dr. Georg Reiser
Prof. Dr. V. Höllt
PD Dr. Thomas Schmitt-John

Submitted on:
29th October 2003

Defense on:
30th March 2004

Dedicated

To my parents, sister and brother
For their love, support, strength and encouragement

Acknowledgements

The work presented in this dissertation was made possible due to help and support of several people. Firstly, I am grateful and indebted to Prof. Dr. G. Reiser for giving me the opportunity to join the Institute for Neurobiochemistry in January 2001 for doing my doctoral work under his guidance. His continuous support, encouragement, motivation and discussion enabled me to move forward in my work.

No words can truly describe the extent of my appreciation for Dr. Fariba Sedehizade, my practical supervisor during the tenure of this work. She has been a pillar of strength for me during all the ups and downs which I faced during the course of experiments. She infused in me the spirit of endless perseverance and motivation. She helped me in developing my scientific attitude through the countless discussions and suggestions.

I am thankful to Dr. Rolf Stricker for introducing me to the field of protein chemistry. His immense knowledge helped me in crossing many hurdles and learning a lot in the process. My appreciation goes to Dr. Rainer Schäfer for the endless and fruitful discussions which were both educational and enjoyable. I would also like to thank Dr. Theodor Hanck for his invaluable suggestions with regard to experiments.

I am grateful to Dr. Abidat Schneider for her excellent technical expertise. She familiarised me to the field of cell culture. Her help and endless support enabled me to carry out several experiments simultaneously. I would also like to thank Mrs. Anke Imrich, Mrs. K. Christoph, Mrs. Petra Hennig, Mrs. Ina Laubinger and Ms. Annette Krüger for their technical help.

My appreciation also goes to Mrs. M. Dullin-Viehweg, secretary of the Graduiertenkolleg, Mrs. I. Klaes, and Mr. P. Ehrbarth for their friendly support.

The time spent at the institute was made a pleasurable, eventful, learning and unforgettable experience due to the presence of colleagues, Dr. Hong Wang, Dr. Mikhail Strokin, Mr. Christoph von Klot, Mr. Mohan Tulapurkar, Ms. Ewa Ostrowska, Ms. Claudia Borrmann, Ms. Denise Ecke, Dr. Elena Sokolova, Mrs. Nastya Galvita, Mrs. Yingfei Wang, Mr. Weibo Lou, Dr. Stefan Kahlert, Dr. Gregor Zündorf and Dr. Werner Laubinger.

I would also like to thank Prof. Dr. B. Sabel for giving me the possibility to come to Magdeburg and start my research career in Germany at the Institute for Medical Psychology in the Graduiertenkolleg program in August 1999. My appreciation goes to the co-workers at the institute for their help, particularly, Ms. Dorothe Poggel, Ms. Iris Müller, Ms. Ulrika Bunzenthal, Mrs. Kerstin Hahn and technical support from Ms. Annette Schulz.

Last but not the least this work was made possible due to love and encouragement of my family and all my friends. Their belief in me gave me the power to move on.

Table of Content

1. Introduction

1.1 Proteases

Proteases or peptidases are enzymes that catalyze the breakdown of peptide bonds (proteolysis) in a protein molecule. Some proteases are very specific and produce a limited proteolysis while others degrade proteins (quaternary and tertiary structure) completely into single amino acid residues. They are either secreted by cells into the surrounding tissues to cause destruction of proteins in extracellular material or they may be secreted into an area for the breakdown of a particular protein. On the basis of their catalytic mechanism, proteases are further divided into five catalytic classes: aspartic, cysteine, metalloproteinase, serine, and unclassified. Of the five, metalloproteinases and serine proteases comprise the largest classes. Examples for metalloproteinases include MMPs (thermolysin), while serine proteases include thrombin, trypsin and chymotrypsin to name a few.

The proteases act not only as simple degradative enzymes but their highly specific mode of action (hydrolysis) can regulate a wide variety of biological processes (Yan and Blomme, 2003). The proteolytic processing involving highly specific and limited substrate cleavage controls the intracellular and extracellular localisation of several proteins and their activation. By virtue of their catalytic activity, proteases regulate almost all biological processes, like cell proliferation, differentiation, migration, apoptosis, wound healing and angiogenesis. Thus, dysregulation of their expression and functional pattern can result in various pathologic conditions, such as neurodegenerative and cardiovascular diseases and cancer (Yan and Blomme, 2003). Therefore, it is of utmost importance to identify and functionally characterise the substrates through which proteases act and manifest their action, since these substrates can be potential therapeutic targets for treatment of pathologic conditions (Yan and Blomme, 2003).

1.2 Protease-activated receptors (PARs)

Serine proteases like thrombin and trypsin not only participate in degradation of extracellular proteins but can also act as a signaling molecule that regulate multiple cellular functions by activating specific cell surface receptors, the Protease-Activated Receptors (PARs). PARs are G-protein-coupled receptor that utilize a unique

mechanism to convert an extracellular proteolytic cleavage event into a transmembrane signal (Coughlin, 2000). PARs belong to family 1 group b of the superfamily of GPCRs and consist of typical 7-transmembrane helics connected by 3 extracellular and 3 intracellular loops together with an extracellular N-terminal and intracellular C-terminal domains (Bockaert and Pin, 1999) (Figure 1.1).

The interesting mechanism of receptor activation involves cleavage of the receptor at a specific site within the extracellular amino terminus, thus unmasking a new N-terminus tethered ligand, which binds intramolecularly to the receptor and activates transmembrane signaling. Six or more specific amino acid residues within the newly exposed tethered ligand interact with extracellular loop 2 (Lerner et al., 1996) and transmembrane domains of the cleaved receptor (Dery et al., 1998; Coughlin, 2000). Thus, PARs are peptide receptors carrying their own ligands, which remain cryptic until unmasked by receptor cleavage due to binding of agonist to extracellular N-terminal domain (Coughlin, 2000). Synthetic peptides that mimic the tethered ligand of receptor can activate the receptor irrespective of agonist and receptor cleavage (Coughlin, 2000). Ultimately, activated receptor interacts with heterotrimeric G proteins in the plasma membrane via intracellular loop 3 (Chen et al., 2001), which transduce the signal.

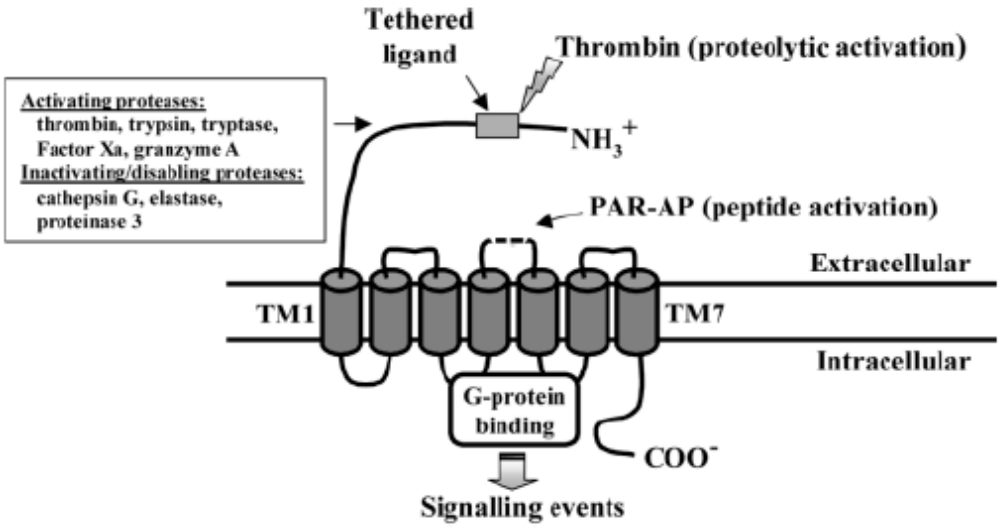

Figure 1.1. Activation Mechanism of PARs (Wang and Reiser, 2003a).
Following irreversible proteolytic cleavage of PAR by thrombin, trypsin or tryptase (depending on the receptor subtype), a new N-terminus is unmasked acting as tethered ligand (boxed segment). This tethered ligand can interact with extracellular loop-2 of the receptor (dashed). A synthetic peptide derived from the N-terminal sequence of PAR (PAR-AP) is able to activate the receptor in the absence of protease-mediated cleavage. Other proteases may also act on the extracellular N-terminus, either exposing the tethered ligand to activate PAR or disabling the tethered ligand to inactivate PARs by cleaving at a site downstream of the tethered ligand sequence (Renesto *et al.*, 1997).

The intracellular loops 2 and 3 have been proposed to play a role in G protein coupling for PAR-1 (Hollenberg and Compton, 2002).

1.3 Irreversible activation and trafficking of PARs

Since the cleavage of the receptor is irreversible, the cleaved receptor cannot be reactivated. Once activated, the receptor rapidly uncouples from the transmembrane signalling and internalised by phosphorylation-dependent mechanism (Coughlin, 2000). The internalised receptor is either targeted to lysosomes or few molecules recycle back to cell surface but remain inactive. PARs are also maintained in large intracellular pools in the Golgi apparatus and in vesicles. Resensitization of the receptor involves mobilization of the intracellular pools (Dery et al., 1998; Coughlin, 1999, 2000).

1.4 Classification and cloning of PARs

Four subtypes of PARs are known: PAR-1-4. PAR-1 and PAR-3 are activated by thrombin (Vu et al., 1991a; Ishihara et al., 1997), PAR-4 is activated by both thrombin and trypsin (Xu et al., 1998), while PAR-2 is activated by trypsin and mast cell tryptase (Nystedt et al., 1994). PAR-1-3 genes co-localise to the same region of the human genome at chromosome 5q13 unlike PAR-4 which is located on chromosome 19p12 (Kahn et al., 1998a; Cupit et al., 1999). Genetic mapping study in human vascular endothelial cells show the presence of PAR-1-3 gene cluster within 110 to 220 kb distance on chromosome 5q13 (Schmidt et al., 1998; Cupit et al., 1999). In case of mouse, PAR-1-3 are located on chromosome 13d2 and PAR-4 on 8b3 (Kahn et al., 1998a). Genetic analysis of the PAR family shows that PAR-1 and PAR-2 arose from a gene duplication event and indeed all 4 subtypes share high homology between them and conserved across species (human and mouse) (Kahn et al., 1998b). The four subtypes have identical gene structure comprising 2 exons, each separated by a very long single intron of 4-22 kb in case of PAR-1-3 and only 274 bp long for PAR-4 (Kahn et al., 1998a; Cupit et al., 1999). In all 4 cases a short first exon encodes the 5'-untranslated sequence, start codon, and signal peptide, and the second, larger exon encodes the receptor protein and 3'-untranslated sequence (Kahn et al., 1998a).

The cDNA has been cloned from human, mice and rat for all 4 receptor subtypes, PAR-1 (Vu et al., 1991a; Coughlin et al., 1992b; Zhong et al., 1992), PAR-2 (Bohm et al., 1996; Nystedt et al., 1994; Nystedt et al., 1995; Saifeddine et al., 1996), PAR-3 (Ishihara et al., 1997; Cupit et al., 1999) and PAR-4 (Xu et al., 1998) (Kahn et

al., 1998b) (Hoogerwerf et al., 2002). PAR-1 was the first receptor of this family to be cloned. It is also referred to as thrombin receptor and represents the prototype of this receptor family since most of the activation paradigm, signalling mechanism and physiological studies elucidating the role of PARs were identified using PAR-1 (Coughlin et al., 1992a; Coughlin, 1994; Cunningham and Donovan, 1997; Ubl and Reiser, 1997; Dery et al., 1998; Coughlin, 2000; Wang et al., 2002b).

cDNA encoding a functional human thrombin receptor (PAR-1) was cloned by direct expression cloning in Xenopus oocytes (Vu et al., 1991a). mRNA from cells highly responsive to thrombin were injected into Xenopus oocytes and the resulting transcript encoding the receptor was purified and tested for calcium release. In oocytes expressing the receptor, thrombin was found to be an extremely potent agonist compared with less effective trypsin. The response to thrombin was found to be blocked by thrombin agonist hirudin indicating the specific nature of thrombin receptor (Vu et al., 1991a). Subsequently thrombin receptor was also cloned from hamster lung fibroblasts (Rasmussen et al., 1991), mouse (Coughlin et al., 1992b) and rat (Zhong et al., 1992). PAR-2 was first cloned in mouse (Nystedt et al., 1994). A cosmid clone containing a 3.7 kb Pst-1 fragment with an ORF encoding a putative 395 amino acid protein similar to human PAR-1 was identified from mouse genomic library under moderate stringency conditions. This clone had 30% identity with human PAR-1 and 28% with mouse PAR-1 (Nystedt et al., 1994). Human PAR-2 was cloned using PCR based approach from human kidney cDNA (Bohm et al., 1996). Cells transfected with human PAR-2 were found to be activated by trypsin and both human and mouse activating peptide and hTRAP, thus confirming the presence of functionally and physiologically active PAR-2 (Nystedt et al., 1995). PAR-3 as a second thrombin receptor was identified when platelets from mice whose thrombin receptor gene was disrupted were still found to be responding to thrombin (Connolly et al., 1996). Human PAR-3 was identified using a PCR- based strategy (Ishihara et al., 1997). Human PAR-3 cDNA was found to have 27% amino acid homology with human PAR-1 and 28% with human PAR-2. PAR-4 the last known member of this family was cloned by identification of PAR-like sequences in Expressed Sequence TAG (EST) libraries (Kahn et al., 1998b; Xu et al., 1998).

A comparison between thrombin receptors (PAR-1,-3 and –4) reveals certain structural differences which determine their ability in responding to agonist. PAR-1 and PAR-3 in their N-terminal exodomain have thrombin-interacting sequences at both N-

and C-terminal to the thrombin cleavage site (Coughlin, 2000). The C-terminal sequence resembles the C-terminal tail of leech anticoagulant hirudin, and similar to hirudin can bind to thrombin fibrinogen-binding exosite. The binding of thrombin to this site on PAR-1 and PAR-3 is important for receptor cleavage at low agonist concentration (Coughlin, 2000). PAR-4 lacks the hirudin-like sequence and hence high thrombin concentration is required for PAR-4 activation (Coughlin, 2000).

1.5 Agonists of PARs

The main agonist of PAR-1, -3 and –4 is thrombin, a multifunctional serine protease. Thrombin is the principal component of the blood coagulation cascade, and also involved in nervous system growth and maintenance. Thrombin is generated from its precursor molecule, prothrombin, which is cleaved by factor Xa, in association with factor Va, calcium and phospholipids (Festoff et al., 1996). Apart from plasma, prothrombin mRNA and protein are also known to be expressed in CNS (Dihanich et al., 1991). Thrombin is a 39 kDa molecule compared to its precursor prothrombin which is 71.6 kDa. During coagulation cascade thrombin mediates cleavage of soluble fibrinogen into insoluble fibrin which forms clot. Thrombin is involved in neurite retraction and this catalytic activity of thrombin is very specific and is known to be reversed on thrombin removal from the tissue culture medium (Festoff et al., 1996), loss of stellate morphology by astrocytes (Cavanaugh et al., 1990), release of endothelin-1 by astrocytes (Ehrenreich et al., 1993). Low thrombin concentration can induce glial cell mitosis (Cavanaugh et al., 1990); expression of c-fos and c-jun mRNA in astrocytic cell line (Trejo et al., 1992). Thrombin can stimulate aggregation of platelets (Berndt and Phillips, 1981), macrophages (Bar-Shavit et al., 1983) and fibroblast (Glenn et al., 1980) which plays important role in protecting the body following injury. Thrombin also play an important role in Alzheimer's disease. It attenuates β-amyloid induced degeneration (Pike et al., 1996).

Thrombin is cleaved to its active form at the site of injury (Friedmann et al., 1999; Friedmann et al., 2001a). Thrombin can induce either apoptosis-neurodegeneration (Donovan et al., 1997; Smirnova et al., 1998; Turgeon et al., 1998) or neuroprotection (Donovan and Cunningham, 1998) in astrocytes and neurons in cultures as well as in vivo. Its concentration-dependent action is well documented with regard to tissue repair and wound healing as reported in the case of several injury models, like OGD in hippocampal organotypic slices (Striggow et al., 2000), optic

nerve crush in rat, a mild trauma model of CNS (Friedmann et al., 1999; Friedmann et al., 2001a) and brain injury (Vaughan et al., 1995; Cunningham and Donovan, 1997).

Most of the effects of thrombin are mediated by its main receptor PAR-1 (Chambers et al., 1998; Weinstein et al., 1998; Cheung et al., 1999), but a recent study (Vergnolle et al., 2002) has highlighted the role of PAR-4 receptor activation in pro-inflammatory properties of thrombin. It cleaves between Arg^{42}-Ser^{43} of the extracellular N-terminal domain of the receptor, in the second extracellular loop of the domain (Suttnar et al., 2000). Thrombin cleavage site on the receptor is followed by a sequence of charged residues which interact with an anion binding site on thrombin, inducing conformational changes in the receptor and thus promoting efficient receptor hydrolysis. The charged domain of the receptor resemble the hirudin domain, which inhibits the thrombin action by binding to its anion site (Vu et al., 1991b). Thrombin cleaves PAR-3 at Lys^{38}-Thr^{39} which also contains a hirudin-like site that interacts with thrombin (Ishihara et al., 1997). PAR-4 can be activated by both thrombin and trypsin. It is cleaved at Arg^{47}-Gly^{48} in the N-terminal sequence. γ-thrombin, which lacks a fibrinogen-binding exosite is as effective in activating PAR-4 as α-thrombin, unlike PAR-1 and PAR-3 where γ-thrombin is much less potent than α-thrombin. This difference is due to the presence of thrombin-binding site within the amino terminal region of PAR-1 and PAR-3 (Xu et al., 1998).

Another protease which acts as agonist of PARs is trypsin. Trypsin is basically known as a digestive enzyme and occurs in gastro-intestinal tract as an inactive zymogen, trypsinogen. Trypsin is activated to its active form by enterokinase. Trypsin cleaves PAR-2 at Arg^{34}-Ser^{35} residues. Trypsin interacts with PAR-2 only at the cleavage site (Nystedt et al., 1994). Apart from PAR-2, trypsin can also activate PAR-1 (Ubl et al., 1998) and PAR-4 (Xu et al., 1998).

Because of the unique activating mechanism of PARs resulting in exposure of the tethered ligand which subsequently binds to the receptor and activates it, it is possible to directly use the synthetic peptides (Activating peptides: AP) mimicking the tethered ligand sequence to activate the receptor without the need for proteolytic cleavage. SFLLR-NH_2, PAR-1 AP derived from human PAR-1 sequence can be used to activate both PAR-1 and PAR-2 (Hollenberg et al., 1997). Now a more specific PAR-1 AP, TRag is also known (Kawabata et al., 1999; Wang et al., 2002a). PAR-2 AP both human and mouse are capable of activating PAR-2 and elicit responses similar to trypsin, but they cannot activate PAR-1 (Hollenberg et al., 1993). Recent studies from

our laboratory have shown that PAR-3 AP (TFRGAP) is capable of inducing Ca^{2+} signalling in astrocytes, albeit to a very modest degree (Wang et al., 2002a). PAR-4 activating peptides are capable of activating the receptor only at a high concentration of the AP, and a longer incubation period leads to toxic effect in astrocytes (Wang et al., 2002a).

Apart from thrombin and trypsin, other serine proteases are also capable of activating PARs but not so strongly. Granzyme A released on cytotoxic T lymphocytes stimulation is capable of activating PAR-1 in neurons and astrocytes (Suidan et al., 1994). Since trypsin is not present in brain, studies were conducted to find PAR-2 agonists in brain or areas where trypsin has no access. Tryptase which is released by mast cells was found to activate PAR-2 with similar efficiency as PAR-2 activating peptides (Molino et al., 1997). Serine proteases not only activate PARs but some of them also inactivate them. Prominent among them are cathepsin G (Molino et al., 1995), elastase and proteinase 3 (Renesto et al., 1997), and plasmin (Parry et al., 1996). Metalloproteinase, like thermolysin (Chen et al., 1996) can inactivate PARs.

1.6 Distribution of PARs in tissues and cell types

Of the four subtype of PARs, PAR-1 is the most intensely and thoroughly studied receptor of this family. Its expression has been reported in embryonic and postnatal brain (Weinstein et al., 1995; Niclou et al., 1998). PAR-1 mRNA is found in variety of cell types like endothelial cells, fibroblasts, monocytes, platelets, osteoblasts, smooth muscle cells, uterine stromal cells, epithelial cells, neurons and glia in brain and cell lines like human embryonic kidney (HEK), glioma cells (NG108) (Vu et al., 1991a; Howells et al., 1993; Jenkins et al., 1993; Arena et al., 1996; Ubl et al., 1998; Striggow et al., 2001; Wang et al., 2002a).

Widespread PAR-2 immunoreactivity has been reported in the developing central and peripheral nervous system (Jenkins et al., 2000). PAR-2 expression has been described in several tissues and cell types like in endothelial and epithelial cells, skin, eye and bone cells, brain, peripheral nerves, in the majority of gastrointestinal tissues, lung, cardiac muscle, blood vessels, kidney, ovary, testis, in CNS during embryogenesis, neurons, astrocytes, glioma cell line, smooth muscle cells, neutrophils (Abraham et al., 2000; D'Andrea et al., 1998; Jenkins et al., 2000; Bohm et al., 1996; Steinhoff et al., 1999; Striggow et al., 2001; Ubl et al., 1998; Wang et al., 2002a; al-Ani et al., 1995; Howells et al., 1997; Corvera et al., 1999).

Studies on PAR-3 and PAR-4 are confined mainly to tissues of hematopoietic origin like platelets, megakaryocytes, bone marrow and spleen (Ishihara et al., 1997) but their expression has also been detected in lung, heart, thyroid, liver, pancreas, small intestine, placenta and testis (Ishihara et al., 1997; Ishihara et al., 1998; Kahn et al., 1998b; Xu et al., 1998; Hoogerwerf et al., 2002; Vergnolle et al., 2002). Human platelets lack PAR-3 but express PAR-1 and PAR-4 (Xu et al., 1998; Kahn et al., 1999), unlike mouse platelet which express both PAR-3 and PAR-4 (Kahn et al., 1998b). In a recent study the presence of all 4 PAR subtypes has been described in cultured rat astrocytes (Wang et al., 2002a). Also, the expression pattern of the 4 receptor subtype was characterized in brain (Striggow et al., 2001). These authors have shown the presence of PARs in different brain areas, particularly in neuronal structures of cortex, hippocampus, amygdala, and hypothalamus.

In mouse platelets, the expression of PAR-3 was found to be necessary for full activation of thrombin since PAR-3 deficient mouse platelets expressing only PAR-4 show delayed and weak thrombin response compared with normal mice platelets (Kahn et al., 1998b). Mouse PAR-3 by itself does not result in any signalling cascade on thrombin stimulation but facilitates thrombin stimulation of PAR-4 by functioning as a tethering protein for the protease (Nakanishi-Matsui et al., 2000). Mice lacking PAR-2 have been shown to have an enhanced response to PAR-1, suggesting possibility of direct PAR-PAR interaction (Damiano et al., 1999b).

1.7 Mechanism of PAR signal transduction

Receptor activation by agonist binding results in conformational change that leads to interaction of receptor with heterotrimeric G proteins. This further leads to catalytic exchange of GTP for GDP on the α-subunit of the G-protein. The α–subunit and $\beta\gamma$ heterodimer can activate different effector enzymes or ion channels until GTP is hydrolysed and G proteins return to their inactive state (Simon et al., 1991). Of all PARs, signalling mechanism for PAR-1 is most studied and well understood. The signalling mechanism for PAR-1 either proceeds via inhibition of cAMP through interaction with inhibitory G proteins (Kanthou et al., 1996) or via stimulation of phospholipase C-catalysed hydrolysis of phosphoinositides, resulting in formation of $InsP_3$, mobilization of intracellular Ca^{2+}, and generation of diacylglycerol, the endogenous activator of protein kinase C (Hung et al., 1992). Extensive studies from our laboratory have highlighted the role of thrombin (PAR-1)- induced proliferation via

MAPK pathway in astrocytes resulting in ERK 1/2 phosphorylation (Wang et al., 2002b). Thrombin-stimulated ERK1/2 activation is mainly mediated by PAR-1 via two branches: the PTX-sensitive G protein/(βγ-subunits)-phosphatidylinositol 3-kinase branch, and the Gq-PLC-(InsP3 receptor)/ Ca^{2+} -PKC pathway. Thrombin- or PAR-1-AP-induced ERK activation is partially blocked by a selective EGF receptor inhibitor. Nevertheless, transphosphorylation of EGF receptor is unlikely for ERK1/2 activation and is certainly not involved in PAR-1-induced proliferation (Wang et al., 2002b; Wang and Reiser, 2003b). Studies using C-tail of PAR-1 to identify molecules involved in downstream signalling (Mahajan et al., 2000; Pai et al., 2001) have shown that not only PAR-1 transmits intracellular signal via G-proteins bound to its 3rd intracellular loop (Chen et al., 2001), but C-tail interaction also results in PAR-1 mediated morphological changes in astrocytes (Mahajan et al., 2000; Pai et al., 2001).

Compared with a large number of studies done to explore PAR-1 signalling pathway, little is known about mechanism of PAR-2 intracellular signalling. Trypsin and PAR-2 AP activation via heterotrimeric G proteins can stimulate IP_3 formation and Ca^{2+} in numerous cell types (Schultheiss et al., 1997). PAR-2 signalling via PTX sensitive pathway has been shown to be associated with tyrosine phosphorylation of SHP-2 (Yu et al., 1997). In enterocytes PAR-2 agonists can stimulate arachidonic acid release and rapid generation of prostaglandins, suggesting activation of phospholipase A2 and cyclooxygenase-1 (Kong et al., 1997). PAR-2 has also been shown to be linked to SAP kinases, JNK and p38MAP kinase (Sabri et al., 2000).

1.8 PAR expression in tissue injury

Several recent studies on PARs have focused on their potential role in regulation of inflammation and response to injury. PAR-1 expression was found to be upregulated as a consequence of spinal cord injury (Citron et al., 2000), and sciatic nerve injury (Niclou et al., 1998), while it is downregulated after facial nerve transection (Niclou et al., 1998). Also cell surface expression of PAR-1 has been investigated under hypoglycemic and hypoxic conditions both in the presence and absence of thrombin (Weinstein et al., 1998). Altered PAR-1 expression also contributes to sclerotic and inflammatory processes in human vasculature (Nelken et al., 1992). PAR-1 expression also increases in rheumatoid and osteoarthritis contributing to inflammatory process (Morris et al., 1996). Thrombin stimulation of PAR-1 leads to platelet aggregation, vasodilation and vasoconstriction, increased vascular permeability and cellular adhesion

and infiltration by chemotaxis (Hung et al., 1992). Out of the 4 receptor subtypes of the PAR family, the role of PAR-2 in the regulation of inflammation is most widely documented. PAR-2 expression was found upregulated after carotid artery injury (Cheung et al., 1999) and in respiratory epithelium of asthmatic patients (Knight et al., 2001). Agonists of PAR-2 are involved in protease-induced neurogenic inflammation (Steinhoff et al., 2000) and cutaneous inflammation (Shpacovitch et al., 2002) via receptor activation. PAR-2 also plays a major role in pathophysiology of vascular and gastric smooth muscle contractility (al-Ani et al., 1995). Besides its pro-inflammatory role, PAR-2 activation has been shown to exert a protective effect in myocardial ischemic-reperfusion injury (Cirino et al., 2000). PAR-1, PAR-2 and PAR-4 are known to modulate cytokine and prostaglandin production in primary human bronchial epithelial cells activation during lung inflammation (Asokananthan et al., 2002). PAR-2 and PAR-4 are upregulated in human coronary artery as a result of inflammatory stimuli (Hamilton et al., 2001), and PAR-1, PAR-2 and PAR-3 are transiently upregulated after experimentally induced ischemia in organotypic hippocampal slice cultures (Striggow et al., 2001). Our recent work has shown that mRNA expression of PAR-1 to -3 was not affected by transient global ischemia (Riek-Burchardt et al., 2002). Taken together, these studies highlight the growing importance of the PAR family in patho-physiological situations of neurodegeneration.

1.9 The yeast-two hybrid assay

The two-hybrid system addresses one of life's fundamental questions: How does one find a meaningful partner? If a protein has a known function, new proteins that bind to it bring additional components into play, ultimately contributing to the understanding of the process under study. Alternatively, a protein's function may be obscure but the protein may be of obvious relevance; for example, its gene may be mutated in human disease. In this case, partners with known roles may turn up and provide essential clues. Thus, the method is a tractable and rapid form of genetics for organisms, such as mammals, that cannot be readily manipulated (MacDonald Paul N., 2001).

1.9.1 Principle of the two-hybrid assay

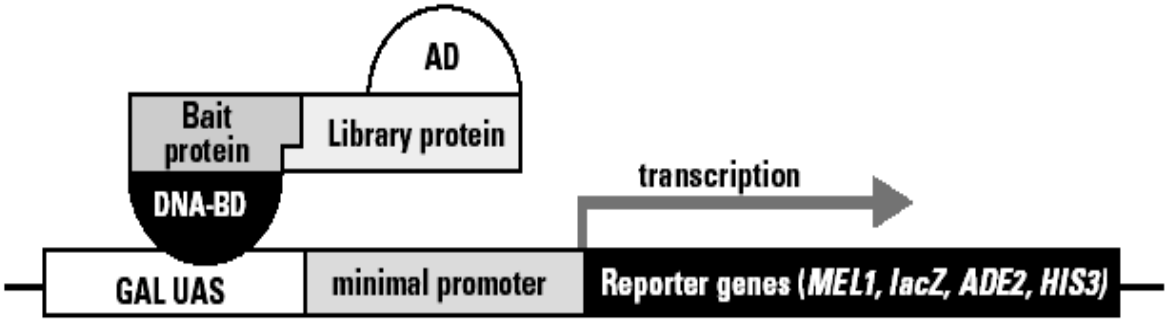

Figure 1.2. The two hybrid principle (Matchmaker Library construction and screening manual, Clontech, Heidelberg, Germany). GAL4-based two-hybrid system provides a sensitive transcriptional assay for detecting protein interactions *in vivo* in yeast. The DNA-BD is amino acids 1-147 of the yeast GAL4 protein, which binds to the GAL UAS upstream of the reporter genes. The AD is amino acids 768-881 of the GAL4 protein and functions as a transcriptional activator.

Transcription-based two-hybrid systems require three tools: one plasmid encoding a protein domain with promoter-specific DNA-binding activity, a second plasmid encoding a protein domain that serves as a transcription activator, and a yeast strain containing transcription-activated reporter genes. The gene encoding a protein of interest (the 'bait') is cloned as an in-frame fusion to the DNA-binding domain (DNA-BD), and genes encoding additional proteins of interest, or a library of proteins (the 'target'), are cloned as in-frame fusions to the transcription activation domain (AD). Both plasmids are then transformed into an appropriate yeast strain. The bait protein is expressed as a fusion to the DNA-BD and is thus localised to the promoter of a reporter gene in the yeast nucleus. The target protein (or library of proteins) is expressed as a fusion to the transcription AD. Interaction between the bait and target results in the co-localisation of the transcription AD to the DNA of the host strain, activating transcription of the adjacent reporter gene and generating a phenotypic signal.

To date, the yeast two-hybrid system has enabled the discovery of many novel proteins that play important roles in diverse biological processes. For example: the use of the two-hybrid system to analyse cell surface receptor and ligand interactions, analysis of protein–protein interactions mediating the yeast pheromone response pathway, and the discovery of new regulators of the cell cycle. Studies on interactions between cell surface ligand–receptor demonstrates that even though the yeast two-hybrid interaction takes place in the nucleus of the yeast cell, it is still applicable to analysing ligand–receptor interactions that normally take place on the cell surface (MacDonald Paul N., 2001).

1.10 Working model and the aims of the thesis project

The main focus of the present project was to study the effect of different forms of brain injury on a family of cell surface receptors known to be involved in tissue repair and modulating brain injury processes (Xi et al., 2003), and further elucidate the role of protein-protein interaction of one of the receptor subtypes in intracellular signalling.

For this purpose the optic nerve crush (ONC) model of rat was used as a prototype of traumatic axonal injury in the central nervous system (Gennarelli et al., 1989; Sautter and Sabel, 1993; Sabel et al., 1997). Axonal damage has now been identified as a major primary response of brain tissue to mechanical insult (Gennarelli et al., 1989). Studying human and experimental animal brains for events surrounding trauma to axons presents several limitations, keeping in mind the complexity of the whole brain (Gennarelli et al., 1989). In such situations a model of axonal damage is required where the lesion is highly specific, graded and reproducible, and lesion severity can be correlated with functional outcome and recovery of function can be followed within a defined time course (Sautter and Sabel, 1993).

For these diverse several reasons ONC injury model provides an ideal substitute for studying pathophysiology of induced trauma which resembled diffuse axonal damage in human as a result of closed head injury (Gennarelli et al., 1989; Sautter and Sabel, 1993). The injury-induced changes in retinal ganglion cell (RGC) axons and response of RGCs such as- transient shrinkage of cells, loss of retrograde transport, cell death and cytoplasmic atrophy have been well described in ONC model (Misantone et al., 1984; Barron et al., 1986). RGCs are a specialized type of nerve cells (neurons) that collect signals from other neurons in the eye and convey this information to the brain.

The nerve fibers, or axons, of RGCs form the optic nerve. The optic nerve is structurally and functionally well separated, unlike fibre tracts in brain or spinal cord, thus allowing specific and precise lesions and clear identification of injury–induced changes. Following ONC, significant spontaneous recovery to near prelesion performance levels occurs in 2-3 weeks (Sautter and Sabel, 1993).

Injury to the optic nerve, either crush or axotomy, have been used previously to study tissue repair mechanism in non-regenerating central nervous system (Tesser et al., 1986; Herdegen et al., 1993; McKerracher et al., 1993a, b; Isenmann and Bahr, 1997; Isenmann et al., 1997; Dieterich et al., 2002). Studies in our laboratory using the ONC model have shown a loss of almost 70-80% RGCs as a result of an early necrosis and subsequent apoptosis within 2 weeks after injury (Sautter and Sabel, 1993; Kreutz et al., 1997; Bien et al., 1999). Using in vivo confocal neuroimaging technique (ICON) it has been shown in our laboratory that following the time course of morphological changes of RGCs after ONC in living rats can help to predict their fate in terms of neuronal survival or death (Rousseau et al., 1999). Increased thrombin levels at the injury site have also been reported in the ONC model of rat (Friedmann et al., 1999; Friedmann et al., 2001a). In this study an increase in thrombin levels as early as 6 h after crush was observed with maximal levels at 1 day after injury (Friedmann et al., 2001a; Friedmann et al., 1999), The observation of such early thrombin up-regulation after crush indicates that thrombin might be involved in pathophysiology of ONC as it is known that thrombin at a higher concentration in brain has a detrimental effect (Striggow et al., 2000).

Aim 1: Since thrombin is an endogenous ligand of protease-activated receptors (PAR-1, -3 and –4), we decided to study the effect of ONC on PAR mRNA expression in retina.

Considering that thrombin is a serine protease whose levels are known to increase even when blood-brain barrier is intact as a result of several types of brain injuries (Xi et al., 2003), we decided to investigate the effect of another type of brain injury i.e., ischemic stroke on PAR mRNA expression. It is known that prothrombin mRNA is expressed in CNS (Dihanich et al., 1991) and that it is up-regulated in brain following cerebral ischemia (Riek-Burchardt et al., 2002) and spinal cord injury (Citron et al., 2000).

Focal ischemia results in inflammatory reaction, including macrophage infiltration, microglia activation, edema formation, upregulation of cytokines and

adhesion molecules, microvascular impairment and blood-brain barrier disruption (Liao et al., 2001; Danton and Dietrich, 2003). The differential response of all the elements involved in inflammation can either be detrimental, leading to secondary brain damage, or beneficial, resulting in neuronal regeneration after injury (Liao et al., 2001; Danton and Dietrich, 2003). Thrombin is known to be produced as a result of an inflammatory reaction at the site of injury (Cirino et al., 2000; Cocks and Moffatt, 2000).

Earlier studies from our laboratory have shown that thrombin receptor-activating peptide mimicked the effects of low concentration of thrombin (50 pM) in reducing ischemic neuronal injury *in vitro* (Striggow et al., 2000); and transient up-regulation of receptors PAR-1 to -3 as a result of OGD in organotypic hippocampal slice cultures (Striggow et al., 2001).

Aim 2: The data on the role of thrombin in brain ischemia including our own previous work prompted us to look at the mRNA expression pattern of PARs after transient focal ischemia in the present study. For this we induced transient focal ischemia by occlusion of the Middle Cerebral Artery (MCA) in rat which is a prototypical and well-established model for studying the outcome of stroke. Occlusion of the MCA was done by microinjection of endothelin-1 near the MCA (Sharkey et al., 1994; Reid et al., 1995). This animal model for studying stroke has the advantage of reduced reperfusion damage. Additionally, the slow onset of reperfusion more closely reflects the clinical situation of stroke.

Receptor activation on the extracellular surface of the cell results in transmission of the response via intracellular signalling that finally culminates in the nucleus resulting in gene activation. Intracellular signalling requires a series of proteins to transfer information from one moiety to another in a sequential manner and in the process of amplifying the signal. Each moiety involved in signalling can interact with several other moieties depending on the preceding signal. Anomalies in the signalling cascade can lead to deleterious effects with major pathological implications. Hence it is important to understand the signalling mechanism in order to unravel its intricacies.

Involvement of PARs in inflammation, tissue injury and neuronal signalling (Vergnolle et al., 2001a) makes them an interesting candidate for studying their intracellular signalling network. Work done in our laboratory has already elucidated the PAR-1 signalling mechanism in astrocytes (Wang et al., 2002b). In previous reports novel protein-protein interactions using the carboxy tail of PAR-1 were found by the classical yeast-two hybrid screen (Mahajan et al., 2000; Pai et al., 2001). These studies

highlighted the role of PAR-1 interacting proteins in signalling to cytoskeleton (Mahajan et al., 2000; Pai et al., 2001).

Aim 3: Since PAR-2 is the most extensively studied and implicated receptor subtype in brain injury such as ONC and ischemia (Napoli et al., 2000; Vergnolle et al., 2001b; Rohatgi et al., 2003), we decided to use this receptor subtype in a yeast-two hybrid screen to find novel interacting protein(s). Then their role in PAR-2 signalling pathway should be identified either under normal or pathophysiological conditions.

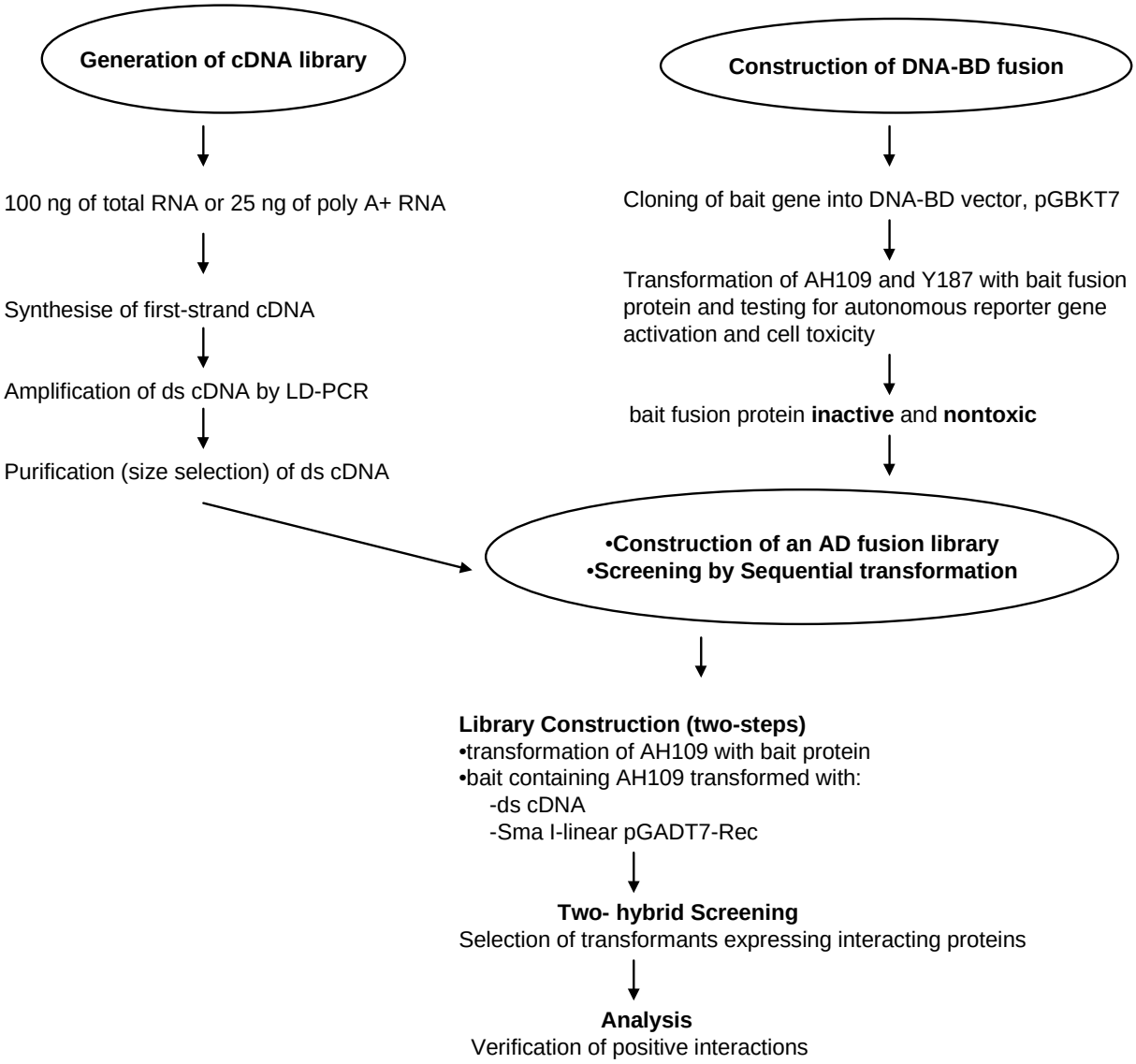

1.11 Yeast-two hybrid library construction and screening protocol

2. Materials and Methods

2.1 Materials

2.1.1 Animals

a) Hsdcpb:WU rats: Pups and adult (12 weeks old) male.

b) Male Sprague Dawley rats

2.1.2 Cell lines

a) Human embryonic kidney (HEK 293-epithelial)
b) Rat N2A (neuronal)
c) NG108 (mouse neuroblastoma x rat glioma hybrid)
d) Retinal ganglion cell (RGC-neuronal)

2.1.3 Bacterial and yeast strains

	Strain	Genotype	Reference
Bacteria: *E coli*	XL1-Blue	*sup*E44, *hsd*R17, *rec*A1, *end*A1, *gyr*A46, *thi*, *rel*A1, *lac*, [F' *pro*AB, *lac*I^q, ZΔM15, *Tn*10(*tet*^{r})]	Sambrook et al., 1989
Yeast:*Saccharomyces cerevisiae*	AH109	MATa, *trp*1-901, *leu*2-3, 112, *ura*3-52, *his*3-200, *gal*Δ4, *gal*80Δ, LYS2 : : $GAL1_{UAS}$-$GAL1_{TATA}$-HIS3, $GAL2_{UAS}$ - $GAL2_{TATA}$-ADE2, URA3 : : $MEL1_{UAS}$-$MEL1_{TATA}$-lacZ, MEL1	James et al., 1996; Clontech
Yeast:*Saccharomyces cerevisiae*	Y187	MATα, *ura*3- 52, *his*3- 200, *ade*2- 101, *trp*1- 901, *leu*2- 3, 112, *gal*4Δ, *met*–, *gal*80Δ,	Harper et al., 1993

		URA3 : : $GAL1_{UAS}$ - $GAL1_{TATA}$ -lacZ, MEL1	

2.1.4 Plasmid vectors

Name	Size(Kb)	Antibiotic resistance	Yeast nutritional selection marker	Manufacturer
pGBKT7	7.3	kanamycin	tryptophan	Clontech, Heidelberg, Germany
pGADT7-Rec	8.0	ampicillin	leucine	
pCMV-HA	3.8	ampicillin	-	
pEGFP-N1	4.7	kanamycin/ neomycin	-	
pEGFP-C2	4.7	kanamycin/ neomycin	-	
pDsRed2-N1	4.7	kanamycin/ neomycin	-	
pcDNA3.1/ Myc-His (B)	5.5	ampicillin/ neomycin	-	Invitrogen, Karlsruhe, Germany

2.1.5 RNA

Rat retina poly A+ RNA Clontech, Heidelberg, Germany

2.1.6 Enzymes

Enzymes and buffer	Manufacturer
Shrimp Alkaline Phosphatase	Boeringer, Mannheim, Germany
Sal I	Gibco BRL (Life Technologies), Karlsruhe, Germany
T4 DNA Ligase	
Bam HI	MBI Fermentas, St. Leon-Rot, Germany
Eco RI	
Eco RV	
Hind III	
Xho I	
Y/Tango+ (10X) buffer	
Sfi I	New England Biolabs, Beverly, MA, USA
RNasin-Ribonuclease inhibitor	Promega, Mannheim, Germany

2.1.7 Kits

Type of kit	Usage	Manufacturer
BigDye Terminator Cycle Sequencing Ready Reaction kit	DNA sequencing	Applied Biosystems, Warrington, UK
ECL+Plus	detection of western blot	Amersham Pharmacia Biotech, Buckinghamshire, UK
MatchMaker Library Construction & Screening kit	cDNA library construction and screening in yeast	Clontech, Heidelberg, Germany
Concert Rapid PCR Purification system	Cleaning of PCR, restriction digestion product	Gibco BRL (Life Technologies), Karlsruhe, Germany

Concert Rapid Gel Extraction system	Cleaning of PCR product from gel	
Invisorb Spin Plasmid Mini kit	Plasmid isolation	Invitek, Berlin, Germany
HiSpeed Plasmid Midi kit	Plasmid isolation	Qiagen, Hilden, Germany
Hotstar Taq Master Mix kit	PCR	
Omniscript Reverse Transcription kit	Making of cDNA	
Qiashredder	Homogenisation of Animal tissue for RNA isolation	
RNase-Free DNase Set	Removal of genomic DNA during RNA isolation	
RNeasy Maxi, Midi and Mini kit (Isolation of RNA)	Isolation of RNA	
Supersignal West Pico kit	Detection of western blot	Pierce, Rockford, IL, USA

2.1.8 Laboratory instruments

Instrument	Manufacturer
ABI PRISMTM 310 Genetic Analyzer	Applied Biosystems Division, Foster City, CA, USA
ProBlott membrane (PVDF membrane)	
Mighty Small II (for western blotting electrophoresis)	Amersham Pharmacia Biotech Buckinghamshire, UK
T3 Thermocycler	Biometra, Göttingen, Germany
Electrophoresis power supply	Bio-Rad Laboratories, München, Germany
Gel electrophoresis system	
Semi-dry Transfer Cell	
Mini PROTEAN II (Tankblot)	

GS-800 Calibrated Densitometer	
LSM510 laser scanning confocal microscope Axiovert 135 fluorescence microscope	Carl Zeiss, Jena, Germany
Sorvall RC-5B Refrigerated Superspeed Centrifuge	Dupont Instruments, Hamburg, Germany
pH Meter (pH526)	WTW
Eagle Eye Still video system	Stratagene, Heidelberg, Germany
Thermomixer comfort	Eppendof
Biofuge A, 13 R, 3.2 RS (centrifuge)	Heraeus, Hamburg, Germany
LaminAir (clean bench)	
Cell culture incubator	
Microplate reader	Molecular Devices
Innova 4230 Refrigerated incubator shaker	New Brunswick Scientific, Nürtingen, Germany
UV/visible Spectrophotometer	Pharmacia Biotech
Gel-blotting-papers	Schleicher & Schuell, Dassel, Germany
Protran BA83 Cellulosenitrat (E) (0.2 µm)	
Protran BA79 nitrocellulose transfer membrane (0.1 µm)	

2.1.9 Chemicals and Reagents

Chemicals	Manufacturer
Protein A	Amersham Pharmacia Biotech, Buckinghamshire, UK
Template Suppression Reagent (TSR)	Applied Biosystems Division, Foster City, CA, USA
Dulbecco's Modified Eagle's Medium (DMEM)	Biochrom, Berlin, Germany
DMEM + HAM'S F12 (1:1)	
Fetal calf serum (FCS)	
Penicillin and Streptomycin	
HBSS (w/o Ca^{2+} and Mg^{2+})	
Ampicillin	
Kanamycin sulphate	
Bio-Rad protein assay dye reagent concentrate	Bio-Rad Laboratories, München, Germany
Bacto Agar	BD Bioscience (Clontech), Heidelberg, Germany
Bacto Tryptone	
Bacto Yeast extract	
Yeast Nitrogen base w/o amino acids	
Amino acid dropout media (DO)	

Ponceau S solution (0.2% in acetic acid)	Boehringer, Mannheim, Germany
G418 Sulphate	Calbiochem, La Jolla, CA, USA
ImmersolTM 518N (Immersion oil for microscopy)	Carl Zeiss, Oberkochen, Germany
HAT supplement	GIBCO BRL, Karlsruhe, Germany
NuPAGE Novex 10% Bis-Tris Pre-Cast Gel	Invitrogen, Groningen, Netherland
NuPAGE Antioxidant	
NuPAGE Transfer Buffer (20x)	
NuPAGE LDS Sample Buffer (4x)	
NuPAGE MOPS SDS Running Buffer (20x)	
X-gal (5-bromo-4-chloro-3-indolyl-β-D-galactopyranoside)	
Accutase	PAA
DOTAP	Roche Diagnostic, Mannheim, Germany
Blotto, non-fat dry milk	Santa Cruz Biotechnology, Heidelberg, Germany
TEMED	SERVA, Heidelberg, Germany
Triton-X-100	
Tween 20	SIGMA, Deisenhofen, Germany
MES (2-[N-Morpholino]ethanesulfonic acid) Hydrate	
Glass Beads, 425-600 microns (unwashed)	
Dimethyl sulfoxide (DMSO)	
DMF (N,N-dimethylformamide)	
β-mercaptoethanol	
Adenine hemisulphate	
Igepal CA630	
Chloral hydrate	

2.1.10 Antibodies

Antibody	Manufacturer
mouse monoclonal antibody against glial fibrillary acidic protein (GFAP)	Boehringer, Mannheim, Germany
rabbit polyclonal antibody against α-crystallin A	Biomol, Hamburg, Germany
rabbit polyclonal IgG against HA-tag	Clontech, Heidelberg, Germany
peroxidase-conjugated anti-mouse and anti-rabbit IgG	Dianova, Hamburg, Germany
mouse monoclonal antibody against Myc	Invitrogen, Groningen, Netherland
rabbit polyclonal anti-GFP	
$Alexa_{555}$ anti-mouse IgG and $Alexa_{488}$	Molecular Probes, Eugene, OR, USA

anti-rabbit IgG	
mouse monoclonal anti-PAR-2 (SAM-11)	Santa Cruz Biotechnology, Heidelberg, Germany
rabbit polyclonal affinity purified antibody against HA-tag	SIGMA, Deisenhofen, Germany
mouse monoclonal antibody against synaptotagmin 1 (cytoplasmic tail)	SYSY-Synaptic Systems, Goettingen, Germany

2.1.11 Buffers and solvents

2.1.11.1 Cell culture medium and solutions

HEK-293 cells- DMEM/HAM'S F12 (1:1) with 2mM Glutamine, 10% FCS, 100U/ml Penicillin, 100 µg/ml Streptomycin

N2A cells- DMEM: 3.7 g/L NaHCO3, 4.5 g/L D-glucose, 1.028 g/L N-Acetyl L-alanyl-L-glutamine, 10% FCS, 100U/ml Penicillin, 100 µg/ml Streptomycin

NG-108 cells- DMEM: 3.7 g/L NaHCO3, 4.5 g/L D-glucose, 1.028 g/L N-Acetyl L-alanyl-L-glutamine, 10% FCS, 100 U/ml Penicillin, 100 µg/ml Streptomycin, HAT supplement (50X) – 200 µl/ 10 cm dish

RGC-5 cells- DMEM: 3.7 g/L NaHCO3, 1.0 g/L D-glucose, 1.028 g/L N-Acetyl L-alanyl-L-glutamine, 10% FCS, 100U/ml Penicillin, 100 µg/ml Streptomycin

HBSS (Hanck's balanced salt solution) without Ca^{2+} and Mg^{2+}

Accutase

G418 Sulphate- stock: 500 mg/ml, working concentration: 500 µg/ ml

2.1.11.2 Buffer and solutions

- DEPC (Diethyl pyrocarbonate) water: 0.1%= 1ml/ 1lt water
- 1x PBS: 137 mM NaCl, 2.6 mM KCl, 8.1 mM Na2PHO4, 1.4 mM KH2PO4, pH 7.4
- 1xTBE: 89 mM Tris, 89 mM Boric acid, 2 mM EDTA, pH 8.0
- 1xTE: 10 mM Tris/HCl, pH 7.4, 1 mM EDTA, pH 8.0

- 10X MOPS: 0,2 M MOPS, 10 mM Na_2-EDTA, 50 mM Na-Acetate, pH 7.0

- Ethidium bromide solution: 10 mg/ml

- TCM: 10 mM Tris/HCl, pH 7.5, 10 mM $CaCl_2$, 10 mM $MgCl_2$

- 4% PFA (Paraformaldehyde) solution: 4% PFA, 120 mM sodium phosphate, pH 7.4, 4% Saccharose

- FTP: Blocking and Washing buffer (immunostaining)-100 ml

10% FCS	10 ml
0.25% Triton-X100	0.25 ml
10X PBS	10 ml

- 4x Lysis buffer (cell lysate): 200 mM Tris/HCl, pH 7.4, 4 mM EDTA, 4 mM β-Mercaptoethanol, 600 mM NaCl, 4% Igepal
and one tablet of Protease Inhibitor Cocktail (Roche Molecular Biochemicals, Mannheim, Germany) per 50 ml

- 1x Lysis buffer (cell lysate)-8 ml

4x lysis buffer	2 ml
0.5 M EDTA	400 µl
EDTA-free complete proteinase inhibitor cocktail	160 µl
H_2O	5.44 ml

- 60% Acrylamid/Bis-100 ml

Acrylamid	58.4 g
N,N‘-Methylen-bisacrylamid	1.6 g

- Resolving buffer (SDS-PAGE-Laemmli): 750 mM Tris/HCl, pH 8.8

- Stacking buffer: 250 mM Tris/HCl, pH 6.8

- SDS solution: 10% (w/v) SDS in H_2O

- PER solution: 10% (w/v) Ammoniumperoxodisulfat in H_2O

- 4x Laemmli Sample buffer: 500 mM Tris/HCl, pH6.8, 8% SDS, 40% Glycerol

- 5x Laemmli Running buffer: 125 mM Tris, 960 mM Glycine, 0.5% SDS, pH 8.5

- 1x Transfer buffer (for Laemmli gels with NC membrane): 25 mM Tris, 192 mM Glycine, 20% (v/v) Methanol

- 100 mM CAPS [3-(Cyclohexylamino)-1-propansulfonic acid] /NaOH, pH 11

- 1x Transfer buffer (for Laemmli gels with PVDF membrane): 10% (v/v) Methanol, 10 mM CAPS/NaOH

- Membrane Stripping buffer: 62.5 mM Tris, pH 6.8, 100 mM β-Mercaptoethanol, 2% SDS

- 20% Protein A slurry : 1 ml 1x PBS and 4 µl 10% sodium azide

- Lysis buffer (for yeast): 10 mM Tris/HCl, pH 8.0, 100 mM NaCl, 1mM EDTA, 2% Triton-X-100, 1% SDS.

- Phenol- chloroform- Isoamylalcohol: 25:24:1

- X-gal (stock solution)- 20 mg/ml in DMF. Stored at -20 C

- Z buffer-1lt

Na_2HPO_4. $7H_2O$	6.1 g
$NaHPO_4.H_2O$	5.50 g
KCl	0.75 g
$MgSO_4.7H_2O$	0.246 g
pH 7.0	

- Z buffer/X-gal solution

Z buffer	100 ml
β-mercaptoethanol	0.27 ml
X-gal (20 mg/ml)	1.67 ml

- PEG/LiAc (polyethylene glycol/ lithium acetate)

	Final conc.	For 10 ml soln
PEG 4000 40%		8 ml of 50% PEG
TE buffer	1x	1 ml of 10x TE
LiAc	1x	1 ml of 10x LiAc

- 5xKCM buffer- 30 ml

		End concentration
3 M KCl	5 ml	0.5 M
1 M $CaCl_2$	4.5 ml	0.15 M
1M $MgCl_2$	7.5 ml	0.25 M

2.1.11.3 Microbial media

- Luria bertini (LB)- 1 lt

Bacto-tryptone	10 g
Bacto yeast extract	5 g
NaCl	10 g
pH 7.0	
bacto agar (for plates)	15 g
Ampicillin	100 µg/ml (final conc.)
Kanamycin	50 µg/ml (final conc.)

- YPDA-1 lt

Difco peptone	20 g
Yeast extract	10 g
0.2% Adenine hemisulfate	15 ml (final conc.= 0.003%)
pH 5.8	
40% Glucose	50 ml (final conc.= 2%)
bacto agar (for plates)	20 g
kanamycin	10-15 µg/ml (final conc.)

- SD minimal media- 1 lt

Yeast nitrogen base w/o amino acids	6.7 g
10X Dropout (DO) solution	100 ml solution / appropriate amount of DO powder
pH 5.8	
40% Glucose	50 ml (final conc.= 2%)
bacto agar (for plates)	20 g

- SOC –250 ml

Bacto tryptone	5 g
Yeast extract	1.25 g
NaCl	0.15 g
KCl	0.125 g
1M Glucose	5 ml (final 20 mM)
1M $MgCl_2$	2.5 ml (final 10 mM)
1M $MgSO_4$	2.5 ml (final 10 mM)

-
-
-

- TSB buffer-150 ml

		End concentration
2x LB-media	75 ml	1x LB
DMSO	7.5 ml	5%
1 M $MgCl_2$	1.5 ml	10 mM
1 M $MgSO_4$	1.5 ml	10 mM
PEG 4000	15 g	10%

Sterile filtered with 0.2µm Filter

- 2xLB-100 ml

bacto tryptone	2 g
Yeast extract	1 g
NaCl	2 g

pH 7.0-7.4

- 10 x -His/-Trp DO supplement- 500 ml

Lysine	0.3 g
Adenine hemisulphate	0.2 g
Leucine	1.0 g

2.1.12 **Oligonucleotides**

(Synthesized by MWG, Biotech, Erbesberg, Germany)

2.1.12.1 PCR Primers

Gene Product	Accession No.	Primer sequence (5'→ 3')	Position	Tm (°C)	PCR product (bp)
PAR-1	M81642	CCTATGAGACAGCCAGAATC (S)	146	55°C	355
		GCTTCTTGACCTTCATCC (AS)	500		
PAR-2	U61373	GCGTGGCTGCTGGGAGGTATC (S)	19	59°C	742
		GGAACAGAAAGACTCCAATG (AS)	760		
PAR-3	AF310076	GTGTCTCTGCACACTTAGTG (S)	18	55°C	581
		ATAGCACAATACATGTTGCC (AS)	598		
PAR-4	AF310216	GGAATGCCAGACGCCCAGCATC (S)	54	64°C	559
		GGTGAGGCGTTGACCACGCA (AS)	612		
GAPDH	M17701	GTGAAGGTCGGTGTCAAC (S)	34	51°C	835
		CAACCTGGTCCTCAGTGTAGC (AS)	868		
α-crystallin A	NM_012534	GGAACATGGACGTCACCAT (S)	8	58°C	526
		CAGGACGAGGGTGCCGAGC (AS)	533		
α-crystallin B	NM_012935	GGACATAGCCATCCACCA (S)	3	56°C	512
		CTGCAGTGACAGCAGGCT (AS)	514		
hsGAPDH	NM_002046	TCCAAAATCAAGTGGGGCGATGCT (S)	322	55°C	600

		ACCACCTGGTGCTCAGTGTAG CCC (AS)	920		

2.1.12.2 Cloning Primers

Gene Product	Accession No.	Primer sequence (5'→ 3')	Position	Tm (°C)	PCR product (bp)
C-tail PAR-2	U61373	TTTGTTGAATTCATGTCGAA AGATTTCAGG (S)	1036	58°C	186
		CTCAGACCCGGATCCAGCTC AGTAGGAGGT (AS)	1206		
Full PAR-2	U61373	CCACGTCTCGAGCCGGGGAT GCGAAGTCTCAGC (S)	1	58°C	1224
		CCCAGCTCAAAGCTTGTAGG AGGTTTTAACACT (AS)	1200		
Full α-crystallin A	NM_012534	GAATTCCGGCTCGAGAACAT GGACGTCACCATC (S)	1	63°C	552
		GCCTGCTCAAAGCTTGGACG AGGGTGCCGAGCT (AS)	540		
Full α-crystallin A	NM_012534	GAATTCCGGGGATCCAACAT GGACGTCACCATC (S)	1	63°C	552
		GCCTGCTCAGATATCGGACG AGGGTGCCGAGCT (AS)	540		
α-crystallin A Domain 1 (CD1)	NM_012534	GAATTCCGGGGATCCAACAT GGACGTCACCATC (S)	1	60°C	198
		GTCCAACACGATATCTGTGC GGAAGAGAGACTG (AS)	186		
α-crystallin A Domain 2 (CD2)	NM_012534	ACAGTGTTGGGATCCGACAT GTCCGGCATCTCTGAG (S)	175	60°C	348
		CTCCTCCCGGATATCTGACA CGGGAATGGCCCT (AS)	507		

2.1.12.3 Sequencing Primers

Annealing temperature in all cases: 55°C

Gene Product / plasmid vector	Accession No.	Primer sequence (5'→ 3')	Position	Comment
pGBKT7	Clontech	GGAGCAGAAGCTGATCTC (S)	1250	
		TATGCTAGTTATGCGGCC (AS)	1345	
pGADT7-Rec Matchmaker AD LD-Insert Screening Amplimer	Clontech	CTATTCGATGATGAAGATACCCC ACCAAACCC (S)		published
		GTGAACTTGCGGGGTTTTTCAGT ATCTACGAT (AS)		
T7 promoter	Invitrogen	GTAATACGACTCACTATAGGGC (S)		published
BGH seq	Invitrogen	CTAGAAGGCACAGTCGAGG (AS)		published
PAR-2 seq	U61373	GCGCTCTGCAAGGTGCTCATT (S)	436	
PAR-2 seq	U61373	CTCAACAGCTGCATAGACCC (S)	1003	
PAR-2 seq	U61373	GTAGACGTGGCTCTGCCTCTG (AS)	969	
α-crystallin A seq	NM_012534	GGCATGCTGACCTTCTCTGG (S)	421	
pEGFP-N1 seq	Clontech	GGTCTATATAAGCAGAGCTG (S)	550	
		CCATGGTGGCGACCGGTGGAT (AS)	682	
pCMV-HA	Clontech	GATCCGGTACTAGAGGAACTGA AAAAC (S)		published

2.1.13 Molecular weight markers

2.1.13.1 Nucleic acid standard marker

GeneRuler 100bp DNA Ladder (1 kb) MBI Fermentas, Germany

GeneRuler DNA Ladder Mix (10 kb)

2.1.13.2 Protein standard marker

Precision Plus (All Blue) (250-10 kDa) Bio-Rad, München, Germany
SeeBlue Plus2 Pre-stained (for Nupage pre-cast) Invitrogen, Netherland

2.2 Methods

2.2.1.1 Optic nerve crush (ONC)

Adult male Hsdcpb:WU rats were kept two animals per cage on a 12 h / 12 h dark/light cycle at a relative humidity of 40-50% at 22°C with food and water available *ad libitum*. 12 weeks old animals were anaesthetised intra-peritoneally with Ketanest and Rompun (50 mg/kg and 20 mg/kg, respectively). A partial nerve crush was done with a cross-action forceps as previously described (Sautter and Sabel, 1993). The tips of the forceps were spaced 0.2 mm apart. The left optic nerve was approached from the orbit by a lateral canthotomy under the guidance of a surgical microscope. The optic nerve was exposed by blunt dissection, leaving both retinal blood supply and dura intact. The nerve was then crushed at a distance of 2-3 mm from the eye for a duration of 30 s. After completion of the crush, the canthotomy was sutured and an antibiotic eye ointment was topically applied to prevent inflammation. The right nerve remained untouched. Control (untreated) and optic nerve crush (ONC) treated (after different post-injury time intervals) rats were killed with 7% chloral hydrate, after perfusion with 10 mM phosphate buffered saline, pH 7.0, for 10 min and both eyes were dissected out of the animal. A cut in the cornea released the lens and vitreous body and the retina was separated from the complex of retinal pigment epithelium and choroid-eye cup .

Tissues were immediately frozen in liquid nitrogen and stored at –70°C. In case of pups, eyes were removed from the animals after giving them 7% chloral hydrate and were immediately frozen in liquid nitrogen and stored at –70°C. All animal experiments were performed in compliance with the relevant laws and institutional guidelines.

2.2.1.2 Transient focal ischemia

Endothelin-1-induced transient focal ischemia in rats (e-MCAO): done in co-operation with Dr. Petra Noack and Prof. K.G Reymann (Forschungsinstitut Angewandte Neurowissenschaften (FAN), 39120 Magdeburg, Germany). Induction of ischemic damage was done by Dr. Noack

Male Sprague Dawley rats (300-360 g) were used. The animals were fed with laboratory chow and water ad libitum and maintained in a thermo-regulated environment (17-21°C) during a 12/12 hr light/dark cycle. Animals were anaesthetised with sodium pentobarbitone (40-50 mg/kg) and placed in a stereotaxic frame. A scalp

incision of approximately 1 cm in length was made from a point between the eyes, along the midline towards the back of the skull. The periosteum was then removed from the surface of the skull by scraping, and the surface was swabbed with 3% hydrogen peroxide to dry and clean it. A stainless steel screw (1.5 mm diameter) was inserted into the skull via a drill hole, without piercing the dura. A second drill hole was made for the guiding cannula for endothelin injection (endothelin-cannula: 0.9 mm posterior to bregma and 4.8 mm lateral to midline). The dura was pierced through the hole and the cannula was lowered with the tip located near to the MCA. The entire assembly was sealed and fixed to the skull with dental cement. The animals were allowed to recover for at least 7 days before any further intervention. Throughout the endothelin application, the animals could move freely in their cage, with an injector connected by a flexible tube to a Hamilton syringe. To induce MCAO, rats were given an injection of 250 pmol endothelin-1 in 2 µl 0.9% NaCl solution over a time period of 2 min. After a further minute the cannula was slowly withdrawn.

After the survival time of 12 h, 48 h and 7 days after ischemia, the animals were anaesthetised (chloralhydrate), perfused with 60 ml saline and then decapitated. Brains were taken out under sterile conditions and placed into a rodent brain matrix. A 4 mm thick coronal slice was taken out 7 mm from the frontal pole, dissected along fissura longitudinalis cerebri in ispsilateral and contralateral hemisphere and immediately frozen in liquid nitrogen. The slice from the ipsilateral hemisphere comprises the infarct volume evaluated in a standard ischemic brain, 7 days after induction of damage (Nissl-staining). Nissl-stain and infarct areas were quantified on a Nikon microscope using Lucia software. The infarct volume was calculated by linear trapezoidal extrapolation. As expected, the histological evaluation of the brains showed a time-dependent increase in damage. The infarct volume increased directly proportional to survival time after ischemic injury: The infarct volume at 12 h survival was 30 mm^3, at 48 h survival 42.6 mm^3 and at 7d survival it was 77.5 mm^3 (data not shown). All animal experiments were performed in compliance with the relevant laws and institutional guidelines.

2.2.2 Isolation of Nucleic acids

2.2.2.1 RNA isolation from Animal tissue

Total RNA was isolated from rat retina with the RNA isolation kit (RNeasy Mini kit, Qiagen). Briefly, the frozen tissue was homogenised completely in 350 µl

Buffer RLT containing β-Mercaptoethanol (10 µl β-ME/1 ml Buffer RLT). Lysate was pipetted directly onto a QIAshredder column sitting in a 2-ml collection tube, and centrifuged for 2 min at maximum speed to homogenise. The lysate was centrifuged again for 3 min at maximum speed and only the clear supernatant from this step used in subsequent steps. Added 1 volume of 70% ethanol to the cleared lysate, and mixed well by pipetting for precipitating the RNA. Applied 700 µl of the sample to a RNeasy mini spin column sitting in a 2-ml collection tube, and centrifuged for 1 min at 10,000 rpm. Pipetted 350 µl Buffer RW1 onto the RNeasy column, and centrifuged for 1 min at 10,000 rpm to wash the lysate. Now On-column DNase digestion was performed to remove genomic DNA using the RNase-Free DNase kit (Qiagen, Hilden). Added 10 µl of DNase I stock solution (2.73 Kunitz units/ µl) mixed in 70 µl Buffer RDD (DNase I incubation mix) directly onto the spin-colum membrane and incubated at room temperature for 15 min. Pipetted 350 µl Buffer RW1 into the spin column and centrifuged for 1 min at 10,000 rpm. Transferred the RNeasy column into a new 2-ml collection tube. Pipetted 500 µl Buffer RPE onto the RNeasy column, and centrifuged for 1 min at 10,000 rpm. Pipetted 500 µl Buffer RPE again onto the RNeasy column and centrifuged for 2 min at maximum speed to dry the RNeasy membrane. Transferred RNeasy column into a new 1.5-ml collection tube, and pipetted 30 µl RNase-free water onto the RNeasy membrane. Incubated at room temperature for 10 min and then centrifuged for 2 min at 12,000 rpm to elute. Stored at –80°C.

To isolate total RNA from rat brain, RNeasy Midi or Maxi kit (Qiagen, Hilden) was used depending on the amount of the tissue. The volume of all the solutions and centrifugation time were adjusted accordingly.

2.2.2.2 RNA isolation from Animal cells

Total RNA was isolated from cultured cells (wild type and transfected) using the RNeasy Mini kit (Qiagen, Hilden). The medium was aspirated from the culture dish (6 cm) and cells were lysed with 600 µl Buffer RLT. Cells were homogenised completely by pipetting with 1 ml tip, and to this homogenised suspension 700 µl of 70% ethanol added and mixed well by pipetting. Rest of the procedure was done as described above for total RNA isolation from animal tissue.

2.2.2.3 Plasmid DNA isolation from bacteria (mini-preparation)

Plasmid DNA from transformed bacteria was harvested using the Invisorb Spin Plasmid Mini Kit (Invitek, Berlin). E.coli culture (single colony) was grown under appropriate antibiotic selection pressure in 3 ml LB media overnight at 37°C with shaking at 250 rpm. 2 ml of overnight grown culture was transferred to microcentrifuge tube and centrifuged for 1 min at maximum speed to pellet the cells down. Supernatant was removed completely and pellet was resuspended in 200 µl of Solution I by vortexing. Added 250 µl of Solution II, closed the tube and mixed carefully by inverting the tube only 5 times (no vortexing since it can lead to shearing of chromosomal DNA which contaminates the plasmid DNA). Added 250 µl of Solution III and mixed gently, but thoroughly, by shaking the tube 4-6 times. Centrifuged for 3 min at maximum speed. Decanted the clarified supernatant into the Spin Filter placed in a 2.0 ml Receiver tube. Added 200 µl of Binding Solution to the filled Spin Filter and closed the tube. Inverted the tube one time and centrifuged for 1 min at 10,000 rpm. Discarded the filtrate and added 750 µl of Wash Buffer PL. Centrifuged for 1 min at 10,000 rpm and discarded the filtrate. Then centrifuged for 2 min at maximum speed for complete removal of residual Wash Buffer PL. Placed the Spin Filter into a new 1.5 ml Receiver Tube and allowed the Spin Filter to air dry for 1 min for complete removal of ethanol in Wash Buffer. Then 30 µl of Elution Buffer added directly onto the membrane of Spin Filter and incubated at room temperature for 10 min. Finally centrifuged for 2 min at 10,000 rpm to recover the plasmid DNA. Stored at -20°C.

2.2.2.4 Plasmid DNA isolation from bacteria (Midi-preparation)

Plasmid DNA from transformed bacteria was harvested using the HiSpeed Plasmid Midi Kit (Qiagen, Hilden). 50 ml of overnight grown transformed bacteria culture was centrifuged for 1 min at 5000 rpm to recover cell pellet. Bacterial pellet was resuspended in 4 ml of Buffer P1 containing RNase A. Added 4 ml of Buffer P2, mixed gently, and incubated at room temperature for 5 min. Then added 4 ml of chilled Buffer P3, mixed immediately but gently and poured the lysate into the barrel of the QIAfilter Midi Cartridge. Incubated at room temperature for 10 min to allow precipitation of protein and genomic DNA at the top of the solution. In the mean time applied 4 ml of Buffer QBT to equilibrated a Qiagen-tip 500 and allowed the column to empty by gravity flow. Then removed the cap from the QIAfilter outlet nozzle and

gently inserted the plunger into the cartridge and filtered the cell lysate into already equilibrated Qiagen-tip. Allowed the cleared lysate to enter the resin by gravity flow. Washed the Qiagen-tip with 2 x 10 ml Buffer QC. After washing was done cartridge was placed in a fresh falcon tube and plamid DNA was eluted with 5 ml of Buffer QF. DNA was precipitated with 3.5 ml of Isopropanol (room temperature) and centrifuged immediately for 30 min at 5000 rpm. Supernatant was carefully discarded and DNA pellet was washed with 2 ml of 70% ethanol and centrifuged for 10 min at 5000 rpm. Again supernatant was discarded carefully and pellet was allowed to air-dry. Dried DNA pellet was redissolved in 100-200 µl TE buffer depending on size of bacterial pellet initially obtained. Stored at -20°C.

2.2.2.5 Plasmid DNA isolation from Yeast

Plasmid DNA was isolated from yeast using the method of Hoffmann and Winston (1987). Briefly, 10 ml of appropriate SD- media (SD/-Leu) was inoculated with a single colony (transformed yeast) in a 50 ml Erlenmayer flask and grown for 3 days at 30°C, 250 rpm. Cells were harvested by centrifuging for 5 min at 5000 rpm. Pellet was resuspended in 200 µl of yeast lysis buffer. Added 0.3 g of acid washed glass beads (soaked in nitric acid, washed briefly in distilled water and dried). Added 200 µl of Phenol-Chloroform-Isoamylalcohol (PCI) (25:24:1). Vortexed 3-4 times thoroughly. Centrifuged for 5 min at maximum speed. Transferred supernatant (aqueous phase) very carefully to a fresh tube. Performed the PCI extraction one more time. To the supernatant added 15 µl of 3M sodium acetate (1/10 vol) and 116 µl of Isopropanol (0.77 volume). Incubated for 5 min at room temperature. Centrifuged for 5 min at maximum speed. Discarded the supernatant and washed the DNA pellet with 300 µl of 70% ethanol. Ethanol washing did twice. Allowed the DNA pellet to air-dried and then redissolved in 25 µl of 10 mM Tris. Stored the plasmid DNA at -20°C.

2.2.2.6 Isolation of DNA fragment from agarose gel

To isolate DNA fragment (PCR or cDNA-insert in plasmid) from agarose gel, Concert Rapid Gel Extraction Kit (Gibco BRL) was used. The area containing the DNA fragment was cut from the gel. Care was taken to minimized the surrounding agarose excised with the fragment. For 1% agarose gel maximum 400 mg of gel slices used per 1.5 ml tube. Added 30 µl of Gel solubilization buffer (L1) for every 10 mg of gel. Incubated the gel slices in buffer at 50°C for minimum 15 min. Mixed the tube

every 3 min. After gel slice appeared dissolved, incubated the tube for 5 min more. Pipetted the dissolved gel slices solution into a cartridge placed in a 2.0 ml wash tube. Centrifuged for 1 min at maximum speed. Discarded the flow-through. Added 500 µl of Solubilization buffer (L1) to the cartridge and centrifuged again. Discarded the flow-through. Added 700 µl of Wash buffer (L2) (containing ethanol) to the cartridge and incubated for 5 min at room temperature. Centrifuged for 1 min at 14,000 rpm. Discarded the flow-through. Centrifuged at maximum speed to remove residual wash buffer. Placed the cartridge into a fresh 1.5 ml recovery tube and added 30 µl of pre-warmed TE buffer (70°C) directly to the center of the cartridge. Incubated for 10 min at room temperature and then centrifuged for 2 min at 12,000 rpm. Discarded the cartridge and stored the DNA at -20°C.

2.2.2.7 Cleaning of DNA fragment

DNA fragments after PCR amplification and restriction digestion were cleaned using the Concert Rapid PCR Purification kit (Gibco BRL). Added 400 µl of Binding Solution (H1) to ≤ 100 µl of amplification reaction. For higher amount adjusted the volume of Binding Solution (H1) 4:1 amplification reaction. Added the sample mix into the cartridge placed in a 2.0 ml wash tube. Centrifuged for 1 min at 12-14, 000 rpm. Discarded the flow-through. Added 700 µl of Wash Buffer (H2) (containing ethanol) to the cartridge and centrifuged for 1 min at 12,000 rpm. Discarded the flow-through and centrifuged again to remove the residual wash buffer. Placed the cartridge into a new 1.5 ml receiver tube and added 30 µl of pre-warmed TE buffer (70°C) directly onto the center of cartridge. Incubated for 10 min at room temperature and then centrifuged for 2 min at 12,000 rpm. Discarded the cartridge and stored the cleaned DNA at -20°C.

2.2.2.8 Precipitation of Sequencing PCR DNA

Sequencing PCR product was precipitated with sodium acetate and 100% ethanol. Briefly, to 80 µl H_2O added 10 µl of 3M Sodium Acetate. To this 20 µl of sequencing PCR reaction mixture was added and mixed thoroughly. Then added 250 µl of chilled 100% ethanol and incubated on ice for 5 min. Centrifuged for 15 min at 14,000 rpm. Supernatant discarded and pellet resuspended in 300 µl of 70% ethanol. Centrifuged again for 15 min at 14,000 rpm. Discarded the supernatant carefully and allowed the pellet to air-dry or at 37°C. DNA sample prepared for Sequencer (ABI

PRISMTM 310 Genetic Analyzer). DNA pellet was then resuspended in 25 µl of Template Suppression Reagent (TSR) buffer (ABI PRISM, Applied Biosystems Division, Foster City, CA, USA). Vortexed and centrifuged briefly. Sample denatured for 2 min at 95°C and then kept on ice for 2 min. Reaction mixture then transferred to the small 0.5 ml sequencing tube (without lid) and capped with rubber stopper suitable for the capillary in the sequencing machine.

2.2.2 Quantification of Nucleic acids

Quantity of Isolated DNA and RNA was measured by the UV absorption ratio 260 nm /280 nm using an Ultrospec 2000 UV/visible spectrophotometer (Pharmacia Biotech, Freiburg, Germany). Prepared 1:10 dilution of sample and measured in quartz cuvette (5.00 mm thickness). Measurement at 260 nm gave the absorption of nucleic acid, at 280 nm the protein absorption and 320 nm gave the salt present in the sample. The sample concentration was obtained in µg/ ml. A factor of 2 was used to calculate the actual concentration of the nucleic acid present in sample in µg/ ml. Absorption ratio of 260 nm/ 280 nm gave the quality of the nucleic acid (ratio > 1.7 considered okay). Quality of the nucleic acid was checked on a 1% agarose/TBE gel pre-stained with ethidium bromide (10 mg/ml).

2.2.3 Biochemical analysis of Nucleic acids

2.2.3.1 Hydrolysis of DNA with restriction endonucleases

Restriction digestion of DNA was done with restriction enzyme and its appropriate 10x reaction buffer. Recombinant plasmids were cut either with one or two enzymes simultaneously. For single digestion appropriate reaction buffer (10x) was used at a final concentration of 1x, while for double digestion Y^+/Tango buffer (10x) used at a final concentration of 2x.

	Single digestion	Double digestion
DNA	1-2 µg	5 µg
Enzyme 1 (10 u/µl)	1 µl	2 µl
Enzyme 2 (10 u/µl)	-	2 µl
Buffer (10x)	1x	2x
H_2O	variable	variable
	30 µl	30 µl
Incubation time	3-4 h at 37°C	10-12 h at 37°C

In case of double digestion involving Sfi I enzyme, DNA was first digested with enzyme 1, cleaned, quantified and then digested with Sfi I at 50°C in the presence of BSA (10 mg/ml-100x) at a final concentration of 100 µg/ml. After digestion, reaction mix was cleaned using Concert Rapid PCR Extraction kit (Gibco BRL), DNA quantified as described previously and 100 ng DNA checked on 1% agarose/TBE gel pre-stained with ethidium bromide in case of PCR DNA or plasmid vector digestion for cloning. To check for the presence of DNA insert in the recombinant plasmid whole of digestion mix was loaded on the gel. For subcloning purpose, after digestion of recombinant plasmid whole of digestion mixture was loaded on the gel and then the desired DNA fragment was cut from the gel and purified for further processing.

2.2.3.2 Gel electrophoresis

2.2.3.2.1 Agarose gel electrophoresis of DNA

To check the quality of DNA (PCR product, recombinant plasmid DNA, restriction analysis) 1% agarose (SIGMA) gel in 0.5x TBE buffer made. Gel was pre-stained in ethidium bromide (10 mg/ml) (SIGMA). DNA samples were prepared in 6x loading buffer (containing bromophenol blue dye) (MBI Fermentas). Gel was run in 0.5x TBE for 60 min at 80 V for PCR samples and at 100 V for plasmid DNA. Depending on the fragment size either GeneRuler 100bp DNA Ladder (1 kb) or GeneRuler DNA Ladder Mix (10 kb) (MBI Fermentas) used. DNA bands were visualised under UV-Transilluminator in an Eagle Eye II video system (Stratagene, Heidelberg, Germany).

For Semi-quantitative analysis of the PCR product, 10 µl of each reaction was used for electrophoresis. PCR signals were quantified in arbitary units (A.U) from optical density x band area. PCR signals were normalized to the GAPDH signal of the corresponding RT product to get a semi-quantitative estimate of the gene expression. PCR data were obtained for each sample and for each gene from two independent experiments and the results were averaged for statistical analysis of n animals.

2.2.3.2.2 Agarose gel electrophoresis of RNA

Quality of isolated RNA was checked in a 1% agarose / MOPS (N-Morpholino-3-propansulphonic acid) gel. 0.1% DEPC-H_2O was used for making all the solutions required for RNA gel including the sample preparation. 3% Hydrogen

peroxide (H_2O_2) used for decontaminating the gel assembly. RNase-free agarose (SIGMA) gel made in 1x MOPS buffer (SERVA, Heidelberg). Gel pre-stained with ethidium bromide (10 mg/ml). 200 ng of RNA used with 6x Loading buffer. Gel was run in 1x MOPS buffer for 1 h at 80 V. 18S and 28S RNA bands were visualised under UV-transilluminator in an Eagle Eye II video system (Stratagene, Heidelberg, Germany).

2.2.3.3 Polymerase Chain Reaction (PCR)

To check for the presence of the gene of interest either in the animal tissue or cell line (wild type and transfected), PCR was performed. PCR signal was amplified using the gene-specific primers (PAR-1-4, GAPDH, □-crystallin A and B) designed from the sequence available in the Genbank. For standard PCR, 20-22 bp long primers were designed, AT and GC content was checked and the difference in the melting temperature (Tm) between the forward and reverse primers was kept not more then 2-4ºC. The primer sequence was checked using the NCBI BLAST search for probable similarity with unrelated genes. In all cases forward and reverse primers were designed flanking an intron to make sure that the amplification signal comes from mRNA and not genomic DNA.

PCR reaction was done in 0.2 ml thin wall tubes in T3 Thermocycler (Biometra). Negative control without template performed to check for self-annealing of primer pair. PCR with RNA was also done to check the intron-flanking primers. Each primer pair was checked with several annealing temperatures depending on the Tm of the primer pair to get a single and specific PCR band. For semi-quantitative analysis of PAR mRNA expression different amounts of starting material and different number of cycles: 20, 25, 30, 32, 35 and 40 cycles checked for each primer pair to get the linear range of the amplification product. Finally PCR was done for 35 cycles.

2.2.3.3.1 Reverse Transcription- Polymerase Chain Reaction (RT-PCR)

To reverse transcribe the isolated total RNA from either animal tissue or cells Omniscript Reverse Transcription kit (Qiagen, Hilden) was used. 1 µg of total RNA was used to make cDNA in a 0.5 µl tube. RT reaction was set as follows:

RNA	1 µg
RT Buffer (10x)	2 µl
dNTP mix (5 mM each)	2 µl
Oligo-dT primer (0.5 µg/µl) (Gibco BRL)	2 µl
Omniscript Reverse Transcriptase (4 u/µl)	1 µl
RNasin (10 u/µl) (Promega)	1 µl
H_2O	variable
	---
	20 µl

RT was done in T3 Thermocycler (Biometra). The reaction was incubated for 1 h at 37°C, followed by 5 min at 95°C and then rapidly cooled at 4°C. cDNA was stored at -20°C.

PCR reaction was done with the cDNA generated from the RT step using the Hotstar Taq Master Mix kit (Qiagen, Hilden). The reaction mixture was pipetted as follows:

cDNA	1-2 µl
Hotstar Taq Master Mix	25 µl
5‘ primer (10 pmol/µl)	2 µl
3‘ primer (10 pmol/µl)	2 µl
H_2O	variable
	---
	50 µl

The PCR reaction was done using the following programme (for Hotstar Taq polymerase):

Lid temperature = 110°C

Preheating =	On	
Initial denaturation =	95°C	15 min
35 cycles: Denaturation	94°C	30 sec
Annealing	variable	1 min 30 sec
Extension	72°C	1 min
Final extension =	72°C	10 min
	4°C	pause

10 µl of reaction used for gel electrophoresis to check for the presence of the desired gene product.

2.2.3.3.2 Sequencing PCR

For sequencing reaction, either 100 ng of cleaned PCR DNA or 1 µg of recombinant plasmid DNA used with 2 µl primer (10 pmol/µl) and 4 µl Big dye (contains DNA polymerase, fluorescent dye-labelled dNTPs, buffer) (Applied Biosystems, Warrington, UK), added H_2O to a final volume of 20 µl. The PCR conditions were:

Denaturation	98°C	for 2 min
25 cycles: Denaturation	96°C	for 30 sec
Annealing	55°C	for 30 sec
Extension	60°C	for 4 min + 25 sec increament/cycle
Pause	4°C	

After PCR, DNA was precipitated and prepared for Sequencing .

2.2.4 Cloning

2.2.4.1 Generation of DNA insert by PCR

To clone a particular DNA fragment into plasmid vector for generating a recombinant plasmid, PCR was done to amplify either the full coding sequence or particular region of interest from the gene. Cloning primers were designed from the sequences available in the Genbank. 30-33 bp long primers were designed flanking the 5‘ and 3‘ region of interest. Care was taken to have similar annealing temperature for the primer pair. Suitable restriction enzyme sites were included in the primer based on the multiple cloning site (MCS) of the plasmid vector into which the fragment was to be cloned. DNA fragment to be cloned was checked for the presence of sequence matching the restriction site. Primers were designed in a way to ensure that the right amino acid codon frame remained intact in the recombinant plasmid. For cloning the full cDNA, stop codon was mutated in the 3‘primer when cloned into a vector with a 3‘ detection tag. 1 µl of cDNA used for generating the required cDNA fragment with 2 µl of each primer (10 pmol/µl) using the Hotstar Taq Master Mix kit (Qiagen, Hilden). PCR cycling conditions were similar to described above for normal PCR with appropriate annealing temperature.

5 µl of amplified fragment was loaded on the agarose gel to check for the correct fragment size. PCR reaction mix cleaned using Concert Rapid PCR

purification kit (Gibco BRL), quantified, restriction digested, again cleaned to remove digestion buffer, quantified and checked on the gel for correct size.

2.2.4.2 Dephosphorylation of digested plasmid

The restriction enzyme treated plasmid was dephosphorylated with Shrimp Alkaline Phosphatase (Boeringer Mannheim) to remove the phosphate groups from the linear plasmid and avoid self-ligation during the ligation process.

Restriction digested DNA	1-2 µg
Shrimp Alkaline Phosphatase (1 u/µl)	1 µl
Dephosphorylation buffer (10x)	1x
H_2O	variable
	20 µl

Incubated for 1 h at 37°C followed by 10 min at 65°C for denaturing the enzyme. After phosphatase reaction, plasmid vector was cleaned again to remove the reaction buffer.

2.2.4.3 Ligation of plasmid and DNA insert

To generate recombinant plasmid, dephosphorylated restriction digested plasmid was ligated with the DNA insert having the same restriciton sites at their 5‘ and 3‘ end using the T4 DNA Ligase (Gibco BRL). All the restriction enzymes used in the present study generate sticky ends.

Plasmid vector	1x
DNA insert	3x
T4 DNA Ligase (1 u/µl)	1 µl
Ligase buffer (5x)	4 µl (1x)
H_2O	variable
	20 µl

Ligation was done in (T3) Thermocycler (Biometra) using following reaction conditions:

16°C	8 h
22°C	4 h
37°C	2 h
Pause	4°C

Ligation mixture was then used to transform bacteria to generate recombinant plasmid.

2.2.5 Microbiological techniques

2.2.5.1 Transformation of bacteria with plasmid DNA

2.2.5.1.1 Transformation of E.coli by heat-shock method ($CaCl_2$ based)

For transformation of E.coli, XL1-Blue strain was used. To make competent cells single colony of XL1-Blue was grown in 5 ml LB media overnight at 37°C with shaking at 250 rpm. 1 ml of overnight bacterial culture was then transferred to 100 ml of fresh LB media and continued to grow at 37°C with shaking till the cells reached their logarithmic phase i.e, OD_{600}= 0.3-0.4. Then the bacterial suspension was centrifuged at 6000 rpm in SS 34 Rotor in Sorvall centrifuge (pre-cooled) for 5 min at 4°C. Supernatant was discarded and cell pellet was resuspended in 10 ml of ice-cold 100 mM $CaCl_2$ solution. The cell suspension was then incubated on ice in cold room (4°C) for 1 h. Centrifuged for 5 min at 6000 rpm at 4 °C. Supernatant discarded carefully and pellet resuspended in 1 ml of ice-cold 100 mM $CaCl_2$ containing 30% glycerine (1 ml solution= 700 µl 100 mM $CaCl_2$+ 300µl of 100% glycerine). From this competent cell suspension aliquots of 200 µl made, frozen in liquid nitrogen and stored at -80°C.

To transform bacteria, 200 µl of $CaCl_2$ competent cells for each reaction thawed on ice. To the cells added 100 µl of cold TCM buffer and either 10-20 ng of super-coiled plasmid DNA or 20 µl of ligation mix. Incubated on ice for 20 min and then heat –shock given for 90 sec at 42°C. Transformation reaction mix immediately incubated on ice for 1 min. 700 µl of LB media (pre-warmed at 37°C and without any antibiotic) added to transformation mix and incubated for 30-60 min with shaking at

37°C. 100 µl of the transformation mixture in case of super-coiled DNA plated on the LB-agar plate containing suitable antibiotic. For ligation transformation, reaction mix was centrifuged briefly, supernatant discarded and pellet resuspended in the residual volume and plated on LB-agar containing suitable antibiotic. LB-agar plates incubated up-side down at 37°C to facilitate growth of tranformants under appropriate antibiotic selection pressure.

2.2.5.1.2 Transformation of E.coli KCM competent cells with plasmid DNA

Transformation of KCM competent cells with plasmid DNA is another method for chemical transformation of E.coli. Briefly, single colony of XL1-Blue E.coli strain grown overnight in 5 ml of LB media (without antibiotic) at 37°C with shaking. 150 ml of fresh media then inoculated with 1 ml of overnight bacterial culture and allowed to grow till the OD_{600} of the culture reached 0.6. Cell suspension was then centrifuged for 10 min at 5000 rpm at room temperature. Supernatant discarded and pellet resuspended in 15 ml (1/10 volume) of TSB buffer. Incubated the suspension on ice for 10 min and then aliquoted 500 µl each of cell suspension. Freezed in liquid nitrogen and stored at -80°C. To transform KCM competent cells using plasmid DNA, 20 µl of KCM buffer added to either 20 µl of ligation mix or 10-20 ng of super-coiled plasmid DNA. H_2O added to made-up the volume till 100 µl. Mixed nicely and incubated on ice. In the mean time thawed the KCM competent cells on ice. 100 µl of cells used per transformation reaction. Mixed properly the cells with DNA and buffer mix and incubated on ice for 30-40 min. Then incubated the reaction mix for 10 min at room temperature (very important). 800 µl of LB media (without antibiotic) added and incubated for 1 h at 37°C with shaking. Either 100 µl of transformation mixture or pellet plated on LB-agar containing suitable antibiotic. Plates incubated up-side down at 37°C overnight to allow transformants to grow.

2.2.5.1.3 Transformation of E.coli by electroporation (electro-transformation)

Transformation efficiency of electroporation method is several folds higher as compared to the chemical transformation. Yeast plasmid DNA was transformed into E.coli by electroporation because isolation of plasmid from yeast results in genomic DNA contamination which reduces the transformation efficiency of the plasmids by

chemical based transformation. For electroporation the salt concentration of plasmid DNA is an important factor. DNA with high salt concentration cannot be electroporated because it interferes with the electrical resistance. To prepare electro-competent cells, E.coli XL1-Blue strain used. Single colony of XL1-Blue inoculated in 5 ml LB media and grown overnight at 37°C with shaking. To fresh 250 ml LB media 2.5 ml of overnight grown culture added and allowed to grow till the OD_{600} of culture media reached 0.5-0.6. Culture media kept on ice for 30 min. All subsequent steps were done at 4 °C. Centrifuged the cold bacterial suspension in GSA-Rotor (Sorvall centrifuge) (pre-cooled) for 10 min at 5000 rpm. Supernatant discarded and cell pellet resuspended in 250 ml of ice-cold sterile H2O. Centrifuged the suspension in GSA-Rotor for 10 min at 5000 rpm. Supernatant discarded. Pellet resuspended in 100 ml of ice-cold sterile H2O. Centrifugation step repeated and supernatant discarded. Cell pellet now resuspended in 30 ml ice-cold 10% (v/v) Glycerine (50 ml Glycerine+450 ml H2O, autoclaved). Centrifuged in SS34-Rotor for 10 min at 10,000 rpm. Supernatant discarded and cell pellet resuspended in 2.5 ml of ice-cold 10% (v/v) Glycerine. 300 µl each of suspension aliquoted in sterile tubes and immediately freezed in liquid nitrogen. Stored at -80°C. For electroporation, competent cells were thawed on ice. 50 µl of cells were taken for each transformation reaction. 5 µl of yeast plasmid DNA added to the competent cells, mixed, transferred to electroporation cuvette (bacterial-0.2 cm gap) and incubated on ice for 10 min. Electric pulse was applied with Gene pulser (Bio-Rad). Electric pulse was given under following conditions: Voltage- 2.5 kV, Capacitance-25 µF and Resistance- 200 ohms to get a time constant of ~4.5 msec. These conditions gave a field strength of 12.5 kV/cm (voltage set/ gap of cuvette). The samples showing resistance either less or more then 200 ohms were discarded (high salt concentration which may result in bursting of cuvette). After the electric pulse 500 µl of SOC media given to cells in cuvette and then transferred the suspension into a fresh tube. One more time 500 µl of SOC media given to clean and remove all the cells from the cuvette and then transferred the rest to the tube. Incubated for 1 h at 37°C with shaking and then plated 100 µl of the transformation mix to the LB-agar plate containing the appropriate antibiotic. Plates incubated up-side down at 37°C overnight to allow transformants to grow.

2.2.5.2 Transformation of Yeast by LiAc (small-scale)

Transformation of *Saccromyces cerevisae* strains AH109 and Y187 was done according to the Clontech yeast protocol handbook. Inoculated 1 ml of YPDA or SD dropout media with several colonies, 2–3 mm in diameter and from ~2 week old plate (SD dropout media used in case of pre-transformed host strain to maintain the selection pressure). Vortexed vigrously for 5 min to disperse the cell clump. Transferred this suspension into a flask containing 50 ml of YPDA or appropriate SD dropout medium. Incubated at 30°C for 16-18 h with shaking at 250 rpm to stationary phase, OD_{600}> 1.5. Transferred the 10 ml of overnight culture to a flask containing 100 ml of YPDA. Checked the OD_{600} of the diluted culture and, if necessary, added more of the overnight culture to bring the OD_{600} upto 0.2-0.3. Incubated at 30°C with shaking at 250 rpm till the OD_{600} reached 0.4-0-6. Placed cells in 50-ml tubes and centrifuged at 1000 x g for 5 min at room temperature. Discarded supernatant and added 50 ml of steril distilled H_2O to resuspend the cell pellet. Pooled the cells into one tube and centrifuged at 1000 x g for 5 min at room temperature. Decanted the supernatant and resuspended the cell pellet in 1.5 ml of freshly prepared, sterile 1X TE/1X LiAc. The cells were ready for transformation. Yeast competent cells should be used within 1 h of preparation for high transformation efficiency. Added 100 ng of plasmid DNA (for single or equimolar amount for co-transformation of two plasmids) and 5 µl (0.1 mg) herring testes carrier DNA to a fresh 1.5 ml tube (carrier DNA denatured at 100°C for 5 min and then chilled on ice. Repeated denaturation two times). Added 100 µl of competent cells and mixed thoroughly followed by addition of freshly prepared 600 µl of sterile PEG/LiAc/TE solution. Vortexed well. Incubated at 30°C for 30 min with shaking at 200 rpm. Added 70 µl of DMSO. Mixed by gentle inversion (no vortexing). Cells were given a Heat shock for 15 min in a 42°C water bath and then chilled on ice for 2 min. Centrifuged for 30 sec at 14,000 rpm at room temperature. Supernatant removed and cells were resuspended in 300 µl of sterile 1X TE buffer. Plated 100 µl on each SD minimal medium agar plate lacking particular amino acid (s) to select for the desired transformants. In yeast, transformants are selected on the basis of the auxotrophic nutritional markers instead of antibiotic selection used for bacteria. To obtain single colonies, also spreaded 100 µl of 1:1000, 1:100, and 1:10 dilution on 100-mm SD agar plates. Incubated plates, up-side-down, at 30°C until colonies appeared (2–4 days).

To calculate the transformation efficiency, colonies (cfu) growing on the dilution plates were counted.

$$\text{Transformation efficiency} = \frac{\text{cfu} \times \text{total suspension vol. (ml)}}{\text{Vol. plated (ml)} \times \text{dilution factor} \times \text{mg of DNA used}} = \text{cfu/mg DNA}$$

To make the master plate, largest colony was picked and restreaked on the same selection medium. Sealed plates with Parafilm and stored at 4°C for 3–4 weeks.

2.2.5.3 Preparation of Microbial culture stock solution

To make stock culture from bacteria, 850 µl of overnight grown culture mixed in 150 µl of sterile 100% glycerine. Vortexed briefly to mix thoroughly and immediately freezed in liquid nitrogen. Stored at -80°C.

To prepare stock culture from yeast, single colony from agar plate was resuspended in 500 µl of YPD medium (or the appropriate SD dropout medium for transformed yeast strains). Vortexed vigrously to disperse the cells. Added sterile 50% glycerine to a final concentration of 25% (125 µl of 50% glycerine to 500 µl YPD). Mixed thoroughly, immediately freezed in liquid nitrogen and stored at -80°C.

2.2.5.4 Testing of DNA-BD fusion protein for toxicity in yeast

To compare the growth rate in liquid culture of Y187 and AH109, cells transformed with the "empty" DNA-BD vector and with the DNA-BD/bait plasmid using the small scale yeast transformation protocol. Transformants were selected on SD/–Trp (since DNA-BD vector can synthesise tryptophan on ist own and hence does not require in the growing medium). An overnight culture was prepared by inoculating one large colony in 50 ml of SD/–Trp/Kana (20̃ g/ml). Incubated 16-24 h at 30°C with shaking at 250 rpm. Checked the OD_{600} to test the difference in growth rate of transformed AH109 and Y187 with empty plasmid or recombinant plasmid ($OD_{600} \geq$ 0.8 is okay, less means bait protein might be toxic).

2.2.6 Generation of cDNA library

To generate a cDNA library for yeast two-hybrid interaction, Matchmaker Library construction and screening protocol (Clontech, Heidelberg) followed.

2.2.6.1 Checking of RNA

Rat retina Poly A^+RNA and Human Placenta Poly A^+RNA (positive control) checked for quality on agarose/ MOPS gel. mRNA mixed with RNA loading buffer denatured at 65°C for 15 min. Both the native and denatured mRNA samples run on gel at 80 V.

2.2.6.2 First-Strand cDNA Synthesise using a Random Primer

First-strand cDNA was made from rat retina poly A^+ RNA (1 µg/µl) (Clontech, Heidelberg) and Human Placenta poly A^+ RNA (control). Following reagents were combined in a sterile 0.25-ml microcentrifuge tube:

1 µl RNA sample (1 µg of poly A^+RNA)
1.0 µl CDS III/6 Primer
2 µl Deionized H_2O
4.0 µl Total volume

Mixed the contents and centrifuged briefly. Incubated at 72°C for 2 min and immediately chilled on ice for 2 min. Centrifuged briefly again. Kept the tube at room temperature and added the following:

2.2 µl 5X First-Strand Buffer
1.0 µl DTT (20 mM)
1.0 µl dNTP Mix (10 mM)
1.0 µl PowerScript Reverse Transcriptase
9.0 µl Total volume

Mixed gently by tapping and centrifuged briefly. Incubated for 10 min at room temperature (25–30°C). Added 1.0 µl (5 milliunits) of RNase I (5 units/ml). Incubated at 42°C for 10 min. Add 1.0 µl of SMART III Oligonucleotide. Incubated at 42°C for 1 h (hot-lid T3 thermal cycler, Biometra). Placed the tube at 75°C for 10 min to terminate first-strand synthesis. Cooled the tube to room temperature, then added 1.0 µl (2 units) RNase H. Incubated at 37°C for 20 min. Proceeded directly with the LD-PCR and stored rest of the first-strand cDNA reaction mixture at –20°C.

2.2.6.3 Amplification of ds cDNA by Long Distance PCR (LD-PCR)

ds cDNA (both the rat retina and Human placenta) were amplified by LD-PCR. Amplification done for 20 cycles (optimum for 1.0 µg starting mRNA to minimize

nonspecific PCR products). T3 thermocycler (Biometra) preheated to 95°C. To prepare sufficient ds cDNA for transformation, two 100-µl PCR reactions set for each experimental sample (rat retina). Set one reaction for the Control sample (Human placenta). In each reaction tube, combined the following components:

2 µl First-Strand cDNA
70 µl Deionized H_2O
10 µl 10X Advantage 2 PCR Buffer
2 µl 50X dNTP Mix
2 µl 5' PCR Primer
2 µl 3' PCR Primer
10 µl 10X GC-Melt Solution
2 µl 50X Advantage 2 Polymerase Mix
100 µl Total volume

Mixed gently by flicking the tube. Centrifuged briefly and placed the tubes in preheated (95°C) thermal cycler. For T3 hot-lid thermal cycler, following program was used:

	95°C	30 sec
20 cycles:	95°C	10 sec
	68°C	6 min + 5 sec increment with each successive cycle
	68°C	5 min
	4°C	Pause

Analyzed a 5-µl aliquot of the PCR product from each sample alongside 1-kb DNA size marker on a 1.2% agarose/EtBr gel. Stored ds cDNA at –20°C until further use.

2.2.6.4 Purification of ds cDNA with a CHROMA SPIN+ TE-400 Column

CHROMA SPIN Columns are packed with resins that fractionate molecules based on size. Molecules larger than the pore size are excluded from the resin and moves quickly through the gel bed when the column is centrifuged, while molecules smaller than the pore size are held back. CHROMA SPIN TE-400 Column was used to select for DNA molecules >200 bp. Swinging bucket rotor used for these columns. Performed the following steps for each experimental and control sample. Inverted the CHROMA SPIN column several times to resuspend the gel matrix completely. Used

one column for each 95 µl cDNA sample. Holding the column upright, grasped the break-away end between the thumb and index finger and snapped off. Placed the end of the spin column into the 2-ml microcentrifuge (collection) tubes, and lifted off the top cap. Centrifuged at 700 x g for 5 min (placed the column-2 ml collection tube into a 15 ml falcon tube for convenient placement in the swinging rotor). Removed spin column and discarded the collection tube and column equilibration buffer. Placed the spin column into the second 2-ml microcentrifuge tube. Carefully and slowly applied the cDNA sample (95 µl) to the center of the gel bed's flat surface. Centrifuged at 700 x g for 5 min. Removed the spin column and collection tube from the rotor and detached them from each other. The purified sample remained at the bottom of the collection tube. At this point combined duplicate experimental samples in a single tube and added the following reagents for cDNA precipitation:

1/10 vol. 3 M Sodium Acetate (pH 4.8)

2.5 vol. 95% ethanol (–20°C)

Mixed gently by rocking the tube back and forth. Placed the tube in –20°C freezer overnight (for better recovery). Centrifuged the tube at 14,000 rpm for 20 min at room temperature. Carefully removed the supernatant with a pipette without disturbing the pellet. Briefly centrifuged the tube to bring all remaining liquid to the bottom. Carefully removed all liquid and allowed the pellet to air dry for ~10 min. Resuspended the pellet in 20 µl of Deionized H_2O and mixed gently. The cDNA obtained was ready for in vivo recombination (Library Construction) with pGADT7-Rec. Store the cDNA at –20°C until used for Two-Hybrid Library Construction.

2.2.6.5 Sequential transformation (Library construction and screening)

To construct AD (Activation Domain) fusion library by in vivo homologous recombination and subsequent library screening in yeast, sequential transformation was done. AH109 was first transformed with DNA-BD/bait protein (C-tail rPAR-2/pGBKT7) using the small-scale yeast transformation protocol and cells containg the DNA-BD/bait protein were selected on SD/-Trp medium. Then the Bait protein containing AH109 (pre-transformed) used for making competent cells and Library scale transformation done with rat retina ds cDNA (CHROMA Spin colume cleaned) and linear pGADT7-Rec vector (sequential transformation).

To prepare competent cells for library transformation, one colony of AH109/bait protein from SD/-Trp plate (~one week old) inoculated in 5 ml of liquid

SD/-Trp medium (to maintain selection pressure) and incubated with shaking at 30°C for 8 h. Then transferred bait containing cell culture to fresh 50 ml SD/-Trp medium in 250 ml flask and continued incubation at 30°C with shaking for 16-20 h (overnight). OD_{600} checked for 0.15-0.3 value. Centrifuged overnight culture at 700 x g for 5 min at room temperature. Discarded the supernatant and resuspended the bait protein containing AH109 cell pellet in 150 ml of YPDA medium. Incubated at 30°C with shaking till the OD_{600} reached 0.4-0.5. Centrifuged at 700 x g for 5 min at room temperature. Discarded supernatant and resuspended cell pellet in 60 ml of sterile H_2O. Repeated the centrifugation step. Discarded the supernatant and resuspended cells in 3 ml of 1x TE/LiAc solution. Resuspension divided into two tubes (1.5 ml each) and centrifuged at high speed for 15 sec. Discarded the supernatant and resuspended each pellet in 600 µl of 1xTE/LiAc solution. Competent cells used immediately for transformation.

Large-scale transformation of AH109/bait protein cells with rat retina ds cDNA and linear pGADT7-Rec plasmid was done. In a sterile 15 ml falcon tube added the following reagents:

20 µl ds cDNA

6.25 µl (3 µg) pGADT7-Rec (Sma-linearized)

20 µl Herring Testes Carrier DNA (10 mg/ml), denatured (100°C for 5 min, then, immediately chilled on ice for 5 min. Repeated two times).

To these, added 600 µl of competent cells (AH109/bait protein) and gently mixed by vortexing. Added 2.5 ml PEG/LiAc solution. Again gently mixed by vortexing. Incubated at 30°C for 45 min. Mixed cells every 15 min. Added 160 µl DMSO, mixed, then placed the tube in 42°C water bath for 20 min. Mixed cells every 10 min. Centrifuged at 700 x g for 5 min. Discarded the supernatant and resuspended the cell pellet in 3 ml of YPD+ medium (specially formulated to promote transformation). Incubated at 30°C with shaking for 90 min. Centrifuged at 700 x g for 5 min. Discarded the supernatant and resuspended in 6 ml of 0.9% NaCl solution. To select for transformants expressing interaction protein, 150 µl of transformation mix plated per 150 mm plate of SD/TDO (triple dropout medium i.e, -Trp-Leu-His) ~40 plates. To determine the transformation efficiency, 30 µl aliquot from 6 ml transformation mix removed and diluted with 720 µl of NaCl solution for a final volume of 750 µl. 150 µl of this diluted solution plated on SD/-LW (3) and SD/-Leu (2) plates. Incubated all the plates up-side down at 30°C until colonies appeared (2-3

days till 6 days). Counted the colonies grown on SD/-Leu plates for No. of transformants/ 3 µg pGADT7-Rec:

No. of colonies x 1000= No. of transformants/ 3 µg pGADT7-Rec

Colonies growing on SD/-LW gave the No. of clones / library:

No. of colonies x 1000= No. of clones screened.

2.2.6.6 Screening for interacting clones

The colonies that grew on the SD/TDO plates (library transformation) after 6 days were streaked on SD/TDO medium again to select for true His+ clones and incubated at 30°C for 5 days. Clones growing on second round of SD/TDO plates were then restreaked on a more stringent medium lacking adenine i.e, SD/QDO (quadruple dropout medium: -Trp-Leu-His-Ade) and incubated at 30°C for 5-7 days to allow for growth of Ade+, His+ clones. The clones grown on SD/QDO plates were used for checking of third reporter gene, lacZ expression by performing Blue/white filter assay on QDO plates. Clones giving either a strong or weak blue color after filter test were picked from second SD/TDO plates and restreaked again on fresh SD/QDO plates and incubated at 30°C for 5-7 days. Blue/white filter test repeated on SD/QDO plates containing true Ade+, His+ clones. The clones which survived the selection for all the three reporter genes after second filter test were used for further analysis. The clones finally selected for further analysis were also restreaked on SD/QDO plates and stored as master plates.

2.2.6.7 Controls for library transformation

For control experiment, competent cells were made in an identical manner and along with competent cells for library transformation from a single colony of AH109 (wild type) picked from YPDA plate (culture grown in in YPDA medium only). One positive and one negative control reaction was done. Added the following components in 1.5 ml centrifuge tubes:

Component	Positive Control (µl)	Negative Control (µl)
SV40 Large T PCR Fragment (25 ng/µl)	5.0	5.0
pGADT7-Rec (Sma I-linearized; 480 ng/µl)	0.52	0.52
pGBKT7-53 (500 ng/µl)	0.5	—
pGBKT7-Lam (500 ng/µl)	—	0.5
Herring Testes Carrier DNA (10 mg/ml), denatured	5	5
AH109 Competent Yeast Cells	50	50
PEG/LiAc Solution	500	500

Mixed thoroughly by gently vortexing. Incubate in a water bath at 30°C for 30 min. Vortexed gently every 15 min. Added 20 µl of DMSO to each tube, mixed, and then placed the tube in a 42°C water bath for 20 min. Vortexed gently every 5 min. Centrifuged at high speed for 15 sec. Removed supernatant and resuspended in 1 ml of YPD + medium. Incubated in a water bath at 30°C for 90 min. Mixed every 15 min by gently vortexing. Centrifuged at high speed for 15 sec. Discarded the supernatant and resuspended in 1 ml of NaCl Solution by gently pipetting up and down. Plated 100 µl of a 1:10, 1:100, and 1:1,000 dilution onto 100-mm SD agar plates:

SD/–Leu/–Trp = To check the cotransformation efficiency

SD/QDO (–Ade/–His/–Leu/–Trp) = To select for cotransformants expressing interacting proteins Incubated the plates at 30°C up-side down for 3–4 days, until colonies appeared. Colonies grown on the SD/QDO were used for blue/white filter assay.

2.2.6.8 Colony-lift Filter Assay

This assay was performed to screen the cotransformants that survived the HIS3 growth selection in a GAL4 two hybrid library screening. Also, the bait protein was tested initially before undergoing library transformation for self-activation and subsequent expression of lacZ reporter gene. The protocol followed was as mentioned in Yeast Protocol Handbook (PT-3024-1). Briefly, Fresh transformed yeast colonies (i.e., grown at 30°C for 2–4 days in appropriate SD dropout medium), 1–3 mm in diameter were used. For each plate of transformants to be assayed, presoaked a sterile Whatman filter by placing it in 2.5–5 ml of Z buffer/X-gal solution in a clean 100- or

150-mm plate. Using forceps, placed a clean, dry filter over the surface of the plate of colonies to be assayed. Gently rubbed the filter with the side of the forceps to help colonies cling to the filter. Made marks on the filter to orient the filter to the agar. When the filter was evenly wetted, carefully lifted it off the agar plate with forceps and transferred it (colonies facing up) to a pool of liquid nitrogen. Using the forceps, completely submerged the filter for 15 sec. After the filter was freezed completely, removed it from the liquid nitrogen and allowed it to thaw at room temperature (the freeze/thaw treatment was necessary to permeabilized the cells.). Then carefully placed the filter, colony side up, on the presoaked filter avoiding trapping of air bubbles under or between the filters. Incubated the filters at 30°C and checked periodically for the appearance of blue colonies. The time taken for colonies to produce β-galactosidase to turn blue varies, typically from 30 min to 8 h in a library screening. Prolonged incubation (>8 hr) may give false positives. Positive control was included in the assay. Identified the β-galactosidase-producing colonies by aligning the filter to the agar plate using the orienting marks.

2.2.7 Yeast Mating

This procedure was done to analyze the protein interaction observed after sequential transformation. Yeast mating is a convenient method of introducing two different plasmids into the same host cells. Reporter gene expression only possible when the AD/library plasmid introduced by mating with the plasmid encoding the DNA-BD/bait protein. For this, transformed AH109 (MATa) with the AD/library plasmids and selected on SD/-Leu and SD/-LH (to check for self-activation of AD/library plasmids). Also transformed Y187 (MATα) with the following three plasmids- empty DNA-BD (pGBKT7), DNA-BD/bait (C-tail rPAR-2/pGBKT7) and pGBKT7-Lam (control) and selected on SD/-Trp. After the Trp+ and Leu+ transformants were ready yeast mating procedure was done in microtiter plate (small-scale):

DNA-BD plasmids ↓	AD/library plasmids →				
Empty DNA-BD	x clone 1	x cl.2	x cl.3	x cl.4	x cl.5
DNA-BD/bait	x clone 1	x cl.2	x cl.3	x cl.4	x cl.5
pGBKT7-Lam	x clone 1	x cl.2	x cl.3	x cl.4	x cl.5

Aliquoted 160 µl of YPDA medium to each well. For each AD/library plasmid to be tested, placed a single transformant colony in a 1.5 ml microfuge tube containing 1 ml YPDA. Vortexed vigrously. For each type of DNA-BD plasmid used, placed several transformant colonies in 3 ml of YPDA medium in a sterile, 10 ml conical tube. Vortexed vigrously. Aliquoted 20 µl of AD/library cell suspension and DNA-BD cell suspension to either horizonzal or vertical wells according to the scheme. In between the pipetting, plate was covered with a sterile lid. Placed the microtiter plate on a platform shaker and incubated at 30°C for ~14 h (required 6-18 h) at 200 rpm. Plated 100 µl of each mating culture on 100 mm SD/-LW plates and SD/TDO plates. Incubated the plates up-side down at 30°C for 3-5 days until the diploid cells formed visible colonies. Diploids were marked for His+ from TDO plates, then filter lifted to SD/QDO plates to check for Ade+ clones. β-gal activity assay (blue/white filter test) was done on SD/QDO plates.

2.2.8 Cell culture

The medium used for culturing of cells was sterile and ready-to-use (Biochrom). For culturing of cells (HEK-293, N2A, NG-108 and RGC-5), frozen cells were thawed in 37°C water bath. 1 ml of cryo-preserved cell suspension and 9 ml of complete cell culture medium centrifuged at 1000 rpm for 3 min at room temperature. Pellet resuspended in tissue culture dish (10 cm) (Nunc, Denmark) and incubated in cell culture incubator (Heraeus) in a humidified atmosphere of 95% air, 5% CO_2 at 37°C. HEK-293 (Human embryonic kidney, epithelial) cells were cultured in DMEM (Dulbecco minimum essential medium) / HAM'S F12 (1:1) with 2 mM Glutamine, 10% FCS (fetal calf serum), 100U/ml Penicillin and 100 µg/ml Streptomycin (Biochrom). Mouse N2A (neuronal) cells were cultured in DMEM containing 3.7 g/L NaHCO3, 4.5 g/L D-glucose, 1.028 g/L N-Acetyl L-alanyl-L-glutamine and 10% FCS, 100U/ml Penicillin, 100 µg/ml Streptomycin. NG-108 (mouse neuroblastoma x rat glioma hybrid cells) were cultured in same culture medium as N2A cells but were

selected for hybridoma cells in HAT supplement (50x) (Hypoxanthine aminopterine thymidine) selection pressure (200 µl HAT used/ 10 cm dish) . RGC-5 cells too were cultured in same complete medium as N2A but in the DMEM containing only 1.0 g/L glucose. Culture medium was changed every 2-3 days.

For cell passage, HEK-293 cells were detached with HBSS without Ca^{2+} and Mg^{2+} (Biochrom) for 5 min at room temperature after the medium was aspirated out; for N2A, NG-108 and RGC-5 cells, first the cells were washed with HBSS and then incubated in cell incubator with Accutase (PAA) 1 ml per 6 cm dish for 5 min at 37°C. Cells were splitted 1:20 to 1:50 in fresh complete medium.

2.2.8.1 Freezing of cells

Cells (either wild type or transfected with fusion protein constructs) were frozen in DMSO and FCS for long storage when not required in culture. Briefly, cells grown in 10 cm culture dish were frozen in 2 cryo tubes (Nunc). To each cryo tube added 50 µl DMSO (sterile, room temperature) and 450 µl fetal calf serum (FCS-37°C). Closed the lid and kept at 4 °C. Meanwhile aspirated out the medium from the cells and pipetted Hanck's medium to dissociate the cells at room temperature (in case of HEK cells, but for N2A cells Accutase used at 37°C). Cells detached from the dish and centrifuged at 1000 rpm for 5 min at room temperature. Discarded the medium and resuspended the cells in 1 ml of appropriate complete culture medium. Transferred 500 µl of cell suspension to each of cryo tube containing DMSO and FCS, mixed well and immediately stored at -20°C for 24 h. Then shifted to -80°C for long storage or liquid nitrogen.

2.2.8.2 Lipotransfection

To express the protein of interest as a fusion protein in mammalian expression system, recombinant plasmid was transfected into mammalian -HEK, N2A, NG-108 and RGC cell lines using the Liposomal transfection reagent DOTAP (Roche Diagnostic). Plasmid DNA was isolated using the Invisorb mini plasmid kit (Invitek, Berlin) to obtain clean DNA. Cells were grown 60-80% confluent. 5-10 µg of DNA made to 50 µl with 20 mM HEPES in a tube (for double transfection 5 µg of each plasmid DNA used). In another tube, 30 µl DOTAP mixed with 70 µl of 20 mM HEPES. Mixed the solutions nicely. Then DNA-HEPES solution was mixed with DOTAP-HEPES solution and incubated for 30 min at room temperature. After 30 min,

5 ml of pre-warmed appropriate culture media (depending on the cell type) without serum and antibiotic taken in a fresh tube and mixed with DNA-DOTAP-HEPES solution. The cells were removed from incubator and medium aspirated out. Transfection media containing DNA-DOTAP-HEPES pipetted into the dish very slowly so as not to detach the cells from the surface of the dish. Cells incubated in the transfection media for 8 h and then full medium containing serum and antibiotic given to cells. 48 h after transfection cells were visualised under the fluorescent microscope to check for expression of fusion protein in case of vector containing GFP tag (GFP fusion protein showed green fluorescence). Cells were made stable transfected after 48 h by giving them G418 Sulphate antibiotic (kanamycin and neomycin derivative) (Calbiochem) at a rate of 1 µl/ ml culture medium of 500 µg/ml (stock- 500 mg/ml). In HA-fusion protein transfection, empty pEGFP vector was used as a carrier DNA since pCMV-HA plasmid contains neither kanamycin nor neomycin resistance gene.

2.2.8.3 Subcloning

Cell were selected for 100% transfection by subcloning. In case of GFP-construct transfected cells, cluster of cells exhibiting high fluorescence selected using a plastic ring and propogated as independent clones in culture under antibiotic pressure. Since it was not possible to visualise MycHis -tag fusion protein, cluster of cells seemingly originating from a single cell were selected in a similar way as GFP-fusion protein and propogated as independent clones under antibiotic selection pressure. HA-tag fusion proteins clones were selected on the basis of carrier GFP fluorescence. Independent clones of MycHis fusion and HA-fusion proteins were verified at the transcription and translation level by RT-PCR and western blot or immunostaining, respectively.

2.2.9 Protein chemistry

2.2.9.1 Cell lysate

To make whole cell lysate for protein measurement and subsequent protein studies, confluent cells (10 cm dish) were washed 1x with ice-cold PBS (1x) and lysed in 1 ml of 1x lysis buffer. The cell lysate was gently mixed on a rotator for 15 min at 4°C. Lysate was then sonificated 3x10 sec (40% power) in Ultrasonificator on ice. Then centrifuged at 14,000 rpm in a pre-cooled centrifuge for 15 min. Supernatant was transferred into a fresh tube and pellet discarded. Protein concentration was determined by Bradford method using 1% bovine serum albumin as standard. Lysate stored at -20°C.

2.2.9.2 SDS-PAGE and immunoblotting

Confluent cells stably transfected with Cryaa-MycHis were lysed in cold 1x lysis buffer and lysate made and measured for protein content. 30 µg of each sample precipitated with ice-cold acetone/methanol solution (1:1), denatured in NuPAGE sample buffer system and were loaded to NuPAGE Novex 10% Bis-Tris Pre-cast gels and electrophoresed for 1.30 min at 120 V. Samples were transferred to nitrocellulose membrane (0.2 µm) using a semi-dry transfer system (Biorad) at a constant voltage (10V) and 200 mA for 40 min at room temperature. Membrane stained for protein bands with 0.2% Ponceau S and then blocked in 5% non-fat dry milk overnight at 4°C. Membrane incubated with monoclonal mouse antibody against myc (1:2500) (Invitrogen) for 1 h at room temperature. Membrane washed three times in PBS+Tween (0.1%) (30 min total). Secondary antibody incubation done with peroxidas-conjugated anti-mouse IgG (1:10,000) (Dianova, Hamburg) for 1 h at room temperature. Washing step repeated. Proteins were visualised with enhance chemiluminiscence (Amersham Pharmacia Biotech).

2.2.9.3 SDS-PAGE and immunoblotting for small size protein

To visualise < 10 kDa protein bands, cell lysate prepared from confluent stably transfected cell in two different ways: Firstly as described above and second, with 1x Laemmli sample buffer. Briefly, cells were lysed directly in 1x Laemmli sample buffer containing β-mercaptoethanol and sonificated three times for 10 sec each (40% power). Then the lysate was denatured for 10 min and centrifuged at 14000 rpm for 10 min in a pre-cooled rotor. To the supernatant added equal volume of chloroform.

Centrifuged as before. Upper phase removed to a fresh tube and protein measured using Bradford assay. 1% bovine serum albumin used as a standard. Samples containing 50 µg protein (acetone/methanol precipitated) or 25 µg chloroform extracted lysate were electrophoresed in a NuPAGE Novex 10% Bis-Tris Pre-cast gel using 1x MES running buffer to resolve small size proteins till 3 kDa. Gel electroblotted using a horizontal transfer system (Tankblot). 0.1 µm nitrocellulose membrane (Protran BA79) used in an electroblot for 1 h at 100 V at 4°C. Protein bands stained with Ponceau S and then incubated in 0.2% Glutaraldehyde at room temperature for 30 min to cross-link small proteins to membrane. 5% non-fat dry milk used for blocking the membrane overnight at 4 °C. Membrane incubated with rabbit polyclonal affinity purified antibody against HA-tag (1:300) (Sigma) for 1 h at room temperature followed by 3x 10 min washing in PBS-Tween (0.1%). Then membrane incubated with peroxidase-conjugated anti-rabbit IgG (1:10,000) for 1 h at room temperature. Washing step repeated. Protein bands visualised by enhanced chemiluminescence (Amersham Pharmacia Biotech).

To successfully transfer small sized proteins, several alternatives tried: 15% pre-cast gel and semi-dry transfer system using nitrocellulose membrane (0.1 µm, 0.2 µm); PVDF membrane (CAPS buffer)-different transfer times (40, 30 and 15 min) and current conditions.

2.2.9.4 SDS PAGE (Laemmli) Gel preparation
(for 2 gels with 1 mm thickness and 8 cm width)

Components	12.5% Resolving gel (ml)	15% Resolving gel (ml)	4% Stacking gel (ml)
60% acrylamide/Bis	2.5	3.0	0.335
Resolving gel buffer	6.0	6.0	-
Stacking gel buffer	-	-	2.5
H_2O	3.3	2.8	2.065
10% SDS solution	0.12	0.12	0.05
1x PER solution	0.06	0.06	0.04
TEMED	0.024	0.024	0.01
Bromophenol blue	-	-	0.002

2.2.9.5 Immunoprecipitation and immunoblotting

Confluent cells (HEK-293) stably transfected with both C-tail PAR2-HA+CryaaMycHis were lysed in 1x lysis buffer and lysate was made and measured as described above. 2 mg of lysate was incubated with 10 µg of rabbit polyclonal affinity purified antibody against HA-tag (Sigma) for 4 h at 4°C and then with 20% protein A-conjugated agarose beads overnight with shaking at 4°C [negative controls also run simultaneously-transfected cells with protein A only (no antibody) and HEK-WT with both antibody and protein A]. Immune complex was washed three times with cold 1x lysis buffer, denatured in 1x Laemmli sample buffer, and resolved in 15% SDS-PAGE. Protein transferred to nitrocellulose membrane (Protran BA79, 0.1 µm) using a semi-dry transfer system (Biorad) at constant voltage (10V) and 200 mA current for 40 min. Protein bands visualised on the membrane by 0.2% Ponceau S. Membrane was blocked in 5% non-fat dry millk (made in PBS-Tween, 0.1%) overnight at 4°C. Membrane incubated with mouse monoclonal antibody against myc (1:2500) (Invitrogen) for 1 h at room temperature. After three rinsed (in total 30 min), membrane incubated with peroxidase-conjugated anti-mouse IgG (1:10,000) (Dianove, Hamburg) for 1 h at room temperature. Washing step repeated and protein was visualised by enhanced chemiluminiscence (Pierce supersignal kit).

2.2.9.6 Silver staining

To visualise < 10 kDa bands protein gel stained using this method since its more sensitive then Ponceau S staining. Electrophoresed gel stored in 10% (v/v) methanol and 5% (v/v) acetic acid solution overnight at 4°C. All subsequent steps performed at room temperature with shaking. Incubated the gel in Fixing solution 2 (5% acetic acid and 10% ethanol solution in H_2O) for 30 min. Then two times for 15 min each in Fixing solution 3 (10% ethanol in H_2O). Coloring solutions always prepared fresh. Incubated in color solution A [25 µl 37% (v/v) Formaldehyde in H_2O, 21 µl 43% (w/v) sodiumthiosulfate in H_2O in 50 ml H_2O] for 60 sec. Washed three times in H_2O. Then incubated in color solution B [25 µl 37% (v/v) Formaldehyde in H_2O, 50 ml 0.2% (w/v) silver nitrate in H_2O] for 6 min. Repeated the washing step (2x). Incubated in color solution C [25 µl 37% (v/v) Formaldehyde in H_2O, 0.5 µl

43% (w/v) sodiumthiosulfate in H_2O, 50 ml 6% (w/v) sodium carbonate] till the desired intensity of color developed. Washed gel two times in H_2O. Finally incubated gel in stop solution [3% (v/v) acetic acid and 5% (v/v) glycerine in H_2O]. Stored in stop solution at 4°C. Scaned the gel and then dried for storage.

2.2.9.7 Stripping of membrane for reprobing

To reprobe the membrane with a second primary antibody this procedure was followed: Washed out enhanced chemiluminiscence solution from membrane by washing in PBS-Tween (0.1%). Incubated in stripping buffer for 30 min at 50°C. Washed extensively in PBS-Tween to remove β-mercaptoethanol from the membrane. Blocked overnight in 5% non-fat dry milk at 4°C. Probed with another primary antibody as described above.

2.2.10 Immunocytochemistry

Cells (wild-type or transfected) cultured on coverglass were fixed in 4% paraformaldehyde for 25 min at room temperature, then washed and stored in PBS. All the following steps were perfomed at room temperature. Fixed cells were blocked and permeabilised in FTP buffer for 1 h. Then incubated in either one or two of the primary antibodies together [mouse monoclonal anti-PAR-2 (SAM-11)-1:100 (Santa Cruz); rabbit polyclonal anti- crystallinA-1:100 (Biomol); mouse monoclonal anti-GFAP-1:2000 (Boehringer); rabbit polyclonal affinity purified anti-HA-1:100 (Sigma); mouse monoclonal anti-myc-1:100 (Invitrogen); mouse monoclonal anti-synaptotagmin-1: 200] for 2 h. Washed the cells 3x10 min in FTP buffer. Secondary antibodies used were fluorescent Alexa IgG [Goat-anti-mouse A_{555}-1:100 and Goat anti-rabbit A_{488}-1:100 (Molecular Probes)] for 2 h. Washing step repeated and in case of Hippocampal astrocytes, nucleus was stained with Hoechst 33342 (1:1000) (Molecular Probes) for 7 min in the last washing step. Cells mounted in SIGMA mounting media and visualised with a LSM510 Confocal laser scanning microscope (Carl Zeiss).

2.2.11 Statistics, NCBI-Blast and expasy search

Statistical evaluation for semi-quantitative expression studies were done using the Student's t-test, and ANOVA with Dunnett post test (compare all columns Vs control column) and $P < 0.05$ was considered significant. Data are given as mean values ± standard error of the mean (SEM).

To search for mRNA, protein and primer homology, NCBI genbank programm-BLAST used. Exon-intron distribution found using NCBI Locuslink programm. Identification of protein done using ExPASy Proteomics tools programm.

3. Results

3.1 Expression of PARs after CNS injury

3.1.1 mRNA expression of the 4 PAR subtypes in the rat developing eye and adult retina

The mRNA expression was studied using semi-quantitative RT-PCR method. For this purpose total RNA was isolated from the tissue and checked for quantity and quality before being processed further. As shown in Figure 3.1, only those RNA samples revealing intense fluorescence bands of 18S and 28S rRNA on ethidium bromide stained 1% agarose/ MOPS gel were used further.

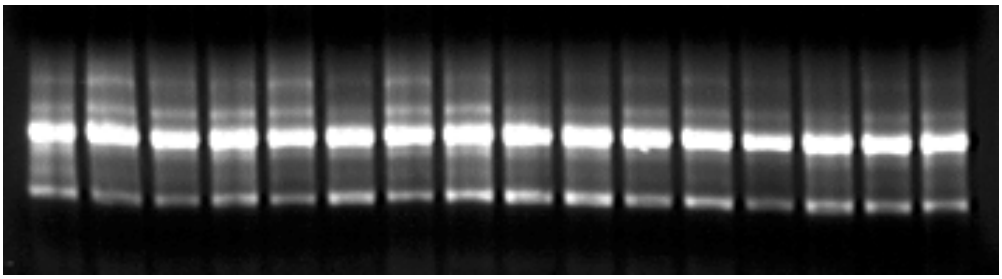

♦

For PCR amplification of the receptor mRNA, gene specific primer pairs were designed from the published rat sequences in the data bank (Table 2.1.12.1 in Materials & Methods). The receptor DNA consists of two exons flanking a very long single intron in the case of PAR-1, PAR-2 and PAR-3, whereas PAR-4 has a very small single intron (Table 3.1). The use of intron-flanking primers in all cases guaranteed that the amplification product was due to mRNA transcript and not to genomic DNA signal. To check this aspect PCR was also carried out with RNA as a starting material and in case of PAR-1, -2 and –3 was negative compared to single band obtained with cDNA. Sequence analysis of the PCR band from cDNA matched completely with the rat sequences published for PAR-1-3 from which the primers were designed. For PAR-4, RNA PCR gave a single band of approximately 850 bp, while with cDNA two bands appeared corresponding to 559 bp and 850 bp (Figure 3.2). On sequencing, PAR-4 PCR band (lower band of 559 bp) matched exactly with the published rat mRNA sequence while PCR band from RNA (850 bp) also gave an in between unmatched sequence of approximately 280 bp corresponding to the small PAR-4 intron. Since it was not

possible to avoid the amplification of 850 bp PAR-4 genomic DNA band during PCR, only the 559 bp mRNA band of PAR-4 considered during analysis of PAR-4 mRNA expression.

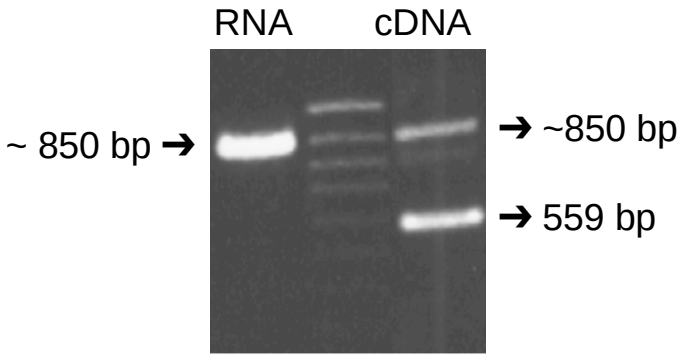

Figure 3.2. PCR with intron-flanking PAR-4 primers. PCR using RNA gave a single band of ~850 bp including the small intron of ~274 bp. cDNA made from the same RNA gave two bands of ~850 bp and 559 bp

Table 3.1 Exon-intron structure of human PARs

Gene	Exon 1	Intron	Exon 2	Chromosome	Reference
PAR-1	1-29 amino acids	22 kb	30-425 amino acids	5q13	Cupit et al, 1999
PAR-2	1-27 amino acids	14 kb	28-397 amino acids	5q13	same
PAR-3	1-22 amino acids	4 kb	23-374 amino acids	5q13	same
PAR-4	1-37 amino acids	274 bp	38-385 amino acids	19p12	Kahn et al, 1998

RT-PCR analysis revealed the presence of mRNA transcripts for all four PAR subtypes in the developing rat eye and adult rat retina. A qualitative estimate of PAR mRNA expression was made in the pup eye at three post-natal stages (P1, P9 and P16). As shown in Table 3.2, PAR-2 and PAR-4 mRNA were clearly expressed in eyes of P1, P9 and P16 animals. While 1 µl cDNA (~ 450 pg) in case of PAR-2 gave a highly pronounced PCR signal (++) in all the 3 stages studied, for the same amount of starting material the PAR-4 signal was moderately detectable (+) in all cases. PAR-1, however, showed a low mRNA expression level in P16 (+/-), since it required 4 µl of cDNA (~

1.8 ng) to achieved a comparable intensity of PCR signal. PAR-1 was highly expressed in P1 and P9 eye (++) using 1 µl cDNA (~ 450 pg). PAR-3 mRNA was expressed at low levels during all the time points studied (+/-), since 5 µl cDNA (~ 2.25 ng) were required for a PCR signal. In adult retina (12 weeks old), PAR-1 mRNA was highly expressed, PAR-2 and PAR-3 were moderately expressed, as compared to low expression of PAR-4.

Table 3.2 Developmental expression of PAR-1-4-mRNA in post-natal rat eyes and adult rat retina. Detection of PARs in P1, P9 and P16 post-natal rat eye and 12 weeks old rat retina by RT-PCR. Expression levels: ++: pronounced signal (1µl cDNA), +: detectable signal (1µl cDNA), +/-: low levels (5µl cDNA). In all the cases cDNA was prepared identically with same amount of total RNA and the same cDNA was used for PCR of all PARs for a particular developmental stage.

Developmental Stage	PAR-1	PAR-2	PAR-3	PAR-4
P1 eye	++ (450 pg)	++ (450 pg)	+/- (2.25 ng)	+ (450 pg)
P9	++ (450 pg)	++ (450 pg)	+/- (2.25 ng)	+ (450 pg)
P16	+/- (1.8 ng)	++ (450 pg)	+/- (2.25 ng)	+ (450 pg)
12 W retina	++	+	+	+/-
Optic nerve	+	+	+	+

3.1.2 the mRNA levels of PAR receptors in retina in response to ONC

Only PAR-1 expression has been studied following nerve injury in the CNS and PNS (Niclou et al., 1998; Citron et al., 2000). In the present study the effect of nerve injury was investigated on the mRNA expression of all 4 receptor subtypes in a partial neurotrauma model. For that purpose, controlled optic nerve crush (ONC) as a model of diffuse axonal injury (Sautter and Sabel, 1993) was used. The mRNA expression pattern of PARs in retina was studied after unilateral ONC using semi-quantitative RT-PCR method. The mRNA levels of all the 4 PAR subtypes altered (upregulated) in both the ipsilateral and contralateral retina as a result of unilateral nerve crush (Figure 3.3 a-d).

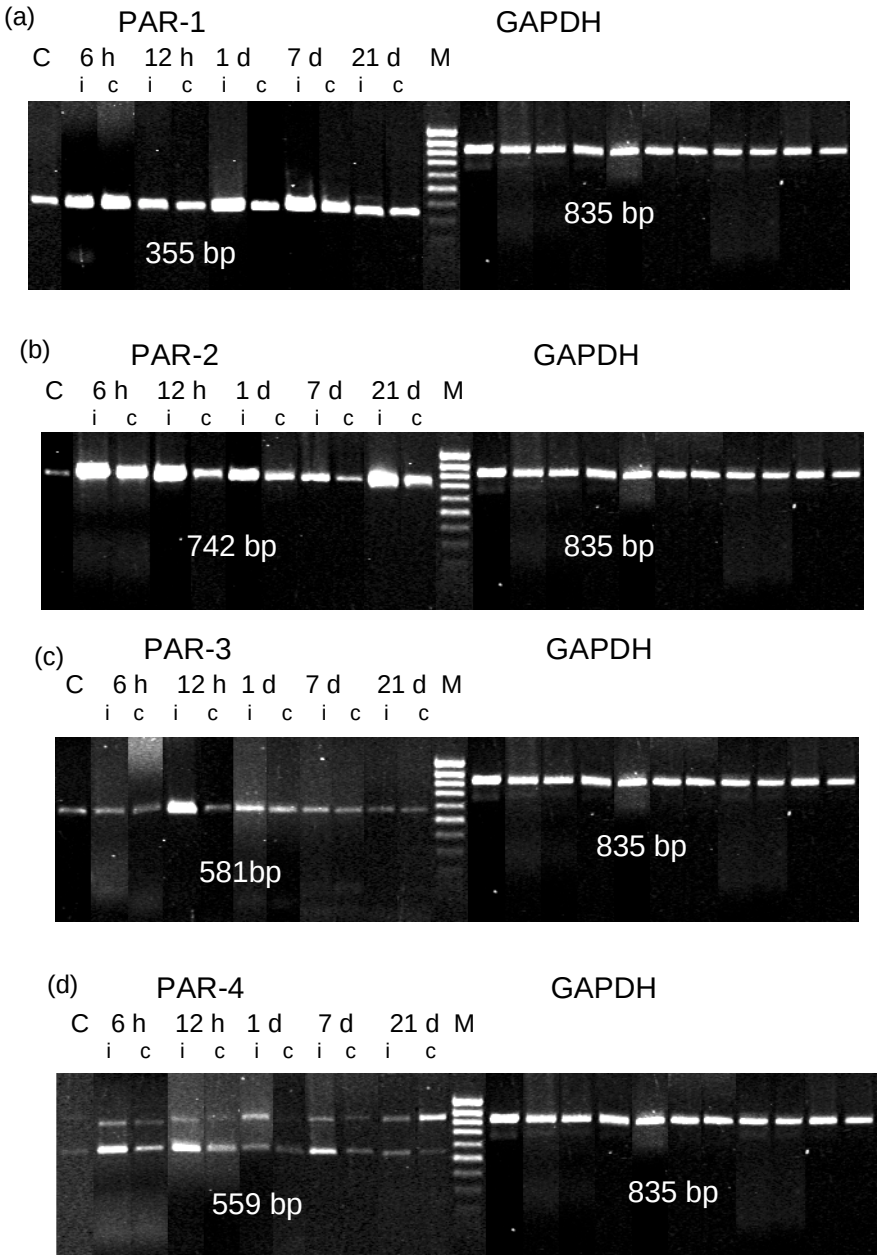

Figure 3.3. RT-PCR detection of PAR-1-4 mRNA expression in retina, control and after ONC. 10 µl of each PCR amplified product was loaded on a 1% agarose gel prestained with ethidium bromide (10 mg/ml). The gels show the mRNA levels of PAR-1(a), PAR-2 (b), PAR-3 (c) and PAR-4 (d) along with GAPDH in control retina (C), and after ONC in ipsilateral (i) and contralateral retina (c) at 6 h, 12 h, 1 d, 7 d and 21 d after crush. Note: In case of PAR-4 only lower 559 bp band considered for mRNA expression analysis.

In retina ipsilaterally injured by ONC, PAR-1 mRNA expression increased moderately (1.5-fold) 6 h after the crush and reached a significantly high, 2.3-fold elevated level on day 7 ($P < 0.001$). By day 21 the mRNA levels were down to 1.2-fold of control values (Fig. 3.4a). Similar to PAR-1 behaviour, PAR-2 mRNA expression increased significantly (1.9-fold; $P < 0.001$) 6 h after the crush, elevated little further to 2.3-fold at 12 h ($P < 0.05$), then decreased to 1.4-fold by the end of one week, but was up to a significantly high value of 1.9-fold ($P < 0.01$) again by day 21 (Fig. 3.4b). PAR-3 mRNA expression remained at basal levels 6 h after the crush, but showed a substantial and significant peak-like increase (2.3-fold; $P < 0.05$) 12 h post-injury, and then declined steadily below the control level at the end of 3 weeks (Fig. 3.4c). Unlike the other PARs, PAR-4 mRNA levels showed a dramatic up-regulation already at 6 h post ONC (3.5- fold; $P < 0.01$) which reached a further peak of 6.1-fold increase at 12 h ($P < 0.001$) and then, just like PAR-1, declined to little above basal levels (1.4-fold) by 21 days (Fig. 3.4d).

In the uninjured contra-lateral retina, surprisingly the mRNA expression for all 4 PAR subtypes was found altered to an extent almost comparably to that of the ipsilateral, injured side. PAR-1 mRNA levels were found elevated (1.8-fold) and remained so till 21 days (1.3-fold; $P < 0.05$) (Fig. 3.5a), similar to PAR-1 mRNA behaviour in the injured side. PAR-2 expression increased significantly (1.8-fold; $P < 0.001$) 6 h after crush and was then maintained elevated around 1.4-fold till day 1 (Fig. 3.5b). On day 7 the mRNA level dropped slightly below basal value but was back at 1.5-fold by day 21 ($P < 0.05$). PAR-3 mRNA levels increased steadily till day 1 and then slowly returned to 0.8-fold of basal levels by day 21 (Fig. 3.5c). In case of PAR-4 the elevated mRNA levels were not as high as found in the crushed injured side, but were still significantly high enough until 12 h (1.9-fold; $P < 0.05$ at 6 h and 2.2-fold; $P < 0.01$ at 12 h), but then a decline pattern excluding day 1 was observed, ending at lower than basal levels by day 21 (Fig. 3.5d).

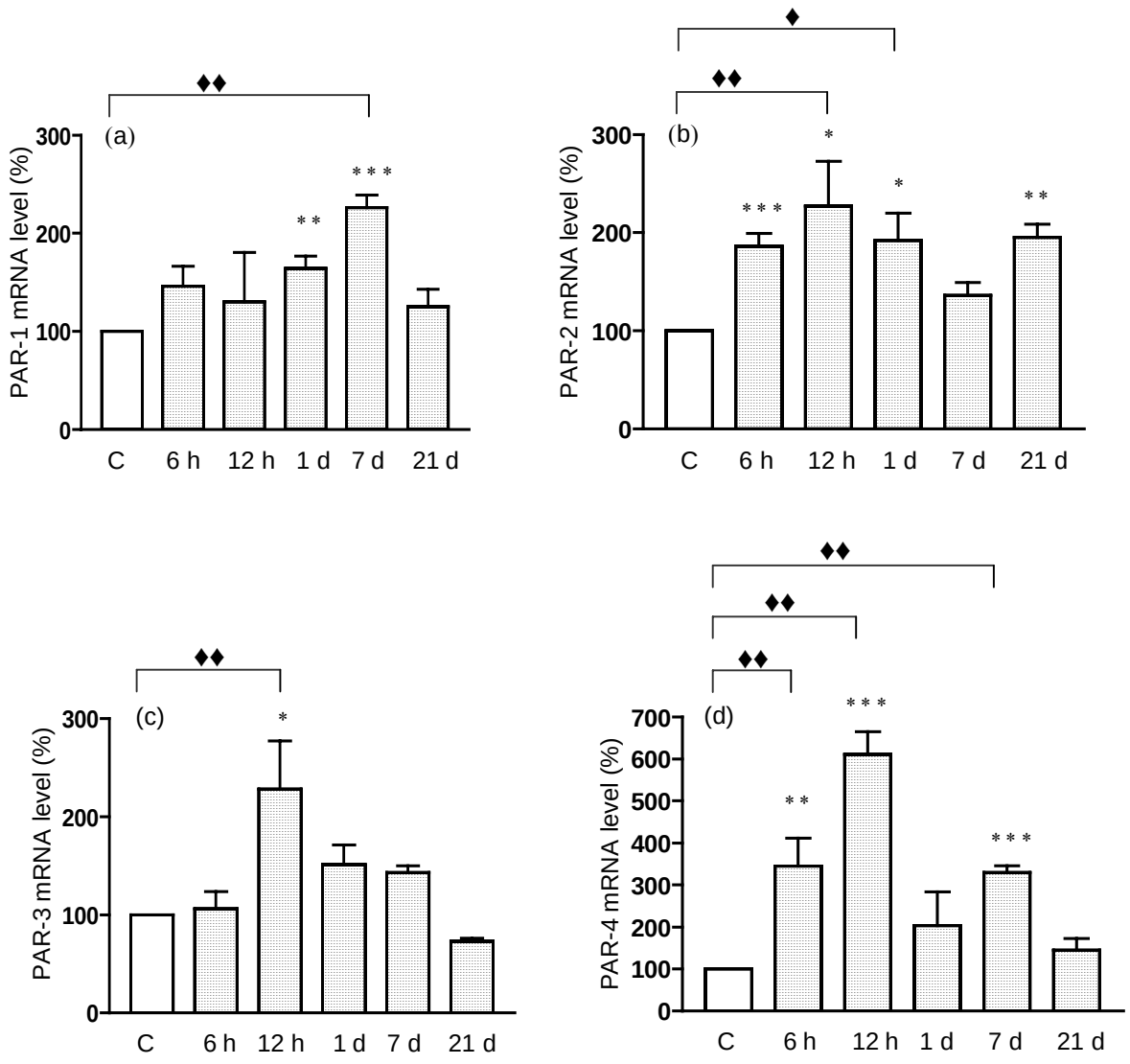

Figure 3.4. Time course of PAR-1 (a), PAR-2 (b), PAR-3 (c) and PAR-4 (d) mRNA expression in retina on ipsilateral injured side after ONC of 12 weeks old rat. Semi-quantitative determination of mRNA level was obtained by densitometric analysis of the PCR product. mRNA signal for each gene was normalized to the GAPDH signal from the same RT product. The expression of the control (untreated) was set as 100%. The PCR data were obtained for each sample and for each gene from two independent experiments and the results were averaged. The cumulative normalized data are presented as mean value ± SEM (n ≥ 3 per group and 1 group corresponds to 2 animals). The statistical significance level (Student t-test: * and Dunnett post test: ♦) for difference from control value is given as *$P < 0.05$, ** $P < 0.01$, *** $P < 0.001$.

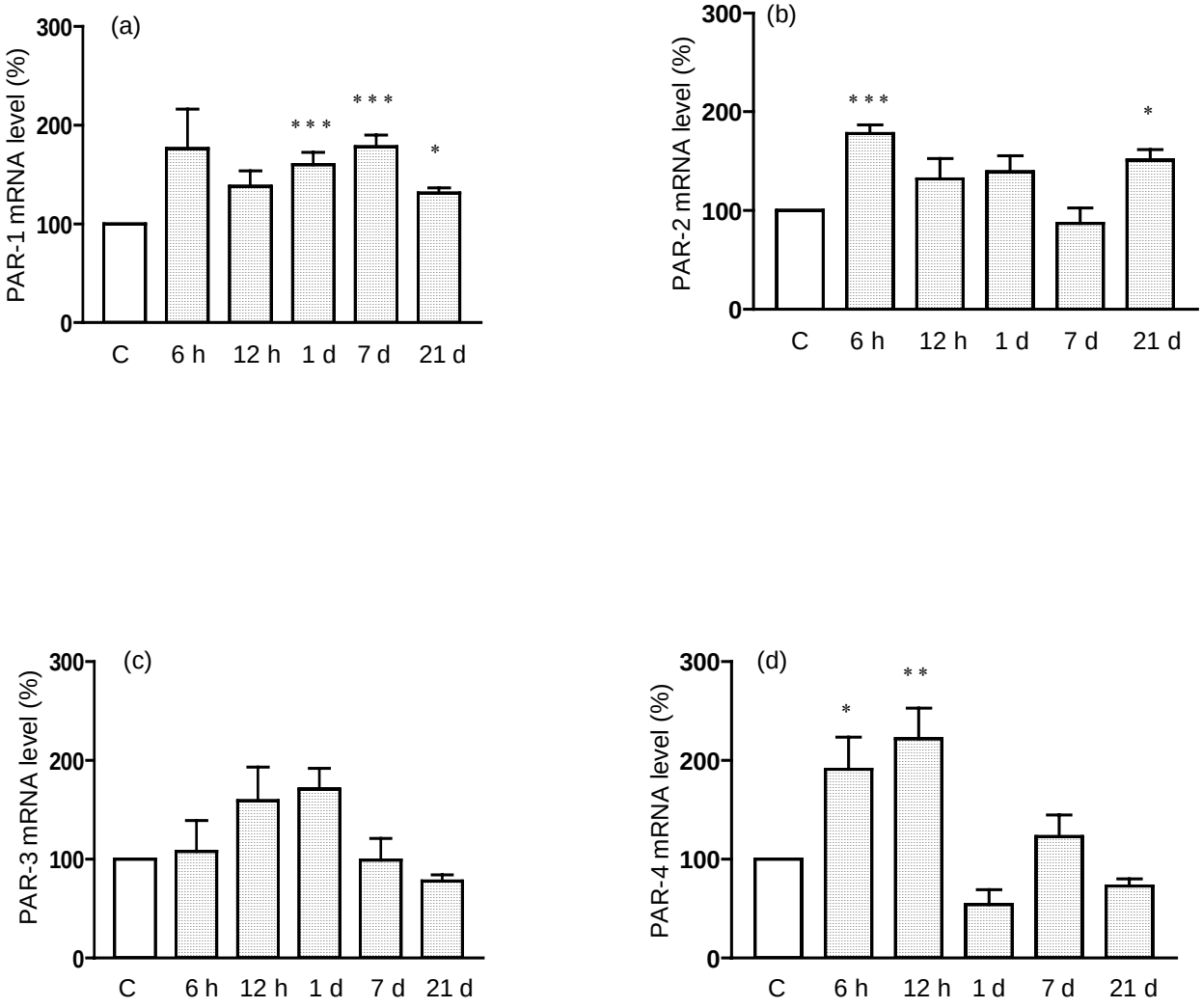

Figure 3.5. Time course of PAR-1 (a), PAR-2 (b), PAR-3 (c) and PAR-4 (d) mRNA expression in the retina on the contralateral uninjured side after ONC. Details as in Figure 3.4

3.1. 3 PAR mRNA levels after transient focal ischemic

To further examine the effect of CNS injury on PAR mRNA expression Endothelin-1-induced focal brain ischemia model was used to asses whether stroke affects the PAR mRNA expression. The change in receptor mRNA expression was assayed by semi-quantitative RT-PCR technique. In the brain of naive animals (control), PAR-1 and PAR-2 mRNA were abundantly expressed, as compared with the moderate expression of PAR-3 and low PAR-4 mRNA levels. Endothelin-1-induced transient focal ischemia in brain near middle cerebral artery (MCA) affects the PAR mRNA expression (Figure 3.6 a-d).

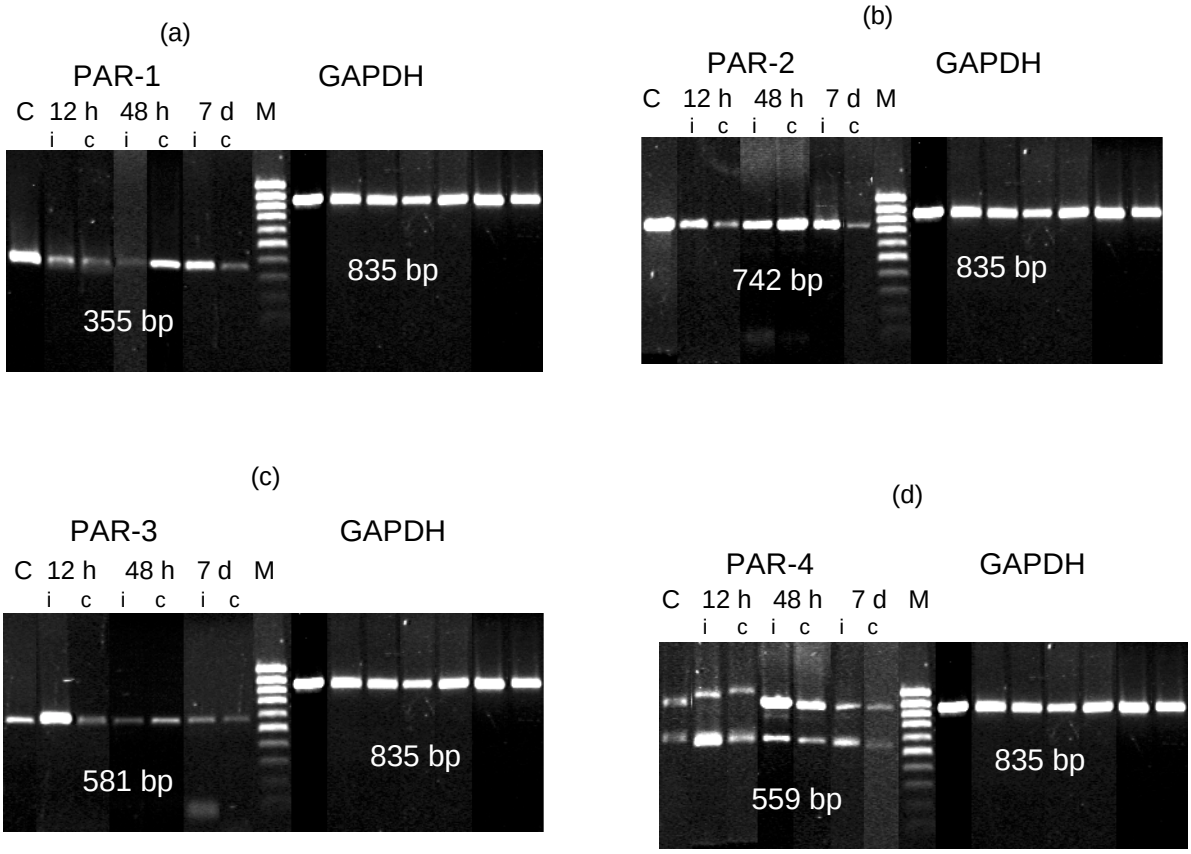

Figure 3.6. RT-PCR detection of PAR-1-4 mRNA expression in rat brain, control (naive), and after transient focal ischemia. 10 µl of each PCR amplified product was loaded on a 1% agarose gel prestained with ethidium bromide (10 mg/ml). The gels show the mRNA levels of PAR-1(a), PAR-2 (b), PAR-3 (c) and PAR-4 (d) along with GAPDH in control (C), and after cerebral ischemia in ipsilateral (i) and contralateral brain hemisphere (c) at 12 h, 48 h, and 7 d after insult. Note: In case of PAR-4 only lower 559 bp band considered for mRNA expression analysis.

Endothelin-induced MCAO yielding focal ischemia results in significant down-regulation of PAR-1 mRNA expression at 12 h after the insult (Fig. 3.6a). Quantitative analysis showed that the mRNA level declined to 0.4-fold of the control value (P<0.05) at 12 h after the insult (Fig. 3.7a). This level further dropped at 48 h after injury to almost negligible values (< 0.1-fold), which was highly significantly reduced (P<0.001). However, PAR-1 showed an upward recovery trend and reached 0.7-fold of control on day 7 (Fig. 3.7a). PAR-2 mRNA expression, like PAR-1, was also down-regulated after the ischemic insult (Fig. 3.6b), but unlike PAR-1, the PAR-2 mRNA levels decreased, but not significantly, and remained static around 0.6-fold during the time course of the study (Fig. 3.7b). PAR-3 showed a transient up-regulation, giving an increase of 1.4-fold at 12 h after injury. Then followed a significant decrease of the PAR-3 mRNA levels to 0.3-fold (P<0.05) at 2 and 7 days after the insult (Fig. 3.7c). PAR-4 mRNA levels were most dramatically increased after endothelin-induced focal ischemia, as compared to the other PARs. PAR-4 mRNA levels increased to a significantly high value of 2.7-fold (P<0.05) at 12 h post-injury and showed a sustained up-regulation (1.5-fold) up to one week following the ischemic insult (Fig. 3.7d). GAPDH expression was used as control standard, because GAPDH remains constant after MCAO in rat (Harrison et al., 2000).

PAR mRNA levels in the contra-lateral hemisphere

Interestingly, also in the contra-lateral brain hemisphere PAR-1, -2 and -3 all revealed a change in mRNA expression patterns. The mRNA levels of all three receptor subtypes were down-regulated to 0.5-fold or less at 12 h after ischemia (P<0.05- 0.001) and then underwent a brief recovery period up to the 48 h time point, but subsequently declined to 0.2–0.3-fold on day 7 after injury (P<0.05-0.01), as shown in Fig. 3.8a, b, c. Hence, the mRNA levels for PAR-1, -2 and –3 were found to be substantially reduced in the contra-lateral brain region. In case of PAR-1 (0.37-fold) and PAR-2 (0.5-fold), the decrease in mRNA levels was as high as in the ipsilateral ischemic hemisphere. PAR-4 mRNA behaved differently. Unlike the other three PAR subtypes in the contra-lateral side, the PAR-4 mRNA levels showed a slight up-regulation of 1.2-fold at 12 h and maintained this increased level until 48 h, but then declined to 0.4-fold (P<0.01) one week after ischemia (Fig. 3.8d).

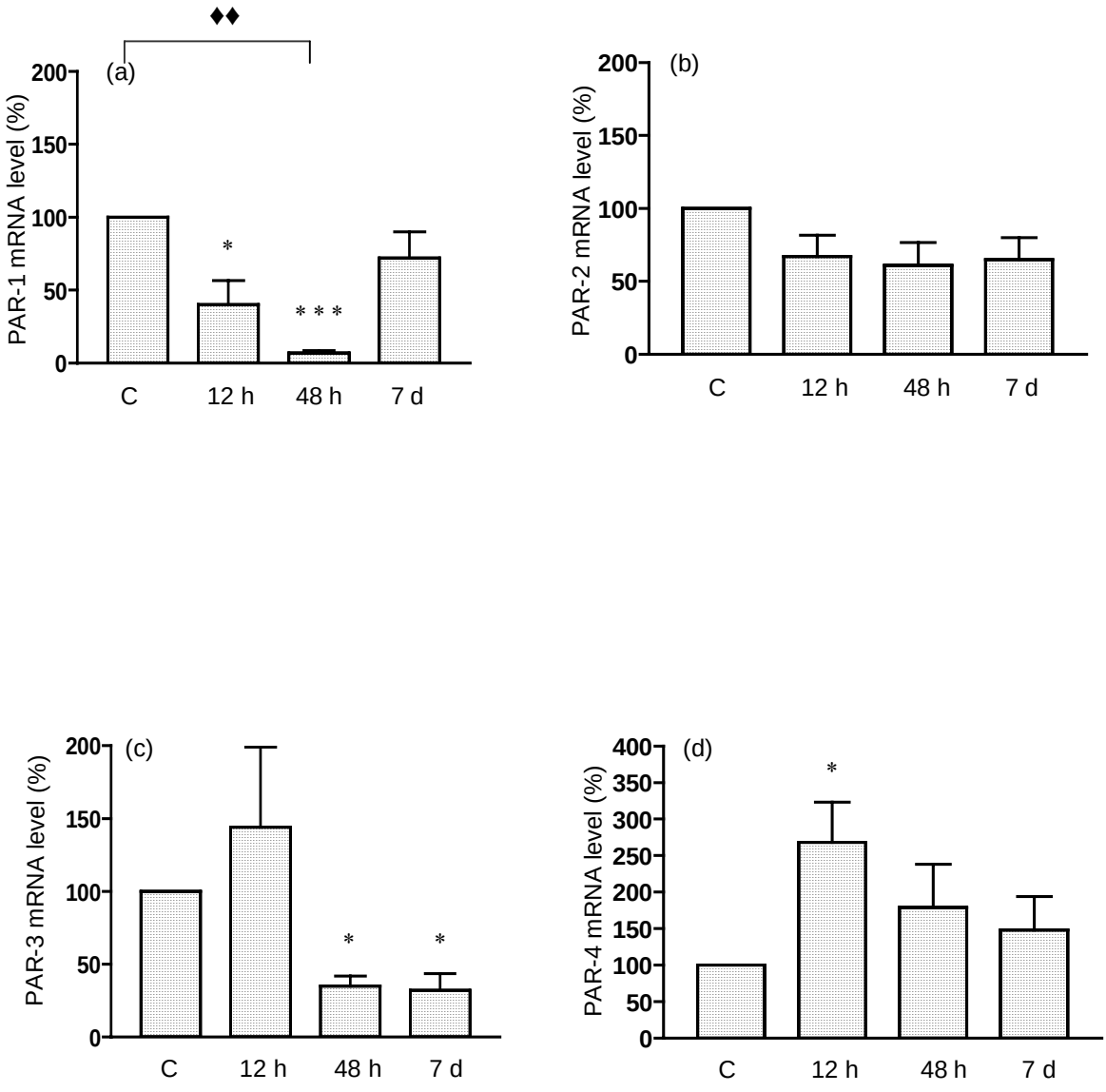

Figure 3.7. Time course of PAR-1 (a), PAR-2 (b), PAR-3 (c) and PAR-4 (d) mRNA expression in the ipsilateral ischemic hemisphere of rat brain after endothelin-1-induced transient focal ischemia. Semi-quantitative determination of mRNA level was obtained by densitometric analysis of the PCR product. mRNA signal for each gene was normalized to the GAPDH signal from the same RT product. The expression of the control (naive) was set as 100%. The PCR data were obtained for each sample and for each gene from two independent experiments and the results were averaged. The cumulative normalized data are presented as mean value ± SEM ($n \geq 3$ per group). The statistical significance level (Student t-test: * and Dunnett post test: ♦) for difference from control value is given as $*P < 0.05$, $** P < 0.01$, $*** P < 0.001$.

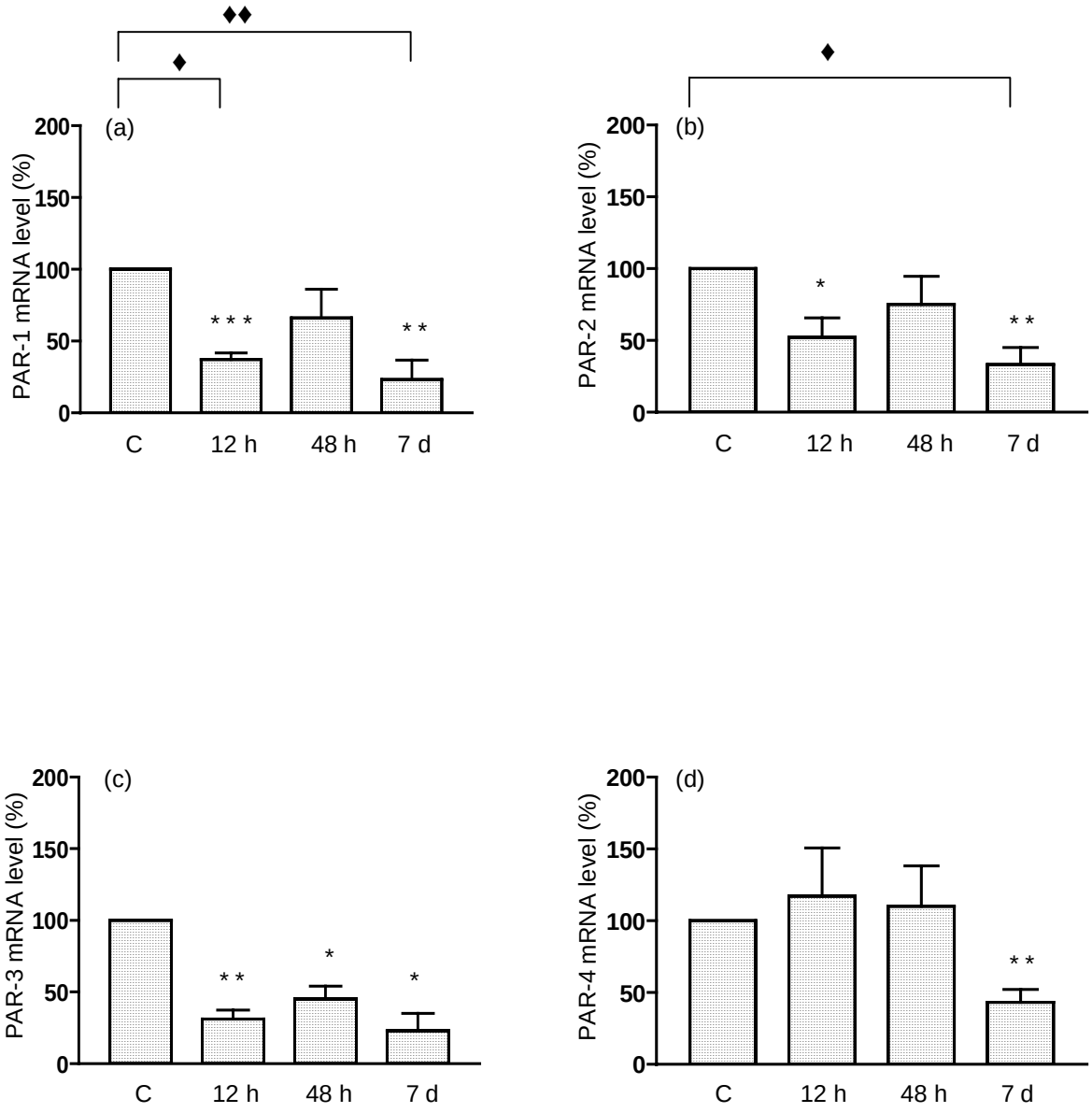

Figure 3.8. Time course of PAR-1 (a), PAR-2 (b), PAR-3 (c) and PAR-4 (d) mRNA expression in the contra-lateral uninjured hemisphere after endothelin-induced *in vivo* transient focal ischemia. Details as in Figure 3.7.

3.2 Identification of a putative interacting protein for PAR-2 using yeast two hybrid system

3.2.1 Construction of DNA-BD/bait fusion protein

To identify a protein which interacts with PAR-2 and thus may be involved in PAR-2 signalling pathway, yeast two hybrid screening was performed with a self-made library. Since PAR-2 is a 7-transmembrane domain G protein-coupled receptor only the C-terminus of the receptor was cloned into the yeast expression plasmid to generate a DNA-BD/bait fusion protein. For this, rat PAR-2 C-tail (Accession No. U61373) from base 1042 until 1197 base, corresponding to 50 amino acids was used. The 152 bp C-tail of rat PAR-2 was cloned between Eco RI and Bam HI restriction sites of yeast DNA-BD vector pGBKT7. Cloning sites and start codon were incorporated before the 1042 bases of the fragment (Figure 3.9) via primers designed for PCR amplifying the C-tail fragment of PAR-2 from rat brain RNA. Since the GAL4 DNA-BD is upstream of pGBKT7 MCS, the original stop codon of the PAR-2 insert was not mutated and used as such. Both the pGBKT7 and C-tail PAR-2 fragment which was generated by PCR were digested, ligated and subsequently transformed into E.coli XL1 blue competent cells. Positive transformants containing the fusion protein were grown under kanamycin selection pressure. The correct sequence of the fusion protein was verified by DNA sequencing. The cloning resulted in a DNA-BD/bait fusion protein containing C-tail of PAR-2 (50 amino acids).

5'GAATTC ATG TCGAAAGATTTCAGGGACCAGGCCAGAAACGCGCTCCTCTG
Eco RI Start ↑ 1042 base

CCGAAGCGTCGCACCGTGAAACGCATGCAGATATCGCTCACCTCCAACAAG
TTCTCCAGGAAATCCAGCTCTTACTCCTCCAGCTCAACCAGTGTTAAAACCT

CCTAC**TGA**GCT **GGATCC-3'**

Stop ↑ Bam HI

1197 base

Figure 3.9. Cloning strategy to create DNA-BD/bait fusion protein. Cloning sites and start codon were incorporated via primers (Table 2.1.12.2 in Materials & Methods) into the PAR-2 fragment. The C-tail PAR-2 fragment was PCR amplified (186 bp) from rat brain, digested and sticky-end ligated into pGBKT7 plasmid having compatible restriction sites. Bacterial transformants were selected for fusion protein by kanamycin selection.

3.2.2 Checking of yeast strains

Yeast strains required for the present work (AH109 and Y187) were checked for proper growth on complete YPDA and several amino acid dropout (DO) media.

3.2.3 Checking of DNA-BD/fusion protein for toxicity

To check if the bait fusion protein is toxic to the yeast strains or not, first both the empty DNA-BD vector and fusion protein were transformed into AH109 and Y187 strains and plated on minimal medium lacking tryptophan (SD/-Trp), since pGBKT7 plasmid can synthesise tryptophan on its own. Growth on SD/-Trp medium was used as a selection marker for pGBKT7 plasmid. Well grown transformed colonies from both the empty plasmid and fusion protein were grown in liquid SD/-Trp culture under kanamycin pressure. Comparison of OD_{600} showed that the DNA-BD/bait fusion protein is not toxic to yeast. The growth rate of fusion protein containing Y187 was slower as compared to transformed AH109 strain.

3.2.4 Checking of DNA-BD/bait fusion protein for transcriptional activation

Since the bait fusion protein should be able to initiate transcription of reporter genes on yeast chromosome only when it was interacting with a protein fused to Activation domain (AD) plasmid, it was important to verify, whether the bait fusion protein was capable of transcriptional activation by itself or not. For this purpose AH109 and Y187 were co-transformed with bait fusion protein and empty AD plasmid (several combinations) as shown in Table 3.3 and plated on different DO media to check for transcriptional activation.

Table 3.3 Testing of bait fusion protein for transcriptional activation. Yeast strains were either single transformed with bait fusion protein, or co-transformed with empty AD plasmid to check if either of the plasmids by itself or in combination could activate the transcription of the reporter genes. Self-activation by bait fusion protein was tested on SD/-HW since bait fusion protein on its own cannot grow in medium lacking histidine. Presence of both the DNA-BD and AD plasmid was checked on SD/-LW (since DNA-BD can grow on –Trp medium and AD plasmid can grow on –Leu medium). To check transcriptional activation with empty AD plasmid, were transformants plated on SD/ -AWLH since growth on -AWLH medium indicates reporter gene expression (His and Ade) and hence probable interaction between the plasmids. Positive blue test indicates expression of 3rd reporter gene, lacZ. +: growth of transformed yeast; negative: no growth of transformed yeast; inactive: negative for transcriptional activation.

AH 109 and Y187 were transformed with the following ↓	SD/-Trp (-W)	SD/-Leu (-L)	SD/-Leu-Trp (-LW)	SD/-Trp-His (-WH)	SD/-Ade-Trp-Leu-His (-AWLH)	Blue/white filter test for lac Z gene	Conclusion
Empty DNA-BD (pGBKT7)	+		negative	negative			
DNA-BD/bait fusion protein (C-tail-PAR-2-pGBKT7)	+		negative	negative	negative		Bait fusion protein inactive
Empty DNA-BD + Sma I-linear AD (pGADT7-Rec)		+	+		negative		inactive
DNA-BD/bait fusion protein + linear AD vector		+	+		negative		inactive
DNA-BD/bait fusion protein + linear AD vector + control PCR fragment		+	+		negative		inactive
Positive control			+		+	+	

The series of experiments, as described in Table 3.3, verified that DNA-BD/bait fusion protein cannot initiate transcriptional activation of reporter genes by itself or together with empty linear AD plasmid.

3.2.5 Generation of ds cDNA for library construction

To fish out a probable interacting protein for PAR-2, a cDNA library was generated as an AD fusion library in yeast utilising in vivo homologous recombination technique. Rat retina PolyA+ RNA (from Clontech, Heidelberg, Germany) was used for generating cDNA library. Quality of PolyA+ RNA was checked on agarose/MOPS gel along with the control tissue ie., Human placenta PolyA+ RNA. Intact PolyA+ RNA both from retina and human placenta (1 µg each) used for synthesising First-Strand cDNA using random primer and SMART III oligonucleotides (as described in Materials & Methods). Use of random primers made sure that the resulting cDNA contained a variety of 5' and 3'-end sequences in equal proportion due to the ability of the random primer to hybridise to many different sequences on the RNA template. Use of SMART III oligonucleotide during cDNA synthesis resulted in generation of ss cDNAs with an anchor sequence, which served as a universal priming site in the subsequent amplification by long-distance PCR. 2 µl of first-strand cDNA used for each LD-PCR reaction. As recommended, LD-PCR was performed for 20 cycles to reduce the generation of non-specific PCR products. 5 µl aliquot of the PCR product was checked on 1.2% agarose gel prestained with ethidium bromide. As expected, the LD-PCR product appeared as a smear on the gel. The ds cDNA was purified using the CHROMA SPIN+TE-400 column. This column allowed retention of DNA molecules >200 bp. For precipitation, the purified ds cDNA recovered from 2 columns (each started with 95 µl of cDNA sample) mixed and processed further. The DNA pellet was resuspended in deionized H_2O and used for in vivo recombination with pGADT7-Rec to generate the AD fusion library in yeast. The steps performed to generate the ds cDNA are outlined in Figure 3.10.

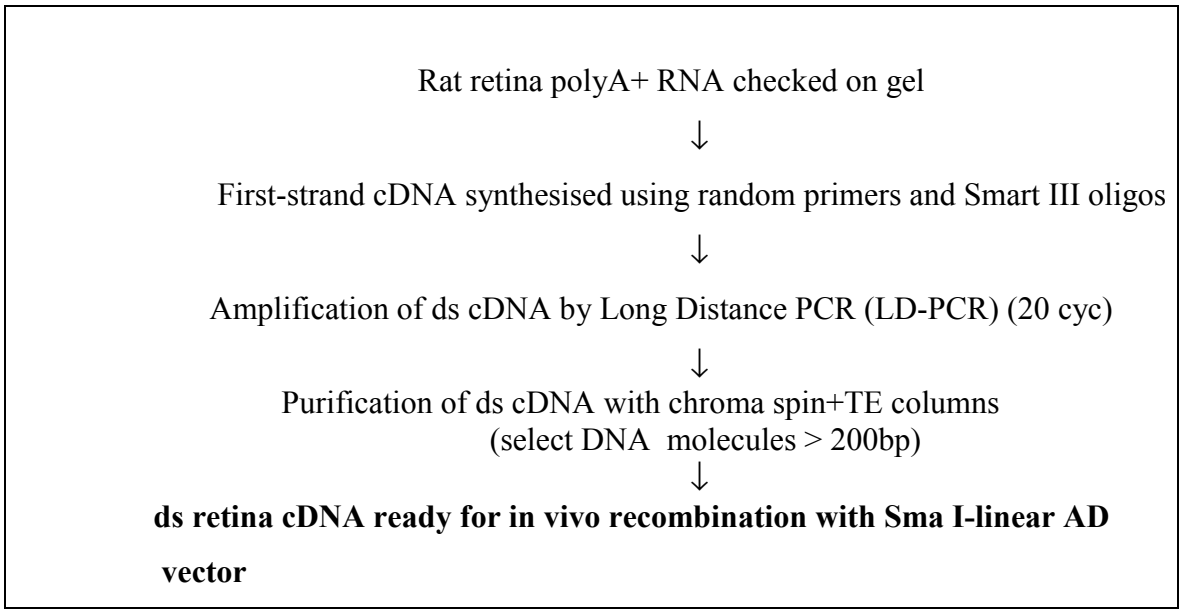

Figure 3.10. Schematic presentation of steps performed to generate ds cDNA from retina for library construction. Details with regard to experimental procedure explained in Materials & Methods.

3.2.6 Construction and Screening of AD fusion library

To construct the AD fusion library and subsequent screening for interacting clones sequential transformation was performed. For this AH109 competent cells were transformed with DNA-BD/bait fusion protein and positive transformants were selected on SD/-Trp medium. Then competent cells from the pre-transformed AH109 (with DNA-BD/bait fusion protein) were made. For this the pre-transformed AH109 was grown in SD/-Trp medium to maintain selection pressure for the recombinant plasmid. These AH109 competent cells were then re-transformed with ds cDNA from retina and Sma I-linear AD plasmid i.e, pGADT7-Rec. Hence AH109 cells were sequentially transformed in the first step with bait fusion protein and then the bait containing cells re-transformed with ds cDNA and linear AD plasmid. In vivo homologous recombination between ds cDNA and Sma I-linear AD vector in yeast resulted in a recircularized AD fusion library plasmid.

Transformants were plated on Triple dropout medium (SD/-TDO ie., -Trp-Leu-His) to select for probable interacting clones. Transformants plated on SD/-Leu gave a transformation efficiency 0.6 x 10^6 transformants / 3µg AD vector and on SD/-Leu/-Trp gave the number of clones screened, which was calculated to be 3.86 x 10^5 clones /

library. The values obtained matched closely with the expected numbers. Simultaneously both the positive and negative controls performed.

Sequential transformation and subsequent library screening gave 336 big clones and 252 small clones on TDO plates. To eliminate false-positive clones initial 588 clones were picked completely from the source and restreaked in a grid fashion on fresh TDO plates. All except 27 clones grew on restreaked TDO plates. To further eliminate false-positive the 561 clones were streaked on a more stringent dropout media lacking adenine also to check for Ade+ clones. Clones lacking ability to grow in –Ade conditions turned pink and subsequently red. Hence the 561 clones streaked on Quadruple Dropout Medium (QDO ie., -Ade-Trp-Leu-His). To further select the clones positive for all 3 reporter genes (Ade+, His+, lacZ) 3rd reporter gene ie., lacZ selection made by performing β-gal filter lift assay. Colonies grown on QDO plates were filter lifted and incubated with X-gal, a substrate for β-galactosidase. LacZ+ colonies turned blue while negative remained white. From 561 clones only 13 clones turned blue within 4 hrs while 98 more turned blue after longer incubation time (8-12 hrs). For further verification all the 111 blue clones were fresh restreaked on QDO plates and blue/white filter test was performed for the second time. In second round 38 clones turned blue within 5 hrs while 27 more were tentative blue after a little longer. 3 clones from the first round of filter test were negative second time around (Figure 3.11). The 65 positive clones after initial library screening were then verified further to identify the probable interacting protein or proteins for PAR-2.

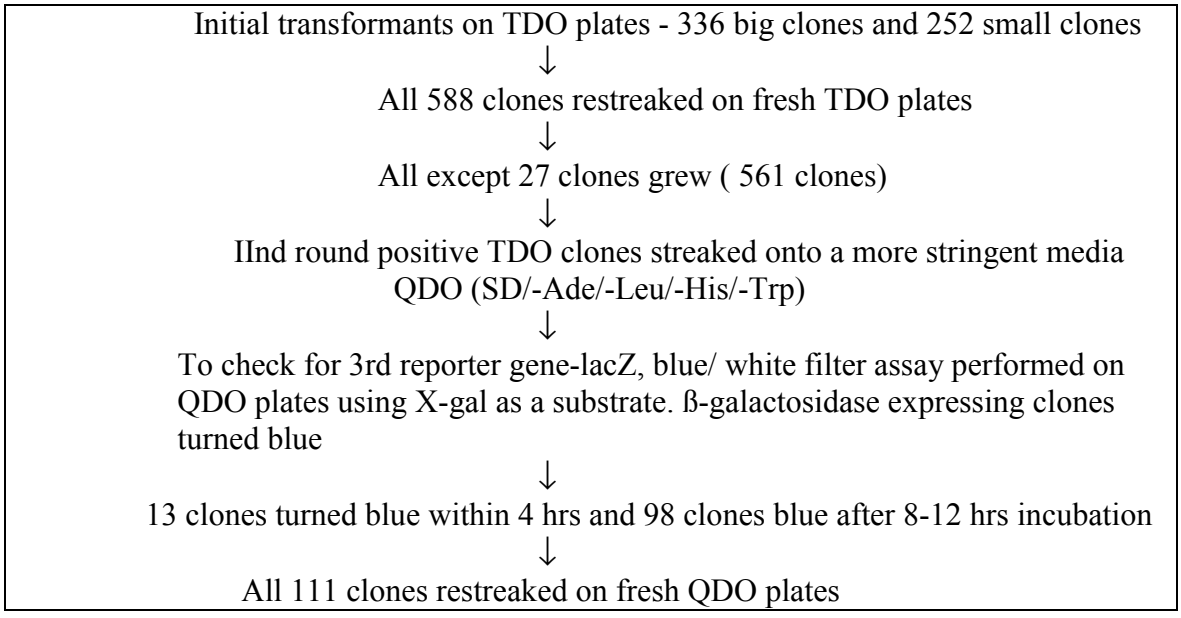

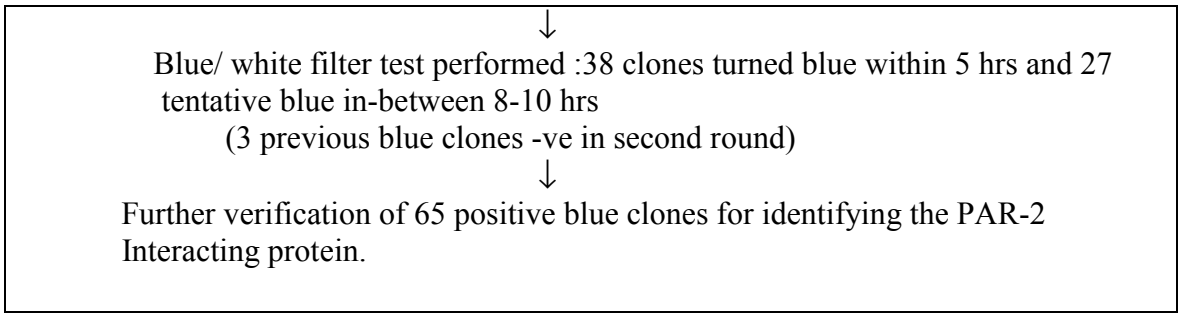

Figure 3.11. Schematic presentation of library screening results.

3.2.7 Analysis of positive clones

Positive yeast clones were grown in SD/-Leu medium to select for AD library plasmids and subsequent plasmid isolation. Plasmid DNA isolated from yeast is always contaminated with genomic DNA due to breakage of yeast chromosome during isolation procedure resulting in low plasmid yields. Hence yeast plasmid DNA is not pure enough for direct sequence or restriction digestion analysis but sufficient to transform E.coli. The isolated yeast plasmid DNA were electroporated into E.coli electro-competent cells and transformants were grown under ampicillin selection pressure to select for AD/library plasmids. Plasmid DNA was isolated from transformed bacteria and restriction digested with Hind III enzyme (since pGADT7-Rec contains 2 Hind III sites) to look for the presence of same AD/library plasmid or inserts. For restriction digestion, 4-2 bacterial clones were checked from each transformed AD/library plasmid. To identify the insert in positive AD/library plasmid, DNA isolated from E.coli was sequenced using the Matchmaker 5' and 3' AD LD-insert screening amplimers. Sequences were checked for probable homology at both the nucleotide and protein levels. Out of 65 positive blue clones only 27 clones gave a meaningful sequence homology both at nucleotide and protein level as described in Table 3.4.

Table 3.4 Nucleotide and Protein homology of positive AD/library plasmid clones. AD/library clones positive for all the 3 reporter gene assay in yeast were further analysed by sequencing after transformation in bacteria.

YTH clone	Nucleotide and Protein homology (rat)	Nucleotide Gene bank Accession number
3/9 B	Crystallin α polypeptide A mRNA (Cryaa)	NM_012534
4/3 A	ATPase, Na+/ K+ transporting, β 2 polypeptide (Atp1b2) mRNA	NM_012507
6/2 A	Iron-regulatory protein 2 (Ireb 2) (Aconitate hydratase or Aconitase)	NM_022863
6/5 D	Glyceraldehyde-3-phosphate dehydrogenase (GAPDH)	XM_216453
6/8 A	Glyceraldehyde-3-phosphate dehydrogenase (GAPDH)	XM_216453
2/2 B	Fibronectin 1 or fibronectin precursor (Fn1)	NM_019143
11/21 A	Polyubiquitin mRNA	NM_138895
12/8 C	Crystallin, α-polypeptide 2 (Cryab)	NM_012935
16/1 B	Crystallin, α-polypeptide A (Cryaa)	NM_012534
20/2 A	Procollagen, type I, alpha 2 (Colla 2)	NM_053356
22/11 B	Cytoplasmic- gamma isoform of actin mRNA And Cytoplasmic β actin (Actx), mRNA	X52815 And NM031144
25/12 A	Crystallin, α polypeptide A (Cryaa), mRNA	NM_012534
33/3 A	Galectin-related inter-fiber protein (Grifin), mRNA (lectin, galactoside-binding)	NM057187
33/20 B	(clone gamma-3) ATP synthase gamma-subunit (ATP5c) mRNA, 3' end cds	L19927
34/19 B	Crystallin, α polypeptide A (Cryaa), mRNA	NM_012534
4/14 A	Mitochrondrial ATP synthase beta subunit mRNA	M19044
6/6 A	Alpha-tubulin (Tuba 1), mRNA	NM022298
11/6 A	mRNA for MEGF8 (multiple EGF-like motifs)	AB011534
17/8 B	Galectin-related inter-fiber protein (Grifin), mRNA	NM057187
23/1 A	Crystallin, α polypeptide A (Cryaa), mRNA	NM_012534
29/11 B	Prohibitin (Phb) mRNA	NM_031851
30/4 A	Myosin heavy polypeptide 3, skeletal muscle, embryonic (Myh3), mRNA And	NM_012604 And

	mRNA for alpha cardiac myosin heavy chain	X15938
30/5 A	Crystallin, α polypeptide A (Cryaa), mRNA	NM_012534
25/3 A	Mitochrondrial ATP synthase beta subunit mRNA And F1-ATPase subunit (beta) mRNA, 3'end	M19044 And M57634
27/19 A	mRNA for MHC class I cell-surface antigen, A1 (F) alpha chain	X99767
23/3 B	Protein phosphatase 2A B regulatory subunit delta isoform mRNA	AF180350
23/3 C	Procollagen, type I, alpha 2 (Colla 2)	NM_053356

3.2.8 Yeast mating

27 clones giving a meaningful nucleotide and protein homology were retested for protein interaction by mating in yeast. For this the DNA/BD-bait fusion protein was transformed in Y187 (Mat α and AD/library plasmids isolated from bacteria were retransformed into AH109 (Mat a) as described in material and methods and selected on SD/-Trp and SD/-Leu respectively. Each AD/library plasmid was mated with DNA/BD-bait fusion protein, empty DNA/BD plasmid and a control plasmid DNA/BD plasmid (pGBKT7-Lam). Diploids were selected on SD/-LW and screened for interaction on TDO and QDO medium. Clones from QDO plates were tested for blue/white filter assay for β-galactosidase (Figure. 3.12).

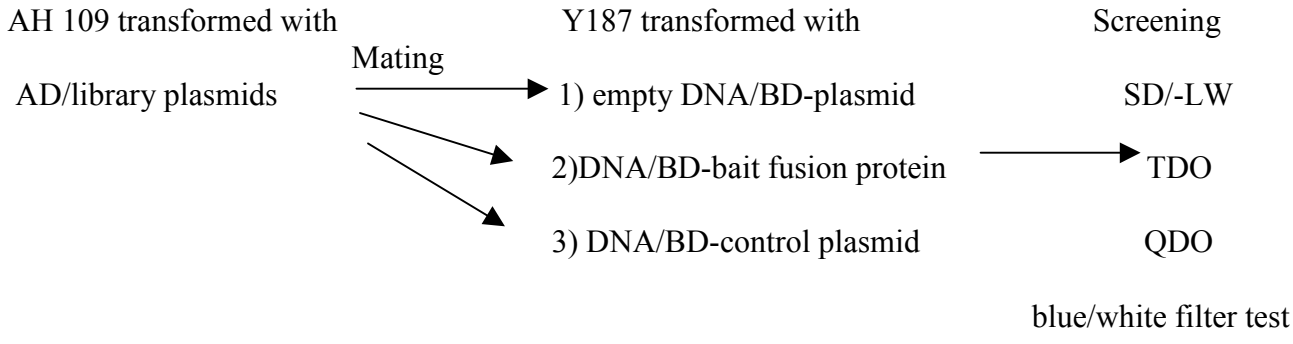

Figure 3.12. Schematic presentation of mating procedure in yeast and subsequent screening for positive clones.

Of the 27 AD/library clones only 1 clone ie., cl. 34/19 B was positive for all 3 reporter gene expression ie., Ade+, His+ and lacZ+ when mated with DNA/BD-bait fusion protein and not with empty or control DNA/BD plasmid.

3.2.9 Identification of the positive clone after mating

Clone 34/19 B was identified as rat crystallin, α̃ polypeptide A (Cryaa) mRNA both at nucleotide and protein level (Table 3.4).

TTTTTTGGGANCCATNNTTNTTNCTTTAATACGACTCACTATAGGGCGAGCG

↓

CCGCC**ATG**GAGTACCCATACGACGTACCAGATTACGCTCATATGGCCATGG
AGGCCAGTGAATTCCACCCAAGCAGTGGGTATCAACGCAGAGTGGGCCATT
ATGGCCGGG**C**ACCATCCAGCACCCTTGGTTCAAGCGCGCCCTGGGGCCCTT
CTACCCCAGCCCGATGTTCGACCAGTTCTTCGGCGAGGGCCTTTTTGAATAC
GACCTGCTTGCCCTTCCTGTCTTCCACCATCAGCCCTTACTACCGGCCAGTCT
CTCTTCCGACAGTGTTGGACTCCGGCATCTTCTGAGGTCCGATCTTGACCGG
GACAAGTTGGCATCTTCTTGGATGTGAAGCACTTNTNTCTGAGGACCCACCG
TGAAGGACTGGAANATTCGTGGAAATCATGGCAACCACAGAGGCAGGATG
ACATGNTNATTTNCCGGAATTACGNCGTNCCGTTGCTTCAAGNGACATCCGC
TTCTGTCTTGTGGGATGATGTACTTTTGGCCAAGGCATTGGTTGATCTGCNA
NAAAGGCTTCCGTNCGAGNAACATTGNCTNCTAAGCTNTGN

Figure 3.13. Sequence of AD/library clone 34/19 B using Matchmaker 5' AD LD-insert screening amplimer. ↓ shows the *in vitro* START site of pGADT7-Rec, underlined nucleotides show the homologous recombination site between pGADT7-Rec and SMART III oligo of cDNA followed by bp 21 (in bold) of AD clone 34/19 B ie., rat α̃-crystallin A nucleotide sequence.

As mentioned in Table 3.4, six AD/library clones gave α̃-Crystallin A protein on sequencing. Since only 1 clone ie., 34/19 B was positive after mating, all 6 clones representing the same α–crystallin A protein were checked for their fragment size in AD/library plasmid (Table 3.5).

Table 3.5 Comparison of fragment size of AD/library clones representing a-crystallin A protein.

AD/library clones of α-crystallin A	Fragment size of α-crystallin A in AD clones (from - till base of available nucleotide sequence)	Fragment size of α-crystallin A in AD clones (in amino acids)
3/9 B	9-361	116
16/1 B	9-367	118
25/12 A	63-330	89
34/19 B	21-955	170
23/1 A	15-363	116
30/5 A	15-370	118

3.2.10 Checking of a-crystallin A clones

Sequence analysis of 6 α-crystallin A clones obtained with Matchmaker 5' AD LD-insert screening amplimer showed two different kinds of patterns. In case of AD clones 34/19 B, 25/12 A and 30/5 A the homologous recombination site between pGADT7-Rec and SMART III oligo of cDNA was immediatelyfollowed by α-crystallin A sequence in-frame. In clones 3/9 B, 16/1 B and 23/1 A the homologous recombination site was followed by ~45-70 bp corresponding to unknown sequence and then in-frame α-crystallin A nucleotide sequence followed.

To recheck for positive clones within the 6 α-crystallin A clones, three of the clones including the positive one from the mating round (25/12 A, **34/19 B** and 30/5 A) were checked for interaction with DNA-BD/bait fusion protein both by sequential transformation and mating. For this the AD/library plasmid DNA was amplified by PCR using the Matchmaker 5' and 3' AD LD-insert screening amplimers. AD/library plasmid DNA (α-crystallin A) and Sma-I-linear pGADT7 were co-transformed in DNA/BD-bait fusion protein containing AH109. For mating, AD/library plasmid DNA (α-crystallin A) and Sma-I-linear pGADT7 were transformed in AH109 and then mated with DNA/BD-bait fusion protein containing Y187. In both cases empty DNA/BD plasmid was used as a control. To check for transcriptional activation by AD/library clones itself, AH109 transformed with the AD/library plasmid PCR DNA and Sma-I-

linear pGADT7 were also plated on SD/-LH and were found to be negative indicating that AD/library clones cannot activate transcription of reporter gene Histidine by itself. Sequential transformation and mating transformants were screened for positive interaction on SD/-LW, TDO, QDO plates and blue/ white filter assay as described earlier in the section for library screening. Only PCR DNA fragment of 34/19 B was found to be positive for all the 3 reporter gene assays with DNA/BD-fusion protein in case of both sequential transformation and mating. For verification of the clone, plasmid DNA of 34/19 B isolated from yeast, electro-transformed into bacteria and sequenced. Sequencing of clone 34/19 B gave the original mRNA and protein sequence.

These experiments with different clones of α-crystallin A gave only clone 34/19 B as positive similar to mating results obtained with different AD/library clones. Databank search about α-crystallin A showed that the protein has a coding region spanning from 13-534 bases ie., 522 bps and 174 amino acids.

3.2.11 Checking for interaction with PAR-2 cytoplasmic loops

Since PAR-2 is a 7-transmembrane domain receptor with 3 cytoplasmic loops apart from the C-terminus region it was important to verify if the interaction observed between C-terminus PAR-2 and AD/library clone 34/19 B was confined to C-tail only or whether clone 34/19 B could interact with cytoplasmic loops as well, since interaction between the third cytoplasmic loop of PARs and G-proteins is known (Chen et al., 2001). For this, rat PAR-2 cytoplasmic loops, Cl-2 (21 amino acids) and Cl-3 (23 amino acids) were cloned between Eco RI and Bam HI site of DNA/BD vector pGBKT7 similar to C-tail fusion protein (this cloning was done by (ATG: biosynthetics, Freiburg, Germany) but sequences of the Cl-2/DNA/BD-fusion protein and Cl-3/DNA/BD fusion protein were verified (Figure 3.14). The Cl-2 and Cl-3 DNA/BD fusion proteins were mated with 3 α-crystallin A clones (25/12 A, 34/19 B and 30/5 A). Appropriate controls were also performed. Mating mixture was screened for all 3 reporter gene expressions. Both the Cl-2 and Cl-3 DNA/BD fusion proteins were found to be negative for all the reporter genes. From these experiments AD/library clone 34/19 ie., α-crystallin A came out as an interacting protein for C-tail of PAR-2 and this interaction seemed to be confined to only the C-tail of PAR-2 and not with PAR-2 cytoplasmic loops.

(A)

5'**GAATTC**GTGCAGAGGTACTGGGTGATCGTGAACCCCATGGGACACTCCAG
GAAGAGGGCCAACATCGCTTAA**GGATCC**-3'

(B)

5'**GAATTC**ATCAAAACGCTCCGCTCTTCCGCCATGGACGAGCACTCGGAGAA
GAAAAGGCGGAGGGCTATCCGCCTCTAA**GGATCC**-3'

Figure 3.14. Cloning strategy of rat PAR-2 cytoplasmic loop 2 and 3. (A) shows the nucleotide sequence of Cl-2 (511-573 bp), and (B) shows the nucleotide sequence of Cl-3 (796-864 bp). In both cases double stranded nucleotide oligos were synthesised and cloned between Eco RI and Bam HI of pGBKT7 plasmid by ATG: biosynthetics, Freiburg, Germany.

3.2.12 Checking for presence of α-crystallin A in different tissues, cell types and cell lines

After identification of a putative interacting protein for C-tail of PAR-2 in yeast, our next step was to identify the tissues and cell types where it occurs under normal conditions. For this, PCR primers were designed (Materials & Methods) from the published nucleotide sequence of rat α-crystallin A and also α-crystallin B isoform (since α-crystallin B is ubiquitously present and shares a high sequence homology with the A isoform). Using the standard RT-PCR technique several tissues, cell types and cell lines were checked for the presence of both isoforms of α-crystallin (Figure 3.15)

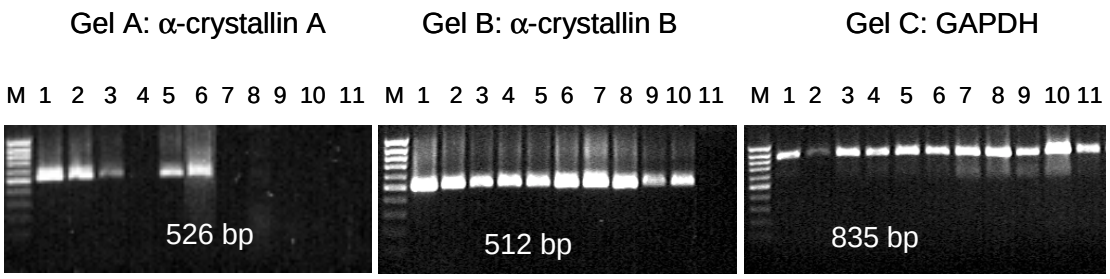

Figure 3.15. Detection of α-crystallin A, α-crystallin B and GAPDH mRNA expression in tissues and cell types. RT-PCR performed to detect presence of α-crystallin A and α-crystallin B in several tissues, cell types and cell lines. Gel A: α-crystallin A, Gel B: α-crystallin B and Gel C: GAPDH. Same cDNA was used for PCRs. Lane 1: retina, lane 2: optic nerve, lane 3: brain, lane 4: Hippocampal neurons, lane 5: Hippocampal astrocytes, lane 6: whole brain astrocytes, lane 7: retinal ganglion cell line (RGC), lane 8:oligodendrocyte cell line (OLN-93), lane 9: N2A cell line, lane 10: mouse neuroblastoma x rat glioma hybrid cell line (NG-108), lane 11: human embryonic kidney cell line (HEK). M: 1 kb DNA ladder.

Table 3.6 Summary of RT-PCR for α-crystallin A and B isoform in different tissues, cell types and cell lines.

Tissue or cell type	α-crystallin A	α-crystallin B
Retina (total RNA and poly A+ mRNA)	+	+
Optic nerve	+	+
Brain	+	+
Rat hippocampal neuronal culture (primary)	-	+
Rat hippocampal astrocyte culture (primary)	+	+
Rat whole brain astrocyte culture (primary)	+	+
Rat retinal ganglion cell line (RGC)	-	+
Rat oligodendrocyte cell line (OLN 93)	-	+
Rat N2A cell line	-	+
NG108 cell line (mouse neuroblastoma x rat glioma hybrid)	-	+

RT-PCR analysis of several tissues showed the presence of α-crystallin A mRNA to be abundant in retina and optic nerve, while it is also expressed in brain. Among the cell types checked it is expressed by rat hippocampal astrocytes and whole brain astrocytes (primary cultures), but not by hippocampal neurons since primary neuronal cultures (mixed) were negative for RT-PCR. Among the cell lines rat RGC and N2A cell lines which are both neuronal were also negative for the α-crystallin A mRNA. Rat oligodendrocyte cell line (OLN-93) and neuroblastoma x glioma hybrid cell line (NG108) too were negative. HEK which is a human epithelial cell line was also

found negative but this may be due to the fact that rat α-crystallin A primers were used for PCR. α-crystallin B isoform was however expressed by all tissues and cell types except HEK (as summarised in Table 3.6).

Primary cultures of rat whole brain astrocytes, hippocampal astrocytes and neurons were also checked by immunocytochemistry for the presence of α-crystallin A (Figure 3.16).

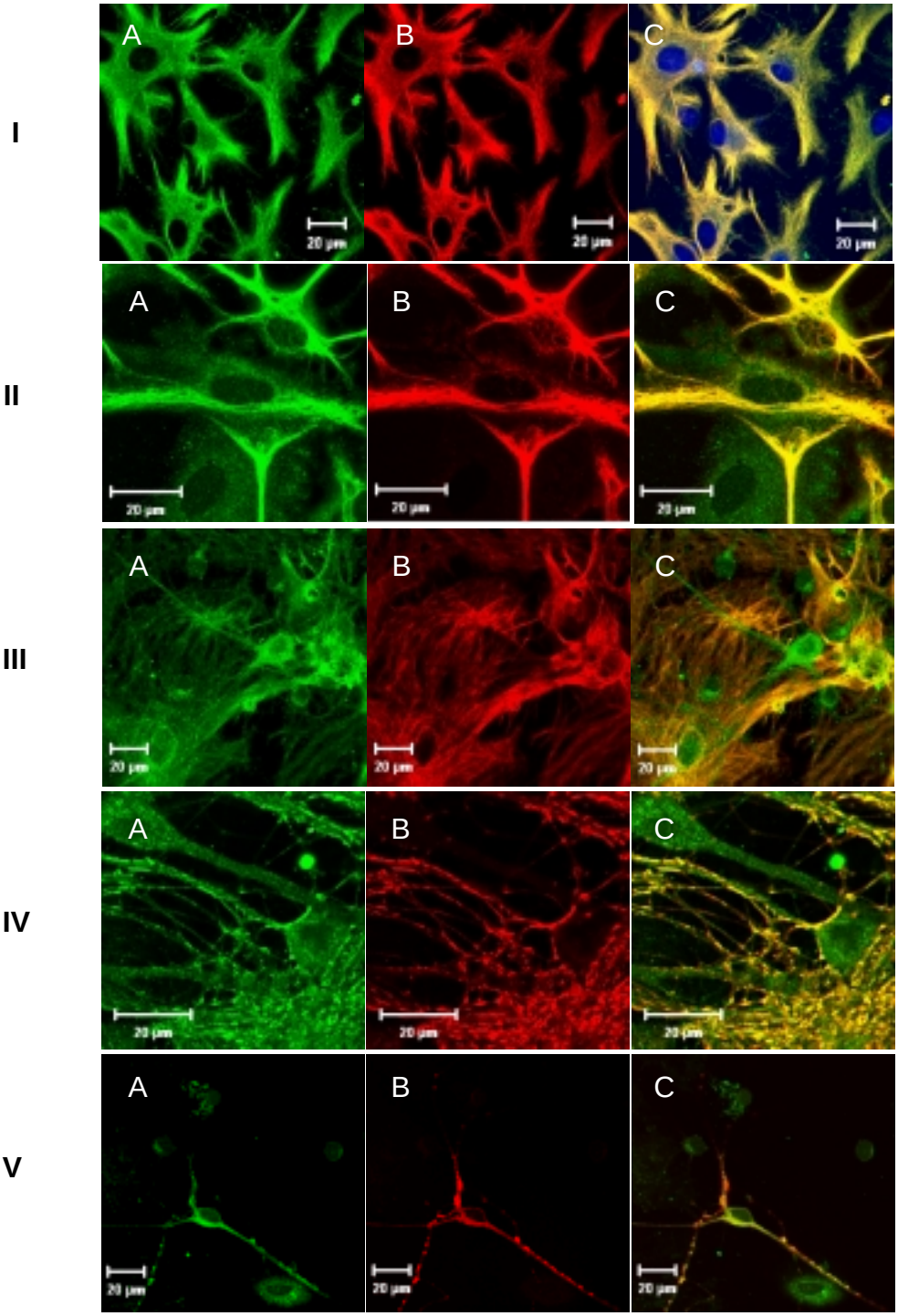

Figure 3.16: Detection of a-crystallin A by immunocytochemistry in primary cultures of rat hippocampal astrocytes (I), whole brain astrocytes (II), and hippocampal neurons (mixed) (III, IV, V). I-V (A): cells were stained for the presence of α-crystallin A using specific antibody (1:100). Fluorescent detection with Alexa A_{488} (green). I-III (B): cells were stained for the presence of GFAP (astrocytic marker) (1:2000) and IV-V (B) with synaptotagmin (neuronal marker) (1:200) using specific antibody. Fluorescent detection with Alexa A_{555} (red). I-V (C): co-localisation of both proteins in cells. Hippocampal astrocytes were also stained with Hoechst for nuclear staining.

Immunocytochemical analysis of the primary cultures showed the presence of α-crystallin A in hippocampal astrocytes (Figure 3.16-I) and whole brain astrocytes (Figure 3.16-II) (co-localised with astrocytic marker-GFAP). Hippocampal neuronal cultures (mixed) stained positive for α-crystallin A (co-localised both with astrocytic marker-GFAP and neuronal marker-synaptotagmin) (Figure 3.16-III, IV and V), unlike the negative RT-PCR results.

3.2.13 Generation of PAR-2 and α-crystallin A fusion proteins

The next step in confirming the interaction observed between the C-tail of rat PAR-2 and its putative interacting protein α-crystallin A in yeast was to recheck the interaction either in prokaryotic or eukaryotic expression systems. A eukaryotic expression system was selected since in mammalian cells, proteins are more likely to be in their native conformations with appropriate post-translational modification and, therefore, results represent biologically significant interactions. To this end rat PAR-2 and α -crystallin A were cloned into several mammalian expression vectors with tag as fusion proteins (Table 3.7).

Table 3.7 List of PAR-2 and α-crystallin A fusion proteins with several expression vectors suitable for mammalian cell culture systems. The gene fragments of interest were amplified by PCR (primers in Material & Method) from rat brain. In all cases the sequence of the fusion protein was verified by sequencing. Normally for transfection 5 µg of plasmid DNA was used but in unsuccessful cases even 10 µg plasmid were tried for transfection. Cells were made stable with fusion protein constructs under suitable antibiotic selection pressure.

Gene	Cloning vector	Restriction sites	Cell lines used for transfection	Transfection results
Full PAR-2	pEGFP-N1	Xho I & Hind III	HEK & N2A	successful
			NG 108 & RBL	unsuccessful
Full PAR-2	pDsRed2-N1	Xho I & Hind III	HEK & RBL	unsuccessful
C-tail PAR-2 (subcloned from pGBKT7)	pCMV-HA	Sfi I & Sal I	HEK (with empty pEGFP-N1 as carrier DNA)	successful
C-tail PAR-2 (subcloned from pGBKT7)	pEGFP-C2	Eco RI & Bam HI	HEK	successful
Full α-crystallin A	pEGFP-N1	Xho I & Hind III	N2A RGC	successful unsuccessful
Full α-crystallin A	pDsRed2-N1	Xho I & Hind III	HEK & RBL	unsuccessful
Full α-crystallin A	pcDNA3.1/Myc-His (B)	Bam HI & Eco RV	HEK	successful
α-crystallin A Domain 1 (CD1)	pcDNA3.1/Myc-His (B)	Bam HI & Eco RV	HEK	successful
α-crystallin A Domain 2 (CD2)	pcDNA3.1/Myc-His (B)	Bam HI & Eco RV	HEK	successful

3.2.14 Cellular localisation of PAR-2 and α-crystallin A

The first step in confirming the interaction outside of the yeast system was to localise both proteins in cells since for any biological interaction to be feasible in a

natural system both proteins should be either in the same cellular compartment or localised in adjacent cell compartments. For this purpose full rat PAR-2-pEGFP-N1 was stably transfected in HEK and N2A cells. PAR-2 fusion protein was localised on the basis of green fluorescence of the GFP vector. Before transfection, wild type cells were checked for endogenous receptor expression. HEK cells endogenously expresses PAR-2, while N2A cells do not. In both HEK and N2A cells, PAR-2-GFP fusion protein could be localised to the plasma membrane with little cytoplasmic distribution, as previously described (Dery et al., 1999) (Figure 3.17 a and 3.17 b).

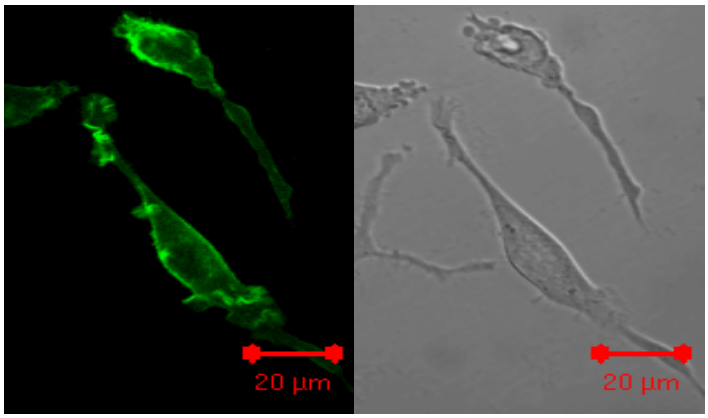

Figure 3.17 a. Subcellular localisation of PAR-2-GFP in N2A cells. Full rat PAR-2 -GFP construct was stably transfected into N2A cells (rat neuronal cells). Membrane localisation of fusion protein detected by GFP fluorescence on confocal laser scanning microscope.

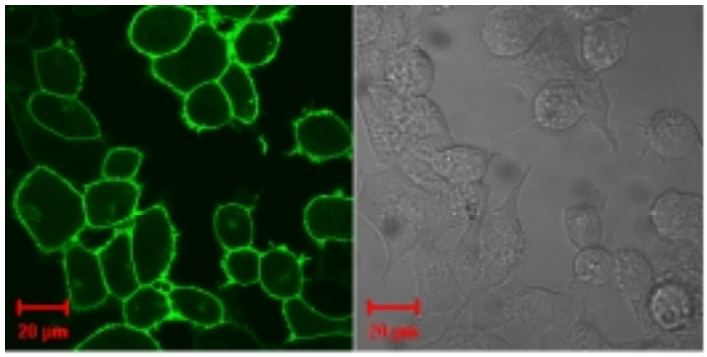

Figure 3.17 b. Subcellular localisation of PAR-2-GFP in HEK cells. Full rat PAR-2 -GFP construct was stably transfected into HEK cells (human embryonic kidney epithelial cells). Membrane localisation of fusion protein detected by GFP fluorescence on confocal laser scanning microscope.

α-crystallin A-pEGFP-N1 fusion protein was stably transfected in N2A cells and green fluorescence of the fusion protein could be localised to the cytosol excluding the

nucleus (Deretic et al., 1994) (Figure 3.17 c). α-crystallin A-MycHis construct stably transfected in HEK cells on immunostaining with anti-myc antibody gave similar cytosolic distribution of α-crystallin A as pEGFP-N1 construct in N2A cells (Figure 3.17 d).

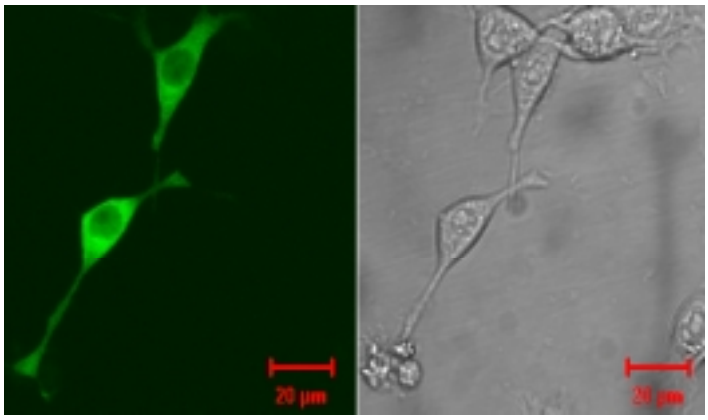

Figure 3.17 c. Subcellular localisation of α-crystallin A-GFP in N2A cells. Full rat α-crystallin A-GFP construct was stably transfected into N2A cells (rat neuronal cells). Cytosolic localisation of fusion protein detected by GFP fluorescence on confocal laser scanning microscope.

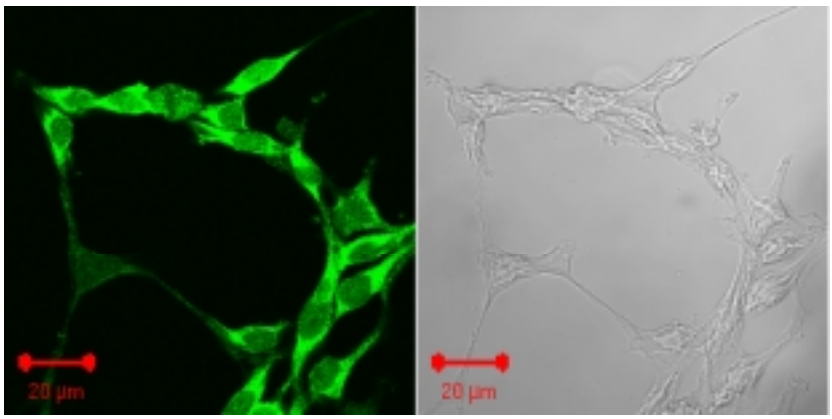

Figure 3.17 d. Subcellular localisation of α-crystallin A-MycHis in HEK cells. Full rat a-crystallin A -MycHis construct was stably transfected into HEK cells. Subcellular localisation of a-crystallin A was detected by immunostaining with mouse monoclonal anti-myc antibody (1:100). Alexa 488 anti-mouse IgG (1:100) depicting green fluorescence of a-crystallin A cytosolic distribution in the cell on confocal laser scanning microscope.

3.2.15 Checking for expression of non-fluorescent fusion protein in mammalian cell culture system

Before proceeding for any biochemical assay to confirm PAR-2 and α-crystallin A interaction *in vitro* in mammalian cell culture system it was important to verify the expression of fusion proteins with non-fluorescent tags (MycHis and HA tag). For this cells were made stable (as described in Materials & Methods). Several individual clones seemed to be originating from one cell source each were propagated under antibiotic selection pressure. The clones were verified both at the transcriptional and the translational level. To check for the presence of insert in the clones at mRNA level RT-PCR was done with the same primer pair used for cloning. The clones positive for mRNA were used for analysis at the protein level by western blot or immuno-staining.

(a) Cryaa-MycHis-HEK:

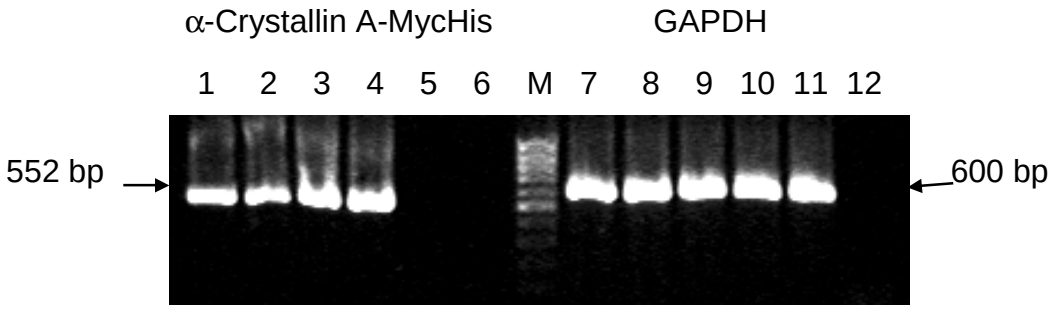

Figure 3.18 a. Detection of α-crystallin A-MycHis PCR signal in transfected HEK cells. 4 independent cell clones were checked for presence of α-crystallin A-MycHis fusion construct mRNA in stably transfected HEK cells by RT-PCR. Lane 1-4: α-crystallin A-MycHis clones, lane 5: untransfected HEK cells, lane 6: negative control (H_2O), lane 7-10: GAPDH signal in transfected clones, lane 11: GAPDH signal in HEK-WT, lane 12: negative control (H_2O).M: 1 kb DNA molecular ladder.

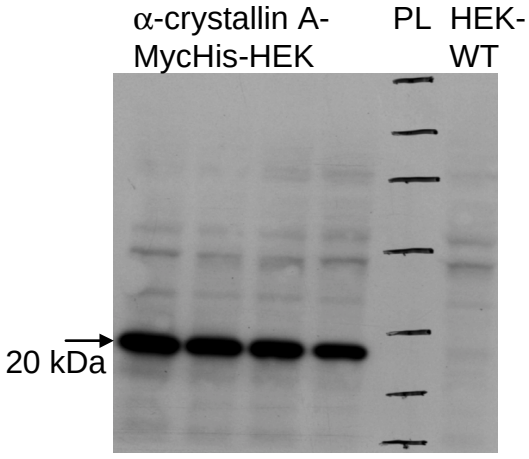

Figure 3.18 b. Detection of α-crystallin A -MycHis by western blot in transfected HEK cells. Independent clones of a-crystallin A -MycHis were checked for protein expression on SDS-PAGE and detected by anti-myc antibody on western blot (20 kDa). Untransfected HEK cells were negative for myc antibody. Details in Material & Methods.

(b) C-tail PAR-2-HA+GFP-HEK: As described in materials and methods it was not possible to make stable transfection with C-tail PAR-2-HA construct in HEK since pCMV-HA vector has no kanamycin/neomycin resistance site for selection with G418 antibiotic. Hence empty pEGFP-N1 plasmid DNA was used as a carrier DNA in this particular transfection and then cells were stably selected on the basis of green fluorescence of the GFP vector. Individual clones were checked for mRNA expression of C-tail PAR-2-HA fusion protein (Figure 3.19 a). It was not possible to check the clones at the protein level by western blot detection due to small size of the protein of ~6.7 kDa. For detection of such a small protein several modifications were applied in western blot and detection including preparation of protein sample, use of 10% precast gel with appropriate buffer (Materials & Methods), 15% Laemmli gel, small pore size nitrocellulose membrane (0.1 μm), PVDF membrane, several different transfer times and conditions in semi-dry transfer system, electroblot using tank transfer system, and anti-HA primary antibody from several companies. To check if the protein was actually expressed or not cell lysate was prepared from transfected cells in different ways (as described in Material & Method) and run on a 10% precast gel (with MES buffer). The gel was then proceeded for Silver staining. It was possible to detect the presence of small 6.7 kDa C-tail PAR-2-HA fusion protein by silver staining technique (Figure 3.19 b).

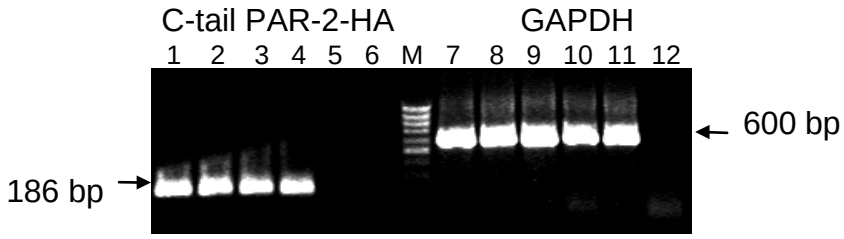

Figure 3.19 a. Detection of C-tail PAR-2-HA PCR signal in transfected HEK cells. 4 independent cell clones were checked for presence of C-tail PAR-2-HA fusion construct mRNA in stably transfected HEK cells by RT-PCR. Lane 1-4: C-tail PAR-2-HA clones, lane 5: untransfected HEK cells, lane 6: negative control (H_2O), lane 7-10: GAPDH signal in transfected clones, lane 11: GAPDH signal in HEK-WT, lane 12: negative control (H_2O). M: 1 kb DNA molecular ladder.

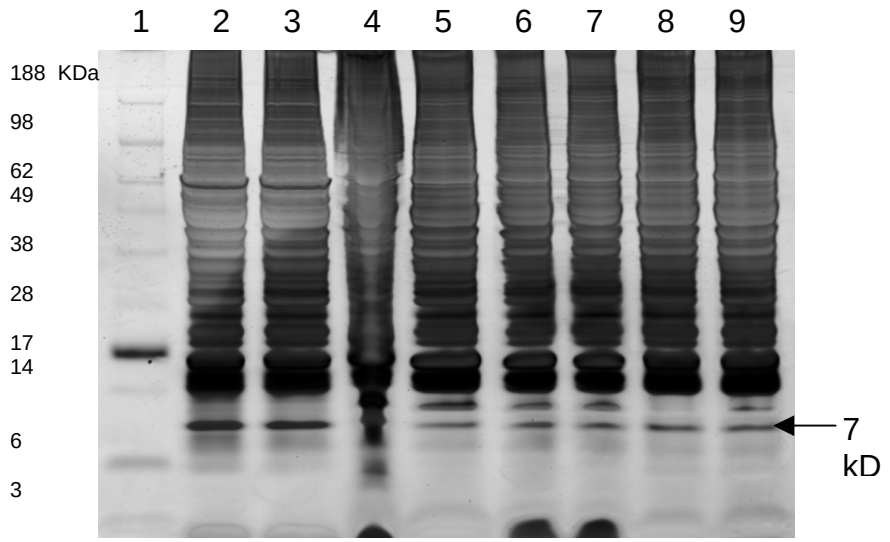

Figure 3.19 b. Silver stained gel for detection of C-tail PAR-2-HA in single and double transfected HEK cells. C-tail PAR-2-HA was transfected either alone or together with α-crystallin A-MycHis in HEK cells. Whole cell lysate prepared by different methods (Materials & Methods) to detect the small ~6.7 kDa protein by silver staining of SDS-PAGE. Lane 1: Protein ladder, Lane 2 & 3: single transfected clone (Acetone/Methanol precipitated), Lane 4 & 5: single transfected clone (lysate prepared by chloroform extraction and then precipitated), Lane 6 & 7: single transfected clone (chloroform extracted lysate), Lane 8 & 9: double transfected clone (acetone/methanol precipitated).

Another way to detect the C-tail PAR-2-HA fusion protein was to perform immuno-staining of the transfected HEK cells. Stable transfected cells exhibiting green fluorescence from GFP vector were stained for the presence of HA fusion protein with anti-HA primary antibody and fluorescent Alexa 555 secondary antibody and were found positive for the HA fusion protein (not shown).

(c) C-tail-PAR-2-HA+Cryaa-MycHis-HEK: HEK cells were double transfected with HA and MycHis fusion proteins. RT-PCR analysis of the double transfected cells showed equal expression of both constructs at the mRNA level (Figure 3.20 a). At the

protein level it was possible to detect Cryaa-MycHis fusion by western blot using monoclonal anti-myc antibody (Figure 3.20 b) but again C-tail PAR-2-HA could not be detected by blotting due to its small size. Silver staining of the double transfected cell lysate showed the presence of the C-tail PAR-2-HA fusion protein as shown in Figure 3.19 b.

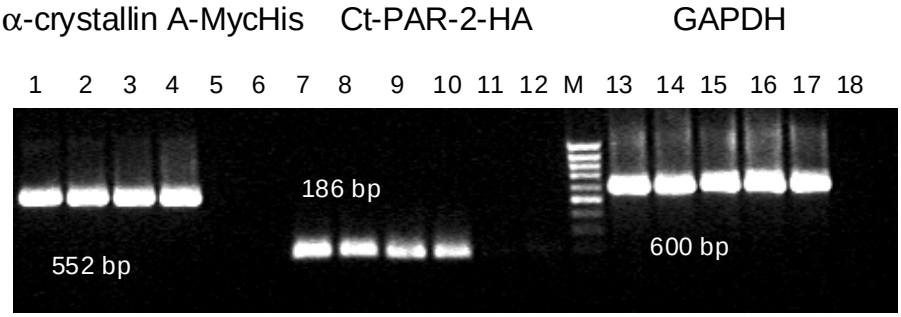

Figure 3.20 a. Detection of α-crystallin A-MycHis and C-tail PAR-2-HA PCR signal in double transfected HEK cells. 4 independent cell clones were checked for presence of α-crystallin A-MycHis and C-tail PAR-2-HA fusion construct mRNA in stably transfected HEK cells by RT-PCR. Lane 1-4: α-crystallin A-MycHis clones, lane 5: untransfected HEK cells, lane 6: negative control,lane 7-10: C-tail PAR-2-HA clones, lane 11: untransfected HEK cells, lane 12: negative control (H_2O), lane 13-16: GAPDH, lane 17: GAPDH signal in HEK-WT, lane 18: negative control. M: 1 kb DNA molecular ladder.

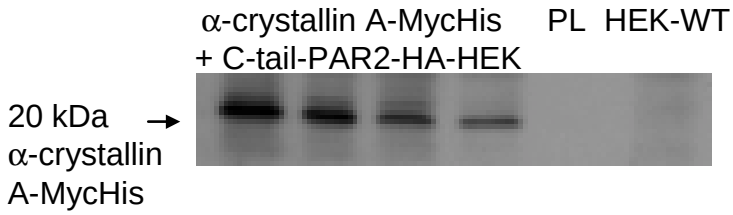

Figure 3.20 b. Detection of α-crystallin A -MycHis by western blot in double transfected HEK cells. Independent cell clones of α-crystallin A -MycHis and C-tail PAR-2-HA double transfected cells were checked for α-crystallin A-MycHis protein expression on SDS-PAGE and detected by anti-myc antibody on western blot (20 kDa). Untransfected HEK cells were negative for myc antibody. PL: protein ladder. Details in Materials & Methods.

(d) α-crystallin A Domain1/Domain 2-MycHis-HEK: HEK cells were stably transfected with either Domain1 (N-terminal) or Domain 2 (C-terminal) of α-crystallin A cloned in

pcDNA-MycHis(B) vector similar to full α-crystallin A. RT-PCR analysis of α-crystallin A Domain1-MycHis transfected cells gave the PCR band of 198 bps as expected (Figure 3.21 a), but due to small size (~ 7 kDa) it was not possible to detect the protein expression on SDS-PAGE. However, both mRNA (Figure 3.21 b) and protein expression (Figure 3.21 c) of α-crystallin A Domain 2-MycHis in transfected cells could be detected.

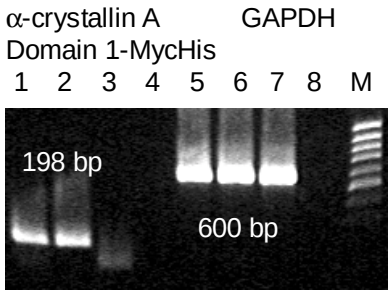

Figure 3.21 a. Detection of α-crystallin A Domain 1-MycHis PCR signal in transfected HEK cells. 2 independent clones were checked for presence of α-crystallin A Domain 1-MycHis fusion construct mRNA in stably transfected HEK cells by RT-PCR. Lane 1-2: α-crystallin A Domain 1-MycHis clones, lane 3: untransfected HEK cells, lane 4: negative control, lane 5-6: GAPDH signal in transfected clones, lane 7: GAPDH signal in HEK-WT, lane 8: negative control (H_2O).M: 1 kb DNA molecular ladder.

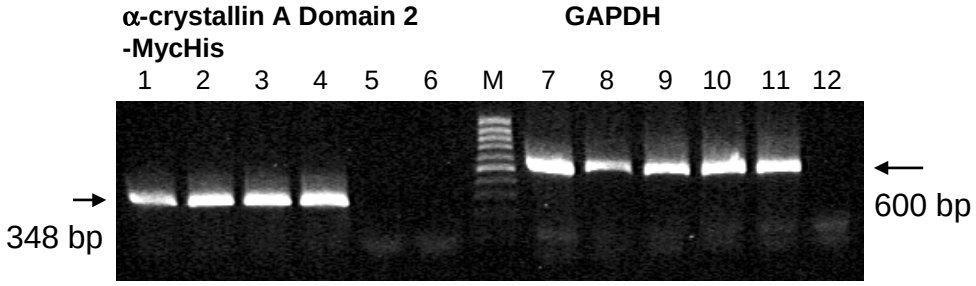

Figure 3.21 b. Detection of α-crystallin A Domain 2-MycHis PCR signal in transfected HEK cells. 4 independent clones were checked for presence of α-crystallin A Domain 2-MycHis fusion construct mRNA in stably transfected HEK cells by RT-PCR. Lane 1-4: α-crystallin A Domain 2-MycHis clones, lane 5: untransfected HEK cells, lane 6: negative control (H_2O), lane 7-10: GAPDH signal in transfected clones, lane 11: GAPDH signal in HEK-WT, lane 12: negative control.M: 1 kb DNA molecular ladder.

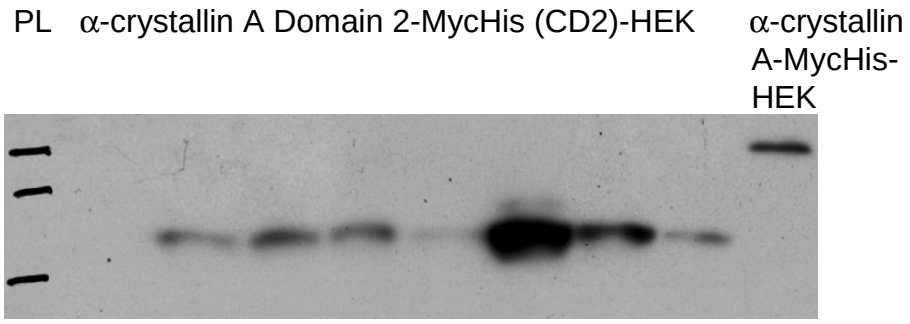

Figure 3.21 c. Detection of α-crystallin A Domain 2-MycHis (CD2) by western blot in transfected HEK cells. Independent clones of α-crystallin A Domain 2-MycHis-HEK were checked for protein expression on SDS-PAGE and detected by anti-myc antibody on western blot (13 kDa). Detection of α-crystallin A -MycHis-HEK used as a positive control for anti-myc antibody. PL: protein ladder. Details in Materials & Methods.

e) C-tail PAR-2-GFP-C2-HEK: C-tail of PAR-2 was subcloned into pEGFP-C2 vector from pGBKT7 in-between EcoRI and BamHI restriction sites. HEK cells were transfected with the construct and were made stable on the basis of green fluorescence of GFP vector. Unlike C-tail PAR-2 HA-HEK construct it was possible to detect the GFP construct because GFP by itself is ~27 kDa. Transfected cells were checked for the expression of fusion protein by western blot using polyclonal anti-GFP antibody (Figure 3.22).

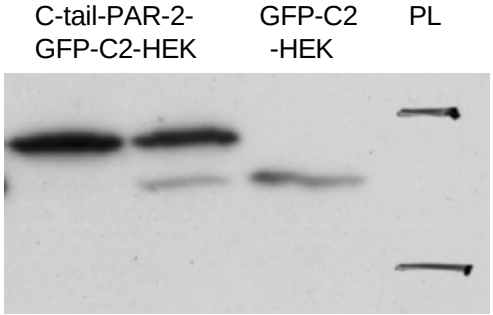

Figure 3.22. Detection of C-tail-PAR-2-GFP-C2 by western blot in transfected HEK cells. Independent clones of C-tail-PAR-2-GFP-C2-HEK (~34 kDa) were checked for protein expression on SDS-PAGE and detected by anti-GFP antibody on western blot. GFP-C2 (empty vector) transfected HEK cells were used as positive control for GFP antibody. PL: protein ladder. Details in Materials & Methods.

3.2.16 Co-immunoprecipitation

To confirm the protein-protein interaction observed in yeast it was important to perform a biochemical assay showing the interaction in another system and thus validating the results obtained in yeast-two hybrid. For this, co-immunoprecipitation assay was done in mammalian expression system. Both the bait and prey constructs after verification for protein expression in double transfected HEK cells were used for co-immunoprecipitation assay. 2 mg of whole cell lysate was used. Double transfected clones precipitated with anti-HA antibody and protein A on detection with anti-myc antibody gave a positive signal indicating that α-crystallin A-MycHis binds to bait C-tail PAR-2-HA and hence could be detected on blot. This proves that there exists interaction between α-crystallin A-MycHis and C-tail PAR-2-HA. The specificity of this interaction was confirmed by negative results obtained when the same double transfected lysate was incubated with only protein A excluding anti-HA antibody. This negative control indicates that the binding of C-tail PAR-2-HA is specific with anti-HA antibody and not by means of protein A. Also incubation of HEK-WT cell lysate with both anti-HA antibody and protein A gave negative results again confirming specificity of interaction (Figure 3.23).

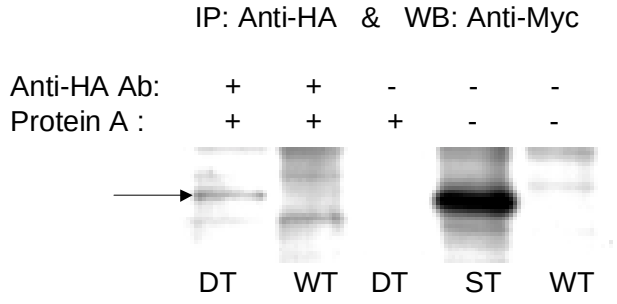

Figure 3.23. Co-immunoprecipitation of double transfected HEK cells. HEK cells transfected with α-crystallin A-MycHis and bait C-tail PAR-2-HA were precipitated with anti-HA antibody (sigma) and protein A. α-crystallin A -MycHis was detected using anti-myc antibody on western blot from the precipitated sample indicating positive interaction between the two proteins. Double transfected lysate without anti-HA antibody and only protein A and HEK-WT lysate with both anti-HA antibody and protein A were negative on western hence indicating the specificity of the co-immunoprecipitation reaction. Single transfected α-crystallin A-MycHis and HEK-WT were used during western blot as a positive and negative control respectively for the anti-myc antibody.

3.2.17 Co-localisation of PAR-2 and α-crystallin A in Hippocampal astrocytes

Out of the tissues and cell types studied, Hippocampal astrocytes apart from retina, optic nerve and brain were positive for α-crystallin A mRNA expression. Hence, to confirm the interaction between PAR-2 and α-crystallin A in a system endogenously expressing both proteins immunostaining of hippocampal astrocytes were done using PAR-2 and α-crystallin A specific antibodies. Hippocampus is known to express PAR-2 (Striggow et al., 2001). Double staining of hippocampal astrocytes with PAR-2 and α-crystallin A antibodies (1:100) and subsequent fluorescent detection by means of Alexa conjugated IgG (488 and 555) gave positive detection for both proteins in the system. Similar to its cellular localisation in transfected N2A cells, α-crystallin A was localised in cytosol of hippocampal astrocytes. PAR-2 showed both membrane and cytosolic localisation. Overly of green (α-crystallin A) and red (PAR-2) fluorescence gave yellow colour indicating that both the proteins are co-localised in hippocampal astrocytes (Figure 3.24). Appropriate negative controls were also done.

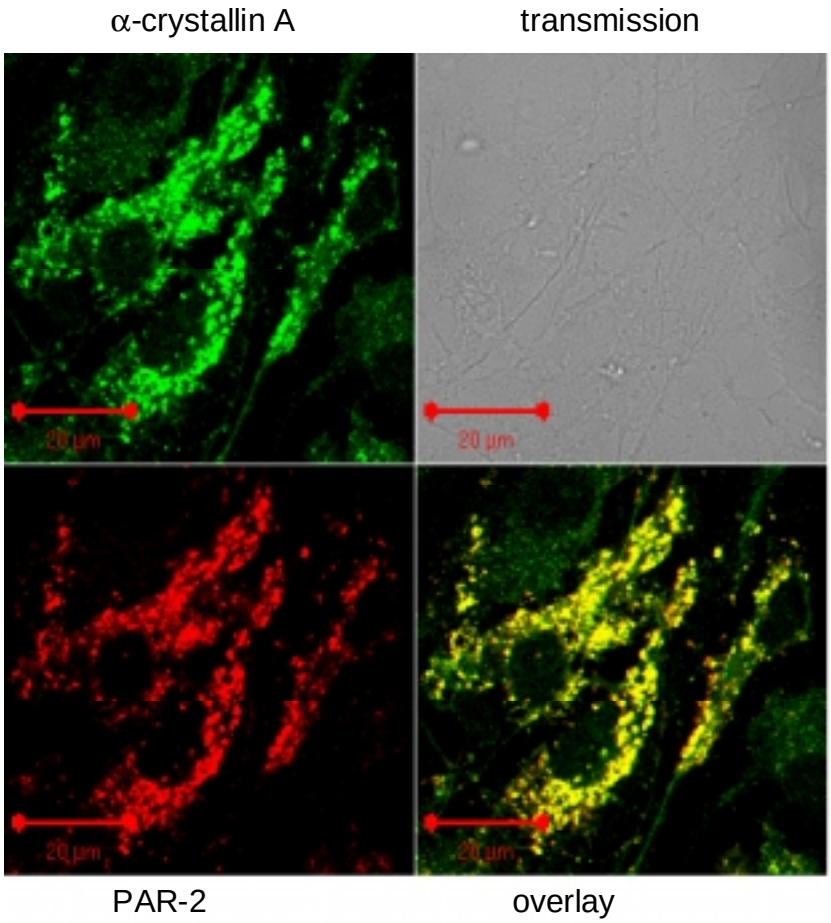

Figure 3.24. Co-localisation of α-crystallin A and PAR-2 in hippocampal astrocytes by immunodetection. Hippocampal astrocytes were stained for the presence of both α-crystallin A and PAR-2 using specific antibodies (1:100). Fluorescent detection with Alexa A488 (green- α-crystallin A) and A555 (red-PAR-2) (1:100) showed co-localisation of both proteins in hippocampal astrocytes.

4. Discussion

4.1 Expression of PARs after CNS injury

In recent years Protease-activated receptor has emerged as one of the key player involved in tissue injury and inflammation (Coughlin and Camerer, 2003). Data particularly on CNS injury, bring into focus the need to study the change in PAR expression after trauma and stroke induced by various stimuli since both serine protease thrombin, which is an agonist for PAR-1, -3 and –4, and PARs play an important role in the sequence of events leading to either brain damage or protection as a result of CNS injury (Gingrich and Traynelis, 2000; Xi et al., 2003).

4.1.1 mRNA expression of the 4 PAR subtypes in the rat developing eye and adult retina

Distribution of PAR-1-4 has been well studied and characterized in several tissues and cell types (Weinstein et al., 1995; Ishihara et al., 1998; Niclou et al., 1998; Steinhoff et al., 1999), but the presence and expression pattern of these receptor subtypes in retina are unknown. Previous studies from our laboratory had shown the presence of these receptors in different areas of brain (Striggow et al., 2001) and in brain astrocytes (Wang et al., 2002a). In the current study, presence and expression of PARs in post-natal rat eye and adult retina were detected for the first time using RT-PCR. A comparison of expression patterns of these receptor subtypes during the different developmental stages of eye (P1, P9 and P16) clearly shows that each subtype is expressed to a different degree.

Unlike for the other PARs, a decrease in PAR-1 mRNA expression from P1 and P9 to P16 in the post-natal eye was observed. The results on PAR-1 mRNA expression during eye development presented in this study are consistent with an earlier study showing a decrease in PAR-1 mRNA intensity from embryonic (E14, E18), post-natal (P0) to adult brain (P28) by Northern analysis (Niclou et al., 1998). Nevertheless, in the same study it was found that in spinal cord the PAR-1 mRNA signal remained identically high throughout the different stages of embryonic and post-natal development (Niclou et al., 1998). However, Niclou et al. (1998) mention that the mRNA signal observed in neural tissue by Northern analysis was comparable to that observed for a neuroblastoma cell line. In the neuroblastoma cells, a physiological response to thrombin due to PAR activation could be found. This

observation suggests that even the low level of these receptors in the embryonic and post-natal stages is probably enough for functional activity. In the retina of the adult rat, we could detect strong signals for PAR-1, moderate signals for PAR-2 and PAR-3, while PAR-4 was expressed at low levels.

4.1.2 The mRNA levels of PAR receptors in retina in response to ONC

In last decade since the cloning of PAR-1, PARs have been studied quite extensively as an important factor in tissue injury (Friedmann et al., 2001a) and injury models (Napoli et al., 2002; Striggow et al., 2000; Xi et al., 2003). These receptor subtypes are also widely implicated in tissue repair (Striggow et al., 2000; Vaughan et al., 1995; Xi et al., 2003). Activation of PARs leads to several downstream processes, like Ca^{2+} influx from intracellular stores (Ubl and Reiser, 1997), various signalling cascades resulting in proliferation (Wang et al., 2002a; Wang et al., 2002b; O'Brien et al., 2001; Saifeddine et al., 1996; Bohm et al., 1998), apoptosis (Cunningham and Donovan, 1997; Turgeon et al., 1998) and inflammation (Steinhoff et al., 2000; Vergnolle et al., 2001a).

In this study all 4 PAR subtypes were found to be upregulated in retina as a result of controlled ONC, a model of partial nerve crush (Sautter and Sabel, 1993). The mild ONC is enough to shear but does not completely axotomize the nerve axons. Studies using this model have shown a loss of almost 70-80% retinal ganglion cells (RGCs) as a result of an early necrosis and subsequent apoptosis within 2 weeks after injury (Sautter and Sabel, 1993; Kreutz et al., 1997; Bien et al., 1999). Near-complete spontaneous behavioural recovery was observed two to three weeks post-injury after the mild crush, but only 28% and 11% of RGCs survived at two and fourteen days, respectively, after crush (Sautter and Sabel, 1993). Upregulation of PAR mRNA levels 6 h after ONC shows an early response to injury. A similar increase in PAR-1 mRNA expression has been reported to occur as a consequence of spinal cord injury (Citron et al., 2000) and non-neuronal sciatic nerve injury (Niclou et al., 1998). In ipsilateral retina after ONC, it was found that PAR-1 mRNA reached maximal levels of 2.3-fold one week post-crush and then came down to basal value by the end of 21 days. Citron et al., (2000) observed a maximal increase in PAR-1 mRNA levels of 4-fold at one day post-injury, then reduced levels by day 3, which declined to basal level by day 28 post-injury. Also sciatic nerve lesion resulted in an increased PAR1 mRNA expression in the proximal and distal part of the lesioned nerve (Niclou et al., 1998). In the case of

sciatic nerve injury a rise in PAR-1 mRNA expression at day 1 with a subsequent very pronounced increase at day 4 and 7 after injury was observed by Niclou et al. (Niclou et al., 1998). In the same study, a substantial decrease in PAR-1 mRNA expression in the lesioned motoneurons of facial nerve was found, which is in contrast to increased PAR-1 mRNA expression after non-neuronal sciatic nerve injury.

The varied behaviour of PAR-1 mRNA expression in response to different types of neuronal and non-neuronal lesions highlights the fact that the receptor expression is not static, but depends on lesion intensity and tissue type. Festoff and co-workers (Citron et al., 2000) attributed the increase in PAR-1 mRNA levels to increased prothrombin mRNA levels at the site of injury. Increase in thrombin levels at the proximal site of injury have indeed been reported (Friedmann et al., 1999; Friedmann et al., 2001a). In these studies a partial ONC in adult rat was used, which is very similar to the approach we have used. In injured optic nerve an up-regulation of thrombin-like activity was found as early as 6 h after the crush (Friedmann et al., 2001a; Friedmann et al., 1999), which peaked at day 1 (40-fold high) and then returned to basal levels by day 4 to 7. The observation of early thrombin up-regulation after crush provides strong support for functional implications of the present finding of PAR upregulation in retina 6 h after nerve crush.

However, the amplitude and time course of increase in mRNA levels observed for the 4 PARs in retina after crush differ from each other. In case of ipsilateral retina, PAR-1 showed a maximal value of 2.3-fold observed on day 7, while PAR-2 and PAR-3 showed this level of mRNA expression only at 12 h post-crush. PAR-4 seems to be the most strongly affected receptor subtype, reaching a maximal level of 6.1-fold at 12 h after crush. The reason for this difference in the expression of the 4 subtypes is not yet clear, but this could be due to differences in the innate regulatory mechanism of these receptors. Detailed studies have already been done to explore the signalling pathways of PAR-1 (Wang et al., 2002a; Wang and Reiser, 2003a), whereas limited information pertaining to intracellular signalling from PAR-2 is available (Kanke et al., 2001), and almost nothing is known about the downstream signalling from PAR-3 and PAR-4.

Another important finding of this study is the fact that as a result of unilateral injury the contralateral uninjured side is also affected, as already seen before by others (Yew et al., 1990; Shibuya et al., 1993; Lam et al., 1996; Bodeutsch et al., 1999). The extent of change in receptor mRNA levels between injured and uninjured retina was

comparable in our study. Compared to the ipsilateral retina, mRNA levels of PAR-1 and PAR-2 in the uninjured side showed a significant maximal increase of 1.8-fold during the time period of study. PAR-4 mRNA levels rose to a significantly high level of 2.2-fold, while increase in PAR-3 level was not so significant. Bodeutsch et al., (1999) observed a moderate c-jun immunoreactivity, up-regulation of astrocytes and microglial cells in the contra-lateral uninjured retina and optic nerve. Bodeutsch et al., (1999) presented interesting reasoning for such a bilateral effect after unilateral lesion: The retinotectal pathway is a very closely linked pathway and both sides behave identical to compensate for the loss of cells even when only one side is injured. According to them this effect of unilateral nerve lesion on the contra-lateral uninjured retina is rather confined to changes at the cellular level with little direct effect on the majority of axons. More recently, Bodeutsch et al., 2000 could demonstrate cell death in the contra-lateral retina as an outcome of unilateral ONC in adult mice. They showed a gradual decrease of retrogradely labeled RGC and their replacement by retinal microglia after ONC. They observed only 25% and 10% of RGCs at 5 and 7 d post-crush, respectively (Bodeutsch and Thanos, 2000).

Schwartz and co-workers (Friedmann et al., 1999; Friedmann et al., 2001a) have shown that thrombin-like activity in the retina remains almost unchanged after the nerve crush, but they detected that prothrombin becomes activated at the site of injury by extravasation from the blood vessels and that injury-induced activity is restricted to the proximal part of injured nerve and associated to retrograde degeneration. This retrograde degeneration towards the optic disk may be somehow responsible for the exposure of retina to increased thrombin levels after injury and hence activation and up-regulation of PARs. Both necrosis and apoptosis have been reported as a cause for retrograde degeneration and cell death of RGCs as a result of optic nerve lesions including crush and axotomy (Garcia-Valenzuela et al., 1994; Rabacchi et al., 1994; Isenmann et al., 1997; Bahr, 2000; Cellerino et al., 2000; Friedmann et al., 2001b). Studies using PAR-1 knockout mice have shown increased RGC survival as compared to the wild-type mice after ONC (Friedmann et al., 2001b). In the same study T cell-induced decrease in endogenous thrombin activity and degeneration was observed when T cells were administrated to rat prior to ONC (Friedmann et al., 2001b). In the present study we can provide a hypothesis explaining cell death in the ONC model of mild trauma. According to data in (Citron et al., 2000), the increase in PAR-1 expression after injury and the presence of active thrombin at

the site of injury cause PAR-1 upregulation and activation. Activation of PARs leads to increased intracellular Ca^{2+}, followed by caspase activation and subsequent apoptosis. Apoptosis of RGCs and its association with rise in intracellular Ca^{2+} is known to be a consequence of lesions of the optic nerve (Cellerino et al., 2000). Cell death in the contra-lateral retina as an outcome of unilateral ONC in adult mice has also been attributed to programmed cell death and subsequent phagocytosis by the retinal microglia cells (Bodeutsch and Thanos, 2000). Earlier studies from our laboratory using *in vivo* confocal neuroimaging technique have followed the time course and extent of change in soma size (Rousseau et al., 1999) and observed increased intracellular calcium activity after ONC (unpublished data). Also seen was an early necrosis followed by apoptosis of RGCs after ONC (Bien et al., 1999) and an increase in mRNA levels for interleukin converting enzyme (ICE; caspase-1) as a result of nerve crush (unpublished data).

With findings from the present study we clarified further the series of events taking place as a result of mild nerve crush in retina. Thus, increase in thrombin activity at the site of injury as a consequence of nerve crush is associated with stimulation of upregulation of PARs. This, in turn, leads to intracellular Ca^{2+} mobilization followed by RGC degeneration due to necrotic and apoptotic mechanisms. Thus, PAR activation in this nerve crush model may act as effector of cell death by an early necrosis and subsequent apoptosis. The evidence pertaining to cell death mechanism in both the injured and uninjured retina and Ca^{2+} increase response rules out the possibility that the observed PAR mRNA increase is only a consequence of stress effects during or after nerve injury (Papadaki et al., 1998; Nguyen et al., 2001a; Nguyen et al., 2001b).

The eventual decrease in the receptor mRNA levels by the end of three weeks after crush, except for PAR-2, to almost basal levels, as seen in this study, may also result from eventual decrease in thrombin activity. Hence, shutting-off the whole hyperactivity cascade that is triggered by an insult to the system, and return back to normal levels is required for basal activity and maintenance of the system.

4.1.3 PAR mRNA levels after transient focal ischemic

To further elucidate the behaviour of PAR mRNA expression in another type of CNS injury, transient focal ischemia as a model of stroke was studied. In the present work, microinjection of endothelin-1 was used as a tool to generate ischemia

with reperfusion resulting in a mild specific stroke damage in rat brain. Endothelin is a peptide of 21 amino acids and the most potent vasoconstrictor known (Levin, 1996). Application of endothelin near the MCA in a model of focal cerebral ischemia results in a dose-dependent, reversible vasoconstriction along with a considerable reduction in cerebral blood flow and causes subsequent cerebral infarction (Sharkey et al., 1994; Reid et al., 1995). Use of endothelin receptor antagonist had shown that endothelin is involved in the development of secondary brain damage (Gorlach et al., 2001). Endothelin levels were found to be elevated in the cerebrospinal fluid (CSF) and plasma of ischemic stroke patients (Lampl et al., 1997) and in patients suffering from subarachnoid hemorrhage and cerebral infarction (Zimmermann and Seifert, 1998). These studies highlight a possible role played by endothelin in the pathophysiology of ischemia and stroke.

Ischemia induced by intracerebral microinjection of endothelin close to the MCA caused infarction in cortical areas. The environment, conditions and brain areas affected by MCAO are largely different from the conditions to which the organotypic hippocampal slices were exposed to during and after OGD (Striggow et al., 2001). Hence it was of no surprise that a different effect in terms of PAR mRNA expression was observed in the present experiments as compared to the study done before (Striggow et al., 2001).

Semi-quantitative RT-PCR analysis of PAR-1-4 expression resulted in a substantial reduction in the mRNA levels of PAR-1 and PAR-2 after the insult in the ipsilateral hemisphere in this study, unlike the up-regulation observed by (Striggow et al., 2001) in the hippocampal slice cultures 24 hrs after 30 min OGD. The mRNA expression pattern of PAR-3 in the present *in vivo* study here and in the *in vitro* experiments (Striggow et al., 2001) both showed a transient increase. In the current study, we obtained a transient increase at 12 h, after which the mRNA levels subsequently declined to lower than half the control levels by the end of one week. In contrast to the results which we obtained for PAR-1 to -3, PAR-4 showed the most striking up-regulation at 12 h after ischemia which declined gradually, but was still maintained at substantially elevated level one week later. This behaviour of PAR-4 after transient focal ischemia is similar to the results obtained for PAR-4 mRNA expression after ONC in retina. In the work by (Striggow et al., 2001), no RT-PCR analysis for PAR-4 was performed. Interestingly, in a recent study from our laboratory PAR-1-3 mRNA expression was found to be unaltered after global ischemia (Riek-

Burchardt et al., 2002). A comparison between the OGD study (Striggow et al., 2001), global ischemia (Riek-Burchardt et al., 2002) and the present study involving transient focal ischemia highlights the specificity in the regulation of PAR mRNA expression as a consequence of different modes of inducing ischemia. Studies assessing the effect of focal ischemia emphasise the role of secondary mechanisms initiated by an acute inflammatory response, including breakdown of blood-brain barrier, edema, induction of proinflammatory cytokines, activation of leukocytes, macrophages and activation of microglial cells (Gehrmann et al., 1992; Buttini et al., 1994; Garcia et al., 1994). Cerebral ischemia exposes the brain tissue to reduced blood glucose in an endogenous immune reactive environment, while such interplay of blood borne immune cells is absent during *in vitro* OGD. The effect of inflammatory stimuli on PAR activation has already been demonstrated in epithelial and endothelial cells (Hamilton et al., 2001; Asokananthan et al., 2002).

PAR-1 was also found to be down-regulated in a human neuronal cell line after hypoglycemia (Weinstein et al., 1998) and the authors proposed this response to be an effective way to attenuate the ability of thrombin to damage the neuronal cells during metabolic insult via PAR-1 activation (Weinstein et al., 1998). In the same study (Weinstein et al., 1998), it was shown that hypoxia and oxidative stress on the other hand had no effect on PAR-1 expression, demonstrating the difference in PAR-1 behaviour following different metabolic insults (Weinstein et al., 1998). Evaluation of the role of PAR-2 in inflammation and tissue injury using a myocardial ischemia-reperfusion model revealed that PAR-2 activation protected against reperfusion-injury and resulted in significant recovery of myocardial function (Cirino et al., 2000).

Besides the changes observed in PAR mRNA expression in the ipsilesional hemisphere, also the contralateral side was found to be affected. Here, PAR-1 to -3 mRNA levels were down-regulated, while PAR-4 showed a transient up-regulation until 48 h and then declined to almost half the control levels. A recent fMRI study examined the bilateral changes and their relation to functional brain recovery after transient focal ischemia in rat (Dijkhuizen et al., 2003). There was a shifting of brain activation to the contralateral side initially after stroke which was directly proportional to the extent of tissue injury. However, the functional recovery was associated more closely with the restoration of activation in the ipsilateral hemisphere (Dijkhuizen et al., 2003). This means that the change in PAR expression on the contra-lateral side in the present study might be part of a compensatory reaction to a severe ischemic effect

resulting in a shifting in brain activity. The changes on the contralateral side could also reflect induction of tolerance.

We found that especially the thrombin receptors PAR-1, 3 and 4 were affected as a result of endothelin-1-induced transient focal ischemia, which implies that thrombin should be produced or present at the site of injury (Smirnova et al., 1996). There is ample evidence in the literature which suggests that prothrombin as the precursor molecule of thrombin is present in brain under normal conditions (Dihanich et al., 1991). Prothrombin is upregulated after global cerebral ischemia (Riek-Burchardt et al., 2002), spinal cord injury (Citron et al., 2000), sciatic nerve injury (Smirnova et al., 1996) and subarachnoid hemorrhage (Suzuki et al., 1999). Increased thrombin-like activity has been detected in CNS and PNS nerve injury models (Smirnova et al., 1996; Friedmann et al., 1999). In case of sciatic nerve injury in mouse it has been shown that injury induced an increase in prothrombin level and subsequently in thrombin enzymatic activity (Smirnova et al., 1996). An earlier study from our laboratory has shown the involvement of endogenous thrombin in ischemia-induced degeneration in the hippocampus (Striggow et al., 2000) thus clearly demonstrating that thrombin is produced in brain in response to ischemia. Additionally, it is known that as a result of stroke, the blood-brain barrier is compromised, giving rise to the possibility of entry of thrombin from plasma into brain (Cunningham et al., 1993; Gingrich and Traynelis, 2000). Also, thrombin is generated at the site of inflammatory reactions after brain damage and PARs orchestrate an important role as mediators of inflammation (Cirino et al., 2000; Cocks and Moffatt, 2000). There are some reports about the role of PARs in inflammation which point to the fact that not only activation of PAR-1 contributes to the thrombin-induced pro-inflammatory action but that also PAR-3 and –4 may be involved (Cirino et al., 2000; Cocks and Moffatt, 2000; de Garavilla et al., 2001; Vergnolle et al., 2002).

Taken together, the diverse roles of PARs including effect of change in PAR expression level in mechanisms related to tissue injury fit well with the results which we have obtained, indicating a possible role for PAR-1, PAR-3 and PAR-4 activation in the sequence of events leading to pathophysiology of focal ischemia.

4.2 Identification of a putative interacting protein for PAR-2 using yeast two hybrid system

The second main aim of the present study was to further the knowledge with regard to trypsin-activated PAR-2, since this is the most well documented receptor subtype in the scenario of injury and inflammation (al-Ani et al., 1995; Damiano et al., 1999a; Steinhoff et al., 2000; Knight et al., 2001; Shpacovitch et al., 2002). Inspite of being studied so thoroughly as an important component after tissue injury and repair little is known with regard to PAR-2 intracellular downstream signalling cascades (Macfarlane et al., 2001). To this effect we tried to identify probable interacting proteins for PAR-2 utilising the yeast two-hybrid screen and enhance our understanding of PAR-2 intracellular signalling mechanism. Already similar studies done with C-tail of PAR-1 have identified creatine kinase (Mahajan et al., 2000) and Hsp 90 (Pai et al., 2001) as PAR-1 interacting proteins.

4.2.1 Library Construction and Screening

The C-terminal of rat PAR-2 (50 amino acids) was cloned in DNA-BD vector pGBKT7 to generate a bait fusion protein. The reasons for selecting only the C-terminus of the receptor as a bait in the present study were two-fold. First, since PAR-2 is a 7-transmembrane receptor it was possible that the transmembrane (TM) region of the receptor might have had problems entering the yeast nucleus and second, there was a successful example in the studies done with PAR-1, which had used only the C-tail of the receptor (Mahajan et al., 2000; Pai et al., 2001).

Before starting with the library transformation and screening, bait protein was tested for proper growth in both solid and liquid complete medium. This was important as some proteins are either expressed in very low amount or are over-expressed and toxic to the yeast cells. In the present study the C-tail of PAR-2 cloned in pGBKT7 i.e., the 'bait' grew at a comparable rate with the empty pGBKT7 vector and hence was suitable to be used for library screening. However, comparison between the two yeast strains AH109 and Y187 transformed with bait showed that bait grew better in AH109 as compared to Y187. Testing of the bait protein for transcriptional activation (Table 3.3) gave negative results, thus confirming that neither the bait protein by itself nor together with empty pGADT7-Rec (library plasmid) is capable of

transcriptional activation of reporter genes in yeast, and hence can be used for yeast library protocol. AH109 and Y187 transformed with bait protein on SD/-Trp/-His did not exhibit any background growth and were negative for HIS3 leaky expression. Therefore, for library transformant screening 3-AT (3-amino-1,2,4-triazole), a competitive inhibitor of yeast HIS3 protein was not used in the medium and since further selection of the positive clones was made for both HIS3 and ADE2 expression it eliminated the need to use 3-AT in the initial library screening.

For screening procedure it was possible either to use a pre-transformed library or to make a cDNA library by itself. For this study it was decided to use the C-tail PAR-2 as a bait with self-made cDNA library. Rat retina poly A+ RNA was used to generate ds cDNA for the library. Since the PAR mRNA expression study showed the presence of PAR-2 in retina and sustained effect of ONC on PAR-2 mRNA expression unlike PAR-1, -3 and –4 (Figure 3.4) it was decided to use retina as the source for preparing ds cDNA for the library.

At every point during library transformation and screening protocol suitable controls were performed simultaneously to keep a check on the whole procedure. During ds cDNA preparation care was taken to use random primer rather then oligo (dT) primer so as to generate cDNA with an equal proportion of 5’ and 3’ end different sequences instead of only 3’ end sequences. The use of SMART III oligo during cDNA synthesis resulted in generation of ss cDNA’s containing the complete 5’ end of the mRNA as well as sequence complementary to the SMART III oligo, which then served as a universal priming site in the subsequent amplification by long-distance PCR (LD-PCR). Thus, ds cDNA generated by LD-PCR containing 5’ SMART sequence and 3’ random primer sequence was suitable for in vivo homologous recombination with pGADT7-Rec during AD fusion library construction in yeast (Figure 4.1).

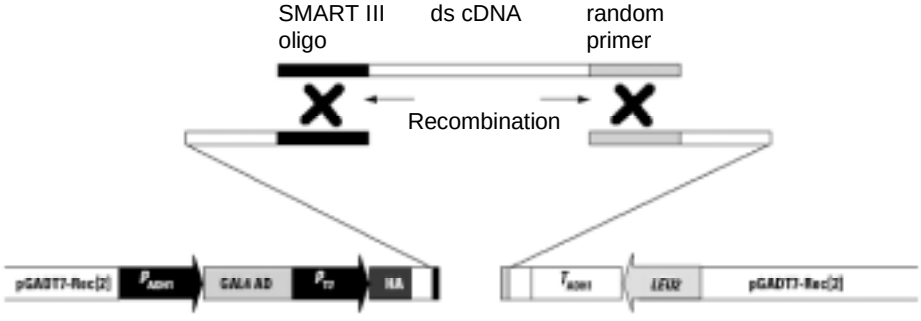

pGADT7-Rec Vector (Sma I-linearized)

Figure 4.1. Construction of AD fusion libraries by recombination-mediated cloning in yeast (Matchmaker Library construction and screening manual, Clontech, Heidelberg, Germany). Co-transformation of ds cDNA with Sma I-linear pGADT7-Rec restores the plasmid with help of yeast repair enzymes to its circular form by recombining sequences at the end of cDNA with homologous sequences at the ends of pGADT7-Rec. The resultant vector is a fully functional GAL4 AD/cDNA expression vector.

For library transformation in yeast, sequential transformation was done unlike the co-transformation as recommended by the Library construction manual (Clontech, Heidelberg, Germany). In case of co-transformation protocol it is possible to introduce the bait protein, ds cDNA and Sma I-linear pGADT7-Rec together into the yeast reporter strain, but the chances of all the three components been taken up by the same yeast cell may not be so good. In order to avoid this problem AH109 was sequentially transformed. First the yeast was transformed with the bait protein and then the bait containing AH109 were made competent under the appropriate selection pressure to retain bait protein in the competent cells and re-transformed with retina ds cDNA and Sma I-linear AD plasmid. The linear pGADT7-Rec was restored to its circular form by recombination with overlapping sequences at the 5' and 3' end of cDNA giving a complete GAL4 AD expression vector (Figure. 4.1). The division of the whole transformation procedure into two separate individual processes was done to maximise the efficiency and increase the probability of bait containing yeast competent cell receiving the AD fusion library plasmid. To validate the library transformation protocol, positive and negative control transformations were done simultaneously. Library transformants were grown on appropriate selection medium to check for transformation efficiency and number of library clones screened. In both cases the value obtained matched with the expected results thus verifying the whole transformation procedure.

To check for positive interacting clones transformants were selected through a series of stringent media suitable for expression of reporter genes. In the first step transformants were selected for His+ reporter gene expression along with tryptophan and leucine which are markers for the DNA-BD and AD plasmids, respectively. The clones were made to grow for 4-6 days so as to provide enough time even for the weak interacting clones to appear. All the clones (big or small) grown after library transformation on TDO plates were restreaked to select for His+ reporter gene expression once again and to eliminate in the process some of the weak clones. The

HIS3 reporter is the most sensitive, but also the least selective, generating large numbers of false positives. As mentioned earlier, since AH109 containing bait protein showed no background growth on SD/-Trp/-His medium hence 3-AT was not used to suppress HIS3 leaky expression. In the second round clones were streaked to select for Ade+ positives. To eliminate false positive clones grown in –His medium, clones were grown under both –Ade and –His selection pressure, since ADE2 reporter is most selective, eliminating almost all false positives. Although ADE2 reporter is too stringent, it provides a powerful secondary screen in combination with other reporter genes (MacDonald Paul N., 2001). Colonies lacking ability to survive -Ade selection turned pink and subsequently red. This phenotypic selection for adenine reporter gene expression, too, helped in reducing the selection of false positive clones. Apart from His+ and Ade+ selection for interacting protein, yeast strain AH109 also allows for third reporter gene assay i.e., lacZ coding for β-galactosidase enzyme. This reporter gene expression is based on phenotypic selection of blue or white colonies. X-gal, the substrate for β-galactosidase has the ability to turn colonies blue in case of positive expression or remained white indicating lack of β-galactosidase expressing positive clones. To check for lacZ gene, colonies were filter lifted from –Ade/-His plates and observed for appearance or lack of blue colour after incubation with X-gal. Thus, screening for all three reporter genes was done individually step by step to avoid selection of false positive clones. Repetition of filter lift assay was done to screen for the positive clones under most stringent conditions. For the transformation and screening procedure use of yeast strain AH109 was most effective, since it utilises not one but three reporter gene constructs which provide the opportunity to eliminate many false positives. In AH109 the three reporter constructs use different promoters (Table 4.1) hence acting as an internal control, because many false positives result from a specific interaction with sequences within the promoter region (MacDonald Paul N., 2001).

Table 4.1. Reporter gene constructs in yeast strains AH109 and Y187 (Matchmaker Library Construction and Screening Manual, Clontech, Heidelberg, Germany). The HIS3, ADE2 and MEL1/lacZ reporter genes in AH109 are under the control of three completely different heterologous GAL4-responsive UAS and promoter elements- GAL1, GAL2 and MEL1, respectively. Strain Y187 contains the lacZ reporter gene under control of the GAL1 UAS.

AH109 Constructs

GAL1 UAS	GAL1 TATA	HIS3
GAL2 UAS	GAL2 TATA	ADE2
MEL1 UAS	MEL1 TATA	lacZ
MEL1 UAS	MEL1 TATA	MEL1

Y187 Construct

GAL1 UAS	GAL1 TATA	lacZ

Clones positive for Ade+, His+ and lacZ+ needed to be identified and verified further. Since the interest was to identify only the AD/library clones for further processing, selection medium favouring growth of AD/library plasmid was used and AD/library plasmids were isolated from the positive clones. The yeast plasmid DNA isolated is not good for any downstream analysis because of heavy genomic DNA contamination, low copy number and low plasmid yield. So in order to obtain AD clones DNA in a pure form and large amount for any further analysis, in the next step E.coli was transformed with yeast plasmid DNA. As the quality of the yeast plasmid DNA isolated is not good, electrical transformation i.e., electroporation was done instead of chemical based transformation of bacteria, as electroporation has several fold higher transformation efficiency compared with chemical transformation. To check for the presence of similar size insert, the clones were digested with a restriction enzyme and subsequently sequenced to identify the fragment.

Of the 65 AD positive clones, sequence of only 27 clones matched with known sequences in the databank both at nucleotide and protein level, while the rest of the clones gave ribosomal RNA, only vector sequence and some sequences not matching with anything known in the databank. It was important to verify the sequences not

only at the nucleotide level but also at the protein level since interaction in yeast occurs at the protein level and any sequence without meaningful protein makes no sense in pursuing further. From the 27 matched sequences some were present only one time while few were represented in duplicate or more. Before analysing the clones further, they were re-tested in yeast one more time for confirmation of interaction and further elimination of false positives by mating procedure.

Yeast mating allowed target proteins expressed in two different haploid yeast strains of opposite mating type to come into contact, resulting in fusion of the two haploids to form a diploid yeast strain. It is possible to determine the interaction between the proteins by analysing the reporter gene expression in the diploid strain. To eliminate the scope for selection of false positives, each AD/library clone was mated with yeast strain expressing three different DNA-BD plasmids: empty pGBKT7, bait-pGBKT7 and control pGBKT7 containing an unrelated fusion protein and selected for Ade+, His+ and lacZ+. True positives are those AD library clones exhibiting reporter gene expression only when AD plasmid is introduced by mating with yeast strain expressing plasmid encoding bait-pGBKT7 (MacDonald Paul N., 2001). After repeating the screening procedure similar to initial library transformation with different stringent growth media to check for reporter genes (Ade+ and His+) and blue colonies for positive lacZ expression only one clone gave positive for all the three reporter genes in the present study when mated with bait-pGBKT7 only and not with control plasmids.

The clone 34/19 B identified as rat crystallin, α̃ polypeptide A (Cryaa) mRNA. Sequence verification of the clone 34/19 B showed the presence of α-crystallin A coding sequence after the SMART III oligo sequence of pGADT7-Rec. The α-crystallin A fragment starts with base pair 21 and found to be in-frame in the AD/library clone. On checking the list of 27 clones six matched with α-crystallin A mRNA, but surprisingly only one clone was positive for all three reporter genes after retesting of AD clones by mating. Sequence analysis of 6 α-crystallin A clones showed the presence of two patterns. In clone 34/19 B, 25/12 A and 30/5 A, SMART III oligo sequence was followed by α-crystallin A mRNA sequence, while in clone 3/9 B, 16/1 B and 23/1 A, in-between SMART III oligo sequence and α-crystallin A mRNA sequence was present 45-60 bps of unknown sequence. However, the α-crystallin A mRNA sequence was in-frame in all 6 clones but in none of the cases the clones were complete. The coding region of α-crystallin A (Accession No.

NM_012534) starts from base 13-534 corresponding to 522 bps and 174 amino acids. Two clones contained the start codon but ~ till bp 360, while two other clones corresponded to fragment size 15-363 bp, one clone was comparatively small from 63-330 bp. The 6th clone i.e., 34/19 B was the longest from 13-955 bp including the 3'-untranslated region of the gene.

Reconfirming for the positive clone between the 6 α-crystallin A clones resulted again in only clone 34/19 B positive for Ade+, His+ and lacZ+. From these experiments it is difficult to find a reason with regard to the difference in behaviour of α-crystallin A clones except that maybe 3'-region of the protein is more important than the initial N-terminal residues since five out of six clones finish at 360 bp or so. But this aspect of region specific interaction of α-crystallin A with C-tail of PAR-2 needs further experimentation and analysis.

Apart from the cytoplasmic tail PAR-2 also contains 3 cytoplasmic loops. Transmembrane signalling involving G-proteins is known to occur via the 3rd cytoplasmic loop of the PAR-1 receptor (Chen et al., 2001). Hence not only the C-tail but the intracellular loops are important components of receptor signalling mechanism. As done in earlier studies of similar type with PAR-1 (Mahajan et al., 2000; Pai et al., 2001) in the present study too cytoplasmic loop 2 and 3 of rat PAR-2 were checked for interaction with α-crystallin A in yeast. The cytoplasmic loop 2 and 3 of rat PAR-2 are very small and consist of only 21 and 23 amino acids, respectively. Cloning of these two loops was done by a company (ATG: biosynthetics, Freiburg, Germany). For this first they synthesised the two loops as ds oligonucleotides and then cloned them into DNA-BD vector between the same restriction sites as the C-tail of PAR-2. The sequence of the cloned loops was confirmed before they were used for yeast mating with three AD clones of α-crystallin A. Mating results were negative for interaction between the cytoplasmic loops and α-crystallin A clones similar to what has been reported with regard to interaction studies concerning C-tail of PAR-1 in yeast (Mahajan et al., 2000; Pai et al., 2001). The AD clones by themselves failed to grow in SD/-Leu/-His plates indicating the lack of transcriptional activation by AD clones on their own. This set of experiment with cytoplasmic loops confirmed that the interaction observed between C-tail of PAR-2, the 'bait' and AD clone 34/19 B i.e., α-crystallin A in yeast is specific and confined to C-tail of PAR-2 and not the cytoplasmic loops of the receptor. However, whether the interaction observed between C-tail of PAR-2 and α-crystallin A is a physiological one, occurs outside the yeast

system and has any meaning in terms of functional significance of the interaction needed to be studied and clarified with further sets of experiments.

4.2.2 Checking for presence of α-crystallin A in different tissues, cell types and cell lines

RT-PCR analysis using gene specific primers to check for the presence of α-crystallin A in several tissues, cell types and cell lines available for this study presented a vivid picture of α-crystallin A mRNA expression. Retina, the source of AD fusion library for finding of PAR-2 interacting protein in the present study was positive for α-crystallin A mRNA expression. In fact intensity of the PCR band indicated abundant amounts of α-crystallin A mRNA in retina. Study involving non-lenticular cells had found abundant amount of α-crystallin A in frog retinal cells, both in soluble form and associated with post-Golgi membranes of photoreceptors (Deretic et al., 1994). PCR signal for optic nerve was also intense compared with moderate amounts obtained in case of brain. To identify the cell types which express α-crystallin A neuronal and glial primary cells as well as several cell lines were checked which gave quite a few surprising results. A glance across Table 3.6 shows that α-crystallin A is not as ubiquitously expressed as the other isoform of α-crystallin i.e., α-crystallin B. Of all, only hippocampal astrocytes and whole brain astrocytes express α-crystallin A. The neuronal cell lines like RGC and N2A along with primary neuronal (mixed) culture also gave negative PCR results for expression of α-crystallin A. Expression of α-crystallin A in retina but absence in neuronal retinal ganglion cell line (RGC) (Krishnamoorthy et al., 2001) suggests that α-crystallin A must be present in Müller cells of retina (astrocytic origin). An oligodendrocytic cell line, too, was negative for α-crystallin A mRNA. RT-PCR result in the present study shows clearly that α-crystallin A has a very selective distribution in brain cells compared to ubiquitously expressed α-crystallin B. Expression study to detect α-crystallin A in various non-lenticular tissues has found that this so-called lens-specific polypeptide is also present in brain, liver, lung, spleen, skin, small intestine and in a number of epithelial and fibroblast cell lines (Srinivasan et al., 1992). Immunocytochemical detection of α-crystallin A in various primary cell cultures confirmed the RT-PCR results in case of hippocampal astrocytes and whole brain astrocytes but not for hippocampal neurons. The primary cultures of hippocampal neurons used in this study

were mixed cultures containing neurons over astrocytic layer. α-crystallin A immuno-staining was co-localised both with astrocyte marker and neuronal marker in the mixed neuronal cultures contrary to the results obtained with RT-PCR. This could be due to difference in levels of α-crystallin A expressed by astrocytes and neurons (RT-PCR using higher amount of starting material and more cycles was positive for hippocampal neurons).

The presence of PAR-2 in different brain areas, including hippocampus (Striggow et al., 2001), retina (found in the present study) and cell types-neurons (D'Andrea et al., 1998) and astrocytes (Wang et al., 2002a) is known. The overlapping tissue and cell type distribution of both PAR-2 and α-crystallin A provides the first line of evidence outside yeast for the likelihood of their being interacting partners.

4.2.3 Generation of PAR-2 and α-crystallin A fusion proteins

Any interaction observed in yeast-two hybrid system is not 100% meaningful or confirmed till it is verified using *in vitro* methods with purified proteins in their initial characterisation since two-hybrid assay occasionally yields false positives. In this regard mammalian expression system was used in the present study to verify the protein interaction between PAR-2 and α-crystallin A. The mammalian expression system permits post-translational modification of eukaryotic proteins which allows a native protein to act in a biological environment, thus exhibiting its natural physiological functions. For detection purposes either full or partial PAR-2 and α-crystallin A were cloned in several mammalian expression vectors with fluorescent and non-fluorescent tags as fusion proteins. As mentioned in Table 3.7, transfection in all cases was not successful. Different approaches were tried to get the transfection of pDsRed2N1 vector working but without success. Cell lines like RGC, RBL and NG108 too proved unsuccessful with DOTAP-based lipotransfection procedure (as described in Material and Methods). Up to 10 μg of DNA also failed to induce transfection in these cell lines. Successfully transfected cells were made stable under antibiotic selection pressure. This proved difficult in case of pCMV-HA fusion protein transfection since pCMV-HA vector has no Kan/Neo resistance site, hence requiring carrier DNA based transfection for stable expression of pCMV-HA fusion protein in cells.

Expression of fusion proteins cloned in vectors with fluorescent tag such as pEGFP was followed in cells by means of green fluorescence of the GFP tag. Colonies of cells originating from one cell cluster were selected for stable propagation as individual clones on the basis of high and even fluorescent cells. For vectors with non-fluorescent tag the selection of clones required checking both at transcription and translation level. Like GFP clones, MycHis and HA fusion protein transfected cells were made stable and grown under appropriate selection pressure. Several clusters of cells each originating from a single cell were propagated as individual clones. The stable clones were checked for mRNA expression of fusion protein construct by RT-PCR using the same primer pair as for generation of PCR product for cloning. On the protein level fusion constructs bigger than 10 kDa were detected by western blot analysis. Full crystallin-MycHis-HEK clones and crystallin Domain 2 clones could be verified in transfected cells for protein expression by western blot. Using the monoclonal antibody against myc antigen gave a positive band at the expected range between 20-25 kDa corresponding to full α-crystallin A protein (Srinivasan et al., 1992). Small size of bait-HA fusion protein (~6.7 kDa) made its detection by western blot not possible. It is already known that detection of proteins smaller then 10 kDa is not easily feasible. Alternative strategies were used to detect the presence of bait-HA fusion protein in transfected cells since fusion construct could be detected at the transcription level. SDS-PAGE of whole cell lysate made using different protocols was stained using silver staining technique. The gel stained by this procedure showed the expression of bait-HA fusion protein in cell lysates (single and double transfected). Silver staining of SDS-PAGE is a more sensitive technique of detecting proteins bands compared to Coomassie Blue staining of the protein gels. Detection of bait-HA fusion construct at the protein level was checked by immuno-cytochemical staining of the transfected cells. Staining of transfected cells with antibodies against HA tag showed the presence of fusion protein in the transfected cells. Thus, by means of silver staining of protein gel and immunostaining it was possible to detect the presence of bait-HA fusion protein in transfected cells. Subcloning of C-tail PAR-2 in pEGFP-C2 vector from pGBKT7 vector made possible the detection of C-tail PAR-2 as a GFP fusion construct by western blot due to bigger size of the fusion protein.

4.2.4 Cellular localisation of PAR-2 and α-crystallin A

After checking the tissue and cell type where PAR-2 and α-crystallin A are present the next step was to identify the cellular localisation of the two proteins. For any protein-protein interaction to take place in a biological system it is necessary that both proteins should be either localised in the same compartment of the cell or in adjacent compartments where it is possible for them to be directly in contact with each other. For localisation study full PAR-2-pEGFP-N1 was transfected in two cell lines: HEK (epithelial) and N2A (neuronal). PAR-2-pEGFP-N1 fusion construct transfection in both HEK cells and in N2A cells resulted in membrane localisation of green fluorescent signal along with little cytoplasmic fluorescence. This pattern of PAR-2-pEGFP-N1 construct localisation has also been described in transfected skin cells (keratinocytes) (Dery et al., 1999). α-crystallin A-pEGFP-N1 fusion protein was localised to cytosol of N2A cells excluding the nucleus. α-crystallin A has been reported to be a cytoplasmic protein (Deretic et al., 1994). Cytosolic localisation of α-crystallin A in cells were further verified by immunostaining of α-crystallin A-MycHis-HEK cells by anti-myc antibody. In α-crystallin A-MycHis-HEK cells also anti-myc antibody detected the presence of fusion protein in the cytosol excluding the nucleus. Cellular localisation of both proteins in adjacent cell compartments or even same cell compartment since C-terminal tail of PAR-2 has cytoplasmic localisation provide further evidence that the interaction between PAR-2 and α-crystallin A can occur in physiological environment.

4.2.5 Co-immunoprecipitation

Protein-protein interaction between C-tail of PAR-2 and α-crystallin A outside yeast was detected in mammalian expression system by co-immunoprecipitation of both proteins. HEK cells transfected with both fusion constructs could be precipitated in the presence of protein A with antibody against HA tag and detected with anti-myc antibody on western blot analysis. Negative results obtained with HEK-WT lysate and lack of binding to protein A in absence of anti-HA antibody by double transfected cell lysate verified the specificity of the interaction. This biochemical assay gave firm indication for existence of interaction between PAR-2 and α-crystallin A under physiological conditions.

4.2.6 Co-localisation of PAR-2 and α-crystallin A in Hippocampal astrocytes

Although localisation studies using transfected cells showed the presence of PAR-2 and α-crystallin A in adjacent compartments it was important to verify this in a system endogenously expressing both proteins. For this primary culture of rat hippocampal astrocytes were stained with specific antibodies against both proteins. Subcellular localisation of PAR-2 and α-crystallin A matched with what was observed in transfected cells and overlay of fluorescence for both proteins showed co-localisation of PAR-2 and α-crystallin A in hippocampal astrocytes.

The series of experiments done until now confirms PAR-2 and α-crystallin A interaction under native, physiological conditions. Hence we could prove by several lines of experimentation that there do exist protein-protein interaction between PAR-2 and α-crystallin A in biological system. In the present study we have identified α-crystallin A as a novel interacting partner for PAR-2. However, for any interaction taking place in nature there has to be a functional rationale behind its occurrence. Which means even PAR-2 and α-crystallin A interaction definitely has a functional significance which needs to be further explored and studied. This interaction might be a part of already existing signalling mechanisms or PAR-2 via α-crystallin A is involved in some novel functional aspect.

4.2.7 α-crystallin A

α-crystallins are major refractive proteins in vertebrate lens, composed of two highly homologous subunits αA and αB. The 20 kDa αA- and αB-crystallin proteins are approximtely 60% identical in amino acid sequence (Deretic et al., 1994; Kantorow and Piatigorsky, 1998). While α-crystallin B is a ubiquitous isoform and shares high homology in its carboxyl-terminal with small heat shock proteins (Ingolia and Craig, 1982), α-crystallin A was considered a lens-specific isoform (Overbeek et al., 1985). PCR analysis and Southern blot analysis established the presence of α-crystallin A in several non-lenticular tissues such as retina, brain, lung, spleen, liver, epithelial and fibroblast cell lines (Srinivasan et al., 1992). Rat α-crystallin A has a 522 bp long mRNA sequence and made up of 173 amino acid residues (Accession No. NM_012534). The coding region consists of two domains: N-terminal domain

represents alpha crystallin A chain, while C-terminal matches with Hsp20/ alpha crystallin family. α-crystallin exists both as soluble and membrane associated forms in retina (Deretic et al., 1994). Apart from maintaining lens transparency, α-crystallin in frog retinal cells is associated with subcellular fraction containing rhodopsin bearing post-Golgi membrane (chaperone activity) and helps in membrane transport in retina (Deretic et al., 1994). α-crystallin A can be phosphorylated in a cAMP-dependent and independent manner (Kantorow and Piatigorsky, 1998). This fact suggests that α-crystallin A is not a passive structural entity of vertebrate lens but is under active metabolic control. It can bind to actin (Wang and Spector, 1996). Low expression of α-crystallin A in Royal college of Surgeons (RCS) rats indicates that α-crystallin A may have a significant role in the development of retinal dystrophy (Maeda et al., 1999). α-crystallin A co-localises with actin cytoskeleton in the cell (Gopalakrishnan et al., 1993) and possibly induces expression of pro-inflammatory cytokines (Bhat and Sharma, 1999). α-crystallin A has also been shown to have anti-apoptotic activity (Andley et al., 2000).

5. Zusammenfassung

Die Degeneration oder das Überleben des Hirngewebes, nach einem Hirn-Trauma oder Verletzung des Zentralen Nerven System (ZNS), hängen stark von der Art, Dauer und der Stärke der Verletzung ab. Eine der wichtige Substanz, die als Folge einer Verletzung des Zentralen Nervensystems nachgewiesen wurde, ist das Thrombin. Die Freisetzung bzw. Produktion von Thrombin im verletzten Gewebe geschieht entweder durch eine beeinträchtigte Blut-Hirn-Schranke oder es wird am Ort der Verletzung direkt durch Spaltung des endogenen Prothrombins produziert. So vermittelt Thrombin seine Wirkung durch Aktivierung der Protease aktivierten Rezeptoren (die so genannte PAR-Rezeptor-Familie). Zu dieser Rezeptor Familie gehören bislang PAR-1, PAR-2, PAR-3 und PAR-4. PAR-1, PAR-3 und PAR-4 gelten als Thrombin Rezeptoren, PAR-2 wird durch Trypsin oder Mastzellen Tryptase aktiviert.

PARs gehören zu der Superfamilie der G-Protein gekoppelten Rezeptoren mit 7 Transmembran-Domänen. Die Aktivierung dieser Rezeptoren wird von extrazellulären Proteasen vermittelt. PARs sind sowohl an der Degeneration als auch an der Reparatur des nach einer Verletzung geschädigten Gewebes beteiligt.

Teil 1: In der vorliegenden Arbeit wurde die mRNA-Expression aller vier PAR-Subtypen im Auge postnataler Ratten und in der Retina adulter Ratten mittels Reverse Transkription Polymerase Kettenreaktion (RT-PCR) gezeigt. Während die PAR-1-mRNA-Expression in den Augen der Neugeborenen eine entwicklungsabhängige Expression mit einer Abnahme der mRNA-Level von P1, P9 zu P16 aufweist, bleibt bei allen untersuchten Altersstadien das Niveau von PAR-2 unverändert hoch und PAR-3 und PAR-4 weisen einen gleichbleibend niedrigen mRNA-Expressionsspiegel auf. In der Retina adulter Ratten zeigte die mRNA-Expression der PAR-1 im Vergleich zu PAR-2 und PAR-3 ein höheres Niveau, während PAR-4-mRNA das geringste Expressions-Niveau aufwies.

Um die mögliche Rolle der PARs bei einem Trauma des ZNS zu untersuchen, wurde mittels semi-quantitaver RT-PCR die mRNA-Expression aller vier PAR-Subtypen in der Retina der adulten Rate nach einer Quetschung des optischen Nervs [optical nerve crush (ONC)], welche ein mildes Trauma des ZNS verursacht, analysiert. Die Expressionsstudie wurde zu verschiedenen Zeitpunkten nach der Applikation des milden Traumas, beginnend mit 6 Stunden bis zu 3 Wochen nach ONC, durchgeführt.

Die mRNA-Expressions-Analyse zeigte bereits 6 Stunden nach der unilateralen ONC eine Hochregulation aller vier PARs in der Retina der behandelten Tiere, mit

Ausnahme von PAR-3, welches erst nach 12 stunden eine Hochregulation der mRNA zeigt. Die mRNA Niveaus der PAR-1, PAR-3 und PAR-4 erreichten drei Wochen nach ONC wieder den Wert der mRNAs in der Retina unbehandelter Tiere. Im Unterschied zu PAR-1, PAR-3 und PAR-4 blieb der mRNA-Expressionsspiegel von PAR-2 zu allen untersuchten Zeitpunkten höher als der entsprechende mRNA-level in der Retina der unbehandelten Tiere.

Interessanterweise wurden vergleichbare Befunde auch in der Retina des kontralateralen, nicht verletzten Auges beobachtet. In früheren Studien wurde als Folge solcher ZNS-Läsionen an Stelle der Verletzung eine Zunahme der Thrombinfreisetzung, in der Retina eine Degeneration der Ganglienzellen sowie Apoptose und Aktivierung von PARs berichtet. Die anfängliche Hochregulation der PAR-mRNA-Expression als eine der Folgen des ONC (Modell eines milden Traumas) könnte als Effektor für den frühen Zelltod wirken. Die Abnahme des mRNA-Expressions-Niveaus auf das Niveau der unbehandelten Tiere würde hingegen die Neuroprotektions-Rolle der PARs beschreiben.

Teil 2: Zur weiteren Charakterisierung der Veränderung der PAR-mRNA-Expression nach einer ZNS- Verletzung wurde die Expression der PAR mRNAs nach einer verübergehenden fokalen Ischämie (transient focal ischemia), bei welcher der reduzierte Blutzufluss zu einer Kaskade pathophysiologischer Effekte, einschließlich Entzündung, Excitoxicität und Blutplättchenaktivierung an der Stelle der Verletzung führt, untersucht. Die fokale Ischämie wurde mittels Mikroinjektion von Endothelin in der Nähe der mittleren cerebralen Arterie induziert. RT-PCR Analysen ergaben für PAR-1 eine signifikante und für PAR-2 eine geringfügige Abnahme der mRNA spiegel. PAR-3 wies anfänglich eine Zunahme, gefolgt von einer Abnahme der mRNA Niveaus auf, und PAR-4 zeigte die höchste Zunahme, das 2,5-fache, der mRNA- spiegel bereits 12 Stunden nach der Ischämie. Auch bei diesem Paradigma stellen wir an der kontralateralen (unbehandelten) Seite eine Veränderung der mRNA-Expression der PARs in Form von Abnahme der mRNA Level von PAR-1, PAR-2 und PAR-3 fest. Eine Abnahme des PAR-4-mRNA spiegels wurde erst 7 Tage nach der Ischämie festgestellt. Die hier gezeigten Befunde legen die Vermutung nahe, dass die Thrombin-Rezeptoren PAR-1, PAR-3, PAR-4 eine wichtige Rolle bei der Pathophysiologie des ZNS nach einem Trauma und auch bei der Ischämie spielen.

Teil 3: Um die intrazellulären Signalwege von PAR-2 näher verstehen zu können, charakterisierten wir in einem weiteren Abschnitt der vorliegenden Arbeit die

möglichen Interaktions-Proteine für PAR-2. Hierfür wurde die Methode des Yeast-Two-Hybrid-Systems gewählt. Die Suche nach Interaktionspartnern wurde mit der Sequenz des C-Terminalen Bereichs von PAR-2 an einer selbst erzeugten cDNA-Bibliothek aus der Retina der Ratte durchgeführt. Die cDNA- Bibliothek suche ergab einen positiven Klon, der sowohl bei der folgenden Cotransformation mit der cDNA-Bibliothek wie auch beim folgenden 'Yeast Mating' eine Interaktion zeigte. Bei diesem Klon handelt es sich um α-Crystallin A. Um den Protein Interaktionsbereich genauer zu definieren, wurden die beiden zytoplasmatischen Schleifen des PAR-2 Rezeptors mit dem α-Crystallin A in Hefe durch 'Yeast Mating' verifiziert. Diese ergab eine spezifische Interaktion nur mit dem C-terminalen Bereich des PAR-2 Rezeptors. Diese Interaktion wurde in Hefe und auch in Säugetier-Zellen verifiziert.

Die Expression des α-Crystallin A wurde mittels RT-PCR in verschiedenen Zell-Linen, wie auch Geweben untersucht. Die mRNA wurde in der Retina, dem optischen Nerv, Hirn und in Astrozyten aus dem Hippokampus in Primärkulturen spezifisch nachgewiesen. Die subzelluläre Lokalisation beider Proteine (PAR-2 und α-Crystallin A) wurde mittels Transfektion von N2A und HEK-293 Zellen entweder mit α-Crystallin A- oder PAR-2- GFP Fusionsprotein untersucht. PAR-2 zeigte wie erwartet eine membranständige Lokalisation, während α-Crystallin A eine zytosolische Lokalisation aufwies. Die in der Hefe festgestellte Interaktion zwischen PAR-2 und α-Crystallin A wurde dann mittels Coimmunopräzipitation und Immunozytochemie in Säugetierzellen verifiziert. Für Coimmunopräzipitation nutzten wir cotransfizierte HEK-293 Zellen, welche beide Proteine (PAR und α-Crystallin A) mit verschiedenen Tags (Myc-His und HA) überexpremierten. Die Immunopräzipitation erfolgte mit einem Antikörper gegen den Tag im PAR-2- Fusionsprotein (Hämagglutinin; HA). Dieser Komplex wurde mit dem Antikörper gegen den Tag im α-Crystallin A Fusionsprotein ebenfalls detektiert. Die Doppel-Immunocytochemischen Untersuchungen an hippokampalen Astrocyten in Primärkultur mit spezifischen Antikörpern gegen α-Crystallin A und PAR-2 bestätigten zum einen die Ergebnisse der subzellulären Lokalisation beider Proteine in den transfizierten Zellen und zum anderen zeigten diese Ergebnisse auch die schon in der Hefe beobachtete Interaktion in Säugetier-Zellen. Für das α-Crystallin A wurde eine co-Lokalisation mit Aktincytoskelett und eine mögliche Rolle bei der Freisetzung von proinflammatorischen Cytokinen beschrieben. Eine weitere detaillierte Untersuchung dieser Interaktion kann die physiologische Bedentung dieser Interaktion klären.

Zusammenfassung: Zeigen Wir in der vorliegenden Arbeit erstmalig: i) die mRNA-Expression von PAR-1-4 im sich entwickelnden Auge der neugeborenen Ratte und in der Retina der 12 Wochen alten Tiere; ii) die Veränderung der mRNA-Expression aller 4 PAR Subtypen bei zwei verschiedenen Paradigmen für ZNS-Verletzung, nämlich Quetschung des optischen Nervs [optical nerve crush (ONC)] oder vorübergehende fokale Ischämie (transient focale ischemie); und iii) die molekulare Identifizierung eines Interaktions-Proteins für PAR-2 in der Retina der Ratte mittels Yeast-Two-Hybrid- Methode.

Die anfängliche Zunahme der mRNA-spiegel der PARs im verletzten Hirngewebe weist auf eine wichtige Funktion dieser Rezeptoren in der Pathophysiologie des zentralen Nervensystems hin. Das unterschiedliche Veränderungsmuster der mRNA- spiegel zu verschiedenen Zeitpunkten nach der ZNS-Verletzung deutet auf eine differentielle mRNA Regulation dieser Gene hin.

Sowohl im ONC- Modell als auch in Modell der fokalen Ischämie konnte ein Effekt der unilateralen Läsion auf die kontralaterale Seite beobachtet werden. Wir konnten ebenfalls einen neuen Interaktionspartner für PAR-2, das α-Crystallin A, identifizieren. Eine Interaktion konnte durch verschiedene experimentelle Ansätze bestätigt werden. α-Crystallin A lokalisiert mit dem Aktincytoskelett in der Zelle und induziert möglicherweise die Expression proinflammatorischer Cytokine. Kenntnis über die physiologische Kontrolle der Interaktion zwischen PAR-2 und α- Crystallin A wird zur Aufklärung der funktionellen Rolle beider Proteine führen.

6. Abstract

Degeneration or survival of cerebral tissue after brain injury depends on the source, intensity and duration of the insult. One serine protease that is closely associated with and produced in response to CNS injury is thrombin. Thrombin enters the injury cascade in brain either via a compromised blood-brain barrier or from endogenous prothrombin. Thrombin mediates its action through the protease-activated receptor family (subtypes PAR-1, -3 and -4), while PAR-2 is activated by trypsin or mast cell tryptase. PARs, belonging to the superfamily of G-protein coupled receptors with a 7-trans-membrane domain structure, are activated by proteolytic cleavage of their N-terminus. PARs are involved in tissue degeneration and repair upon injury.

Part 1: In the present study, we have demonstrated for the first time the expression of all four subtypes of PARs in the post-natal eye and in retina of the adult rat by reverse transcription-polymerase chain reaction (RT-PCR). PAR-1 is developmentally regulated in the eye, with a decrease from P1, P9 to P16, while levels for PAR-2, PAR-3 and PAR-4 remain unchanged throughout. In the retina of the adult rat, PAR-1 is highly expressed, whereas PAR-2, PAR-3 are moderately expressed and PAR-4 is expressed at low levels. To elucidate possible roles of PARs after trauma, we performed semi-quantitative RT-PCR analysis of expression of all 4 PAR subtypes after ONC. mRNA levels of all 4 PARs were upregulated as early as 6 h after unilateral ONC, except PAR-3, which showed a delayed upregulation. PAR-1, PAR-3 and PAR-4 mRNA levels returned back almost to basal levels at 3 weeks post-crush, while PAR-2 mRNA level was still high by the end of 3 weeks after crush. As a result of unilateral lesion, PAR mRNA expression even in the contra-lateral, uninjured side was found to be affected to almost comparable levels as in the injured side. Previous studies have already shown increase in thrombin levels at the site of injury, retinal ganglion cell degeneration by necrosis and apoptosis and PAR activation as a consequence of nerve crush. PAR upregulation as a result of nerve crush in the mild trauma model could act as an effector of early cell death. Eventual return of receptor mRNA to basal levels is consistent with neuroprotection.

Part 2: To further characterise PAR mRNA expression after CNS injury, we studied the model of transient focal ischemia. In the present study we examined the change in mRNA expression levels of PAR-1-4 as a result of transient focal ischemia in rat brain, induced by microinjection of endothelin near the middle cerebral artery. Using semi-quantitative RT-PCR analysis, PAR-1 was found to be significantly down-

regulated, while PAR-2 mRNA levels decreased only moderately after the ischemic insult on the ipsilesional side. PAR-3 was transiently up-regulated, followed by downregulation, and PAR-4 mRNA levels showed the most striking (2.5 fold) increase at 12 h after ischemia in the injured side. In the contra-lateral hemisphere, mRNA expression was also affected. There, decreased mRNA levels were observed for PAR-1, -2 and –3, while PAR-4 levels were reduced only after 7 days. Taken together, these data suggest the involvement of the thrombin receptors PAR-1, PAR-3 and PAR-4 in the pathophysiology of brain ischemia.

Part 3: In order to gain more insight into PAR-2 signalling pathway and the proteins involved downstream of the receptor, we performed a yeast-two hybrid screening to fish out putative interacting partners for PAR-2 (rat). Screening for positive clones both after the initial library transformation (sequential) and subsequently by yeast mating resulted in identification of α-crystallin A as the interacting protein for PAR-2. Lack of interaction between cytoplasmic loop 2 and 3 of PAR-2 and α-crystallin A by yeast mating confirmed the specificity of the interaction between C-tail of PAR-2 and α-crystallin A.

RT-PCR analysis of several tissues and cell lines exhibited a selective expression of α-crystallin A in retina, optic nerve, brain and primary cultures of rat hippocampal astrocytes and whole brain astrocytes. However, presence of α-crystallin A at the protein level in primary cultures of hippocampal neurons indicated high expression of α-crystallin A in hippocampal astrocytes compared with low levels in neurons.

Subcellular localisation of α-crystallin A and PAR-2 as GFP fusion protein in N2A cells showed cytosolic expression for α-crystallin A, while PAR-2 was expressed on plasma membrane with little cytosolic fluorescence. HEK cells transfected with both bait and prey protein on precipitation with antibody against bait protein tag gave positive signal on detection with prey protein tag antibody. Co-immunoprecipitation of C-tail of PAR-2 and α-crystallin A verified the results from the yeast-two hybrid screening. Further, double labelling of hippocampal astrocyte primary cultures confirmed the subcellular localisation of both proteins observed in mammalian expression system, and the overlapping of staining pattern proved that an interaction between α-crystallin A and PAR-2 exist in native biological systems. The physiological control of this interaction will clarify the functional role of both, PAR-2 and α-crystallin A signalling.

7. References

Abraham LA, Chinni C, Jenkins AL, Lourbakos A, Ally N, Pike RN, Mackie EJ (2000) Expression of protease-activated receptor-2 by osteoblasts. Bone 26:7-14.

al-Ani B, Saifeddine M, Hollenberg MD (1995) Detection of functional receptors for the proteinase-activated-receptor-2-activating polypeptide, SLIGRL-NH2, in rat vascular and gastric smooth muscle. Can J Physiol Pharmacol 73:1203-1207.

Andley UP, Song Z, Wawrousek EF, Fleming TP, Bassnett S (2000) Differential protective activity of alpha A- and alphaB-crystallin in lens epithelial cells. J Biol Chem 275:36823-36831.

Arena CS, Quirk SM, Zhang YQ, Henrikson KP (1996) Rat uterine stromal cells: thrombin receptor and growth stimulation by thrombin. Endocrinology 137:3744-3749.

Asokananthan N, Graham PT, Fink J, Knight DA, Bakker AJ, McWilliam AS, Thompson PJ, Stewart GA (2002) Activation of protease-activated receptor (PAR)-1, PAR-2, and PAR-4 stimulates IL-6, IL-8, and prostaglandin E2 release from human respiratory epithelial cells. J Immunol 168:3577-3585.

Bahr M (2000) Live or let die - retinal ganglion cell death and survival during development and in the lesioned adult CNS. Trends Neurosci 23:483-490.

Barron KD, Dentinger MP, Krohel G, Easton SK, Mankes R (1986) Qualitative and quantitative ultrastructural observations on retinal ganglion cell layer of rat after intraorbital optic nerve crush. J Neurocytol 15:345-362.

Bar-Shavit R, Kahn A, Fenton JW, 2nd, Wilner GD (1983) Receptor-mediated chemotactic response of a macrophage cell line (J774) to thrombin. Lab Invest 49:702-707.

Berndt MC, Phillips DR (1981) Interaction of thrombin with platelets: purification of the thrombin substrate. Ann N Y Acad Sci 370:87-95.

Bhat NR, Sharma KK (1999) Microglial activation by the small heat shock protein, alpha-crystallin. Neuroreport 10:2869-2873.

Bien A, Seidenbecher CI, Bockers TM, Sabel BA, Kreutz MR (1999) Apoptotic versus necrotic characteristics of retinal ganglion cell death after partial optic nerve injury. J Neurotrauma 16:153-163.

Bockaert J, Pin JP (1999) Molecular tinkering of G protein-coupled receptors: an evolutionary success. Embo J 18:1723-1729.

Bodeutsch N, Thanos S (2000) Migration of phagocytotic cells and development of the murine intraretinal microglial network: an in vivo study using fluorescent dyes. Glia 32:91-101.

Bodeutsch N, Siebert H, Dermon C, Thanos S (1999) Unilateral injury to the adult rat optic nerve causes multiple cellular responses in the contralateral site. J Neurobiol 38:116-128.

Bohm SK, McConalogue K, Kong W, Bunnett NW (1998) Proteinase-Activated Receptors: New Functions for Old Enzymes. News Physiol Sci 13:231-240.

Bohm SK, Kong W, Bromme D, Smeekens SP, Anderson DC, Connolly A, Kahn M, Nelken NA, Coughlin SR, Payan DG, Bunnett NW (1996) Molecular cloning, expression and potential functions of the human proteinase-activated receptor-2. Biochem J 314:1009-1016.

Buttini M, Sauter A, Boddeke HW (1994) Induction of interleukin-1 beta mRNA after focal cerebral ischaemia in the rat. Brain Res Mol Brain Res 23:126-134.

Cavanaugh KP, Gurwitz D, Cunningham DD, Bradshaw RA (1990) Reciprocal modulation of astrocyte stellation by thrombin and protease nexin-1. J Neurochem 54:1735-1743.

Cellerino A, Bahr M, Isenmann S (2000) Apoptosis in the developing visual system. Cell Tissue Res 301:53-69.

Chambers RC, Dabbagh K, McAnulty RJ, Gray AJ, Blanc-Brude OP, Laurent GJ (1998) Thrombin stimulates fibroblast procollagen production via proteolytic activation of protease-activated receptor 1. Biochem J 333:121-127.

Chen X, Berrou J, Vigneau C, Rondeau E (2001) Role of the third intracellular loop and of the cytoplasmic tail in the mitogenic signaling of the protease-activated receptor 1. Int J Mol Med 8:309-314.

Chen X, Earley K, Luo W, Lin SH, Schilling WP (1996) Functional expression of a human thrombin receptor in Sf9 insect cells: evidence for an active tethered ligand. Biochem J 314:603-611.

Cheung WM, D'Andrea MR, Andrade-Gordon P, Damiano BP (1999) Altered vascular injury responses in mice deficient in protease-activated receptor-1. Arterioscler Thromb Vasc Biol 19:3014-3024.

Cirino G, Bucci M, Cicala C, Napoli C (2000) Inflammation-coagulation network: are serine protease receptors the knot? Trends Pharmacol Sci 21:170-172.

Citron BA, Smirnova IV, Arnold PM, Festoff BW (2000) Upregulation of neurotoxic serine proteases, prothrombin, and protease-activated receptor 1 early after spinal cord injury. J Neurotrauma 17:1191-1203.

Cocks TM, Moffatt JD (2000) Protease-activated receptors: sentries for inflammation? Trends Pharmacol Sci 21:103-108.

Connolly AJ, Ishihara H, Kahn ML, Farese RV, Jr., Coughlin SR (1996) Role of the thrombin receptor in development and evidence for a second receptor. Nature 381:516-519.

Corvera CU, Dery O, McConalogue K, Gamp P, Thoma M, Al-Ani B, Caughey GH, Hollenberg MD, Bunnett NW (1999) Thrombin and mast cell tryptase regulate guinea-pig myenteric neurons through proteinase-activated receptors-1 and -2. J Physiol 517:741-756.

Coughlin SR (1994) Molecular mechanisms of thrombin signaling. Semin Hematol 31:270-277.

Coughlin SR (1999) How the protease thrombin talks to cells. Proc Natl Acad Sci U S A 96:11023-11027.

Coughlin SR (2000) Thrombin signalling and protease-activated receptors. Nature 407:258-264.

Coughlin SR, Camerer E (2003) PARticipation in inflammation. J Clin Invest 111:25-27.

Coughlin SR, Vu TK, Hung DT, Wheaton VI (1992a) Characterization of a functional thrombin receptor. Issues and opportunities. J Clin Invest 89:351-355.

Coughlin SR, Vu TK, Hung DT, Wheaton VI (1992b) Expression cloning and characterization of a functional thrombin receptor reveals a novel proteolytic mechanism of receptor activation. Semin Thromb Hemost 18:161-166.

Cunningham DD, Donovan FM (1997) Regulation of neurons and astrocytes by thrombin and protease nexin-1. Relationship to brain injury. Adv Exp Med Biol 425:67-75.

Cunningham DD, Pulliam L, Vaughan PJ (1993) Protease nexin-1 and thrombin: injury-related processes in the brain. Thromb Haemost 70:168-171.

Cupit LD, Schmidt VA, Bahou WF (1999) Proteolytically activated receptor-3. A member of an emerging gene family of protease receptors expressed on vascular endothelial cells and platelets. Trends Cardiovasc Med 9:42-48.

Damiano BP, D'Andrea MR, de Garavilla L, Cheung WM, Andrade-Gordon P (1999a) Increased expression of protease activated receptor-2 (PAR-2) in balloon-injured rat carotid artery. Thromb Haemost 81:808-814.

Damiano BP, Cheung WM, Santulli RJ, Fung-Leung WP, Ngo K, Ye RD, Darrow AL, Derian CK, de Garavilla L, Andrade-Gordon P (1999b) Cardiovascular responses mediated by protease-activated receptor-2 (PAR-2) and thrombin receptor (PAR-1)

are distinguished in mice deficient in PAR-2 or PAR-1. J Pharmacol Exp Ther 288:671-678.
D'Andrea MR, Derian CK, Leturcq D, Baker SM, Brunmark A, Ling P, Darrow AL, Santulli RJ, Brass LF, Andrade-Gordon P (1998) Characterization of protease-activated receptor-2 immunoreactivity in normal human tissues. J Histochem Cytochem 46:157-164.
Danton GH, Dietrich WD (2003) Inflammatory mechanisms after ischemia and stroke. J Neuropathol Exp Neurol 62:127-136.
de Garavilla L, Vergnolle N, Young SH, Ennes H, Steinhoff M, Ossovskaya VS, D'Andrea MR, Mayer EA, Wallace JL, Hollenberg MD, Andrade-Gordon P, Bunnett NW (2001) Agonists of proteinase-activated receptor 1 induce plasma extravasation by a neurogenic mechanism. Br J Pharmacol 133:975-987.
Deretic D, Aebersold RH, Morrison HD, Papermaster DS (1994) Alpha A- and alpha B-crystallin in the retina. Association with the post-Golgi compartment of frog retinal photoreceptors. J Biol Chem 269:16853-16861.
Dery O, Corvera CU, Steinhoff M, Bunnett NW (1998) Proteinase-activated receptors: novel mechanisms of signaling by serine proteases. Am J Physiol 274:C1429-1452.
Dery O, Thoma MS, Wong H, Grady EF, Bunnett NW (1999) Trafficking of proteinase-activated receptor-2 and beta-arrestin-1 tagged with green fluorescent protein. beta-Arrestin-dependent endocytosis of a proteinase receptor. J Biol Chem 274:18524-18535.
Dieterich DC, Trivedi N, Engelmann R, Gundelfinger ED, Gordon-Weeks PR, Kreutz MR (2002) Partial regeneration and long-term survival of rat retinal ganglion cells after optic nerve crush is accompanied by altered expression, phosphorylation and distribution of cytoskeletal proteins. Eur J Neurosci 15:1433-1443.
Dihanich M, Kaser M, Reinhard E, Cunningham D, Monard D (1991) Prothrombin mRNA is expressed by cells of the nervous system. Neuron 6:575-581.
Dijkhuizen RM, Singhal AB, Mandeville JB, Wu O, Halpern EF, Finklestein SP, Rosen BR, Lo EH (2003) Correlation between brain reorganization, ischemic damage, and neurologic status after transient focal cerebral ischemia in rats: a functional magnetic resonance imaging study. J Neurosci 23:510-517.
Donovan FM, Cunningham DD (1998) Signaling pathways involved in thrombin-induced cell protection. J Biol Chem 273:12746-12752.
Donovan FM, Pike CJ, Cotman CW, Cunningham DD (1997) Thrombin induces apoptosis in cultured neurons and astrocytes via a pathway requiring tyrosine kinase and RhoA activities. J Neurosci 17:5316-5326.
Ehrenreich H, Costa T, Clouse KA, Pluta RM, Ogino Y, Coligan JE, Burd PR (1993) Thrombin is a regulator of astrocytic endothelin-1. Brain Res 600:201-207.
Festoff BW, Smirnova IV, Ma J, Citron BA (1996) Thrombin, its receptor and protease nexin I, its potent serpin, in the nervous system. Semin Thromb Hemost 22:267-271.
Friedmann I, Yoles E, Schwartz M (2001a) Thrombin attenuation is neuroprotective in the injured rat optic nerve. J Neurochem 76:641-649.
Friedmann I, Faber-Elman A, Yoles E, Schwartz M (1999) Injury-induced gelatinase and thrombin-like activities in regenerating and nonregenerating nervous systems. Faseb J 13:533-543.
Friedmann I, Hauben E, Yoles E, Kardash L, Schwartz M (2001b) T cell-mediated neuroprotection involves antithrombin activity. J Neuroimmunol 121:12-21.
Garcia JH, Liu KF, Yoshida Y, Lian J, Chen S, del Zoppo GJ (1994) Influx of leukocytes and platelets in an evolving brain infarct (Wistar rat). Am J Pathol 144:188-199.
Garcia-Valenzuela E, Gorczyca W, Darzynkiewicz Z, Sharma SC (1994) Apoptosis in adult retinal ganglion cells after axotomy. J Neurobiol 25:431-438.

Gehrmann J, Bonnekoh P, Miyazawa T, Hossmann KA, Kreutzberg GW (1992) Immunocytochemical study of an early microglial activation in ischemia. J Cereb Blood Flow Metab 12:257-269.

Gennarelli TA, Thibault LE, Tipperman R, Tomei G, Sergot R, Brown M, Maxwell WL, Graham DI, Adams JH, Irvine A, et al. (1989) Axonal injury in the optic nerve: a model simulating diffuse axonal injury in the brain. J Neurosurg 71:244-253.

Gingrich MB, Traynelis SF (2000) Serine proteases and brain damage - is there a link? Trends Neurosci 23:399-407.

Glenn KC, Carney DH, Fenton JW, 2nd, Cunningham DD (1980) Thrombin active site regions required for fibroblast receptor binding and initiation of cell division. J Biol Chem 255:6609-6616.

Gopalakrishnan S, Boyle D, Takemoto L (1993) Association of actin with alpha crystallins. Trans Kans Acad Sci 96:7-12.

Gorlach C, Hortobagyi T, Hortobagyi S, Benyo Z, Wahl M (2001) Inhibition of endothelin-1 by the competitive ET(A) receptor antagonist Ro 61-1790 reduces lesion volume after cold injury in the rat. Pflugers Arch 441:844-849.

Hamilton JR, Frauman AG, Cocks TM (2001) Increased expression of protease-activated receptor-2 (PAR2) and PAR4 in human coronary artery by inflammatory stimuli unveils endothelium-dependent relaxations to PAR2 and PAR4 agonists. Circ Res 89:92-98.

Harrison DC, Medhurst AD, Bond BC, Campbell CA, Davis RP, Philpott KL (2000) The use of quantitative RT-PCR to measure mRNA expression in a rat model of focal ischemia--caspase-3 as a case study. Brain Res Mol Brain Res 75:143-149.

Herdegen T, Bastmeyer M, Bahr M, Stuermer C, Bravo R, Zimmermann M (1993) Expression of JUN, KROX, and CREB transcription factors in goldfish and rat retinal ganglion cells following optic nerve lesion is related to axonal sprouting. J Neurobiol 24:528-543.

Hollenberg MD, Laniyonu AA, Saifeddine M, Moore GJ (1993) Role of the amino- and carboxyl-terminal domains of thrombin receptor-derived polypeptides in biological activity in vascular endothelium and gastric smooth muscle: evidence for receptor subtypes. Mol Pharmacol 43:921-930.

Hollenberg MD, Saifeddine M, al-Ani B, Kawabata A (1997) Proteinase-activated receptors: structural requirements for activity, receptor cross-reactivity, and receptor selectivity of receptor-activating peptides. Can J Physiol Pharmacol 75:832-841.

Hoogerwerf WA, Hellmich HL, Micci M, Winston JH, Zou L, Pasricha PJ (2002) Molecular cloning of the rat proteinase-activated receptor 4 (PAR4). BMC Mol Biol 3:2.

Howells GL, Macey M, Curtis MA, Stone SR (1993) Peripheral blood lymphocytes express the platelet-type thrombin receptor. Br J Haematol 84:156-160.

Howells GL, Macey MG, Chinni C, Hou L, Fox MT, Harriott P, Stone SR (1997) Proteinase-activated receptor-2: expression by human neutrophils. J Cell Sci 110:881-887.

Hung DT, Wong YH, Vu TK, Coughlin SR (1992) The cloned platelet thrombin receptor couples to at least two distinct effectors to stimulate phosphoinositide hydrolysis and inhibit adenylyl cyclase. J Biol Chem 267:20831-20834.

Ingolia TD, Craig EA (1982) Four small Drosophila heat shock proteins are related to each other and to mammalian alpha-crystallin. Proc Natl Acad Sci U S A 79:2360-2364.

Isenmann S, Bahr M (1997) Expression of c-Jun protein in degenerating retinal ganglion cells after optic nerve lesion in the rat. Exp Neurol 147:28-36.

Isenmann S, Wahl C, Krajewski S, Reed JC, Bahr M (1997) Up-regulation of Bax protein in degenerating retinal ganglion cells precedes apoptotic cell death after optic nerve lesion in the rat. Eur J Neurosci 9:1763-1772.

Ishihara H, Zeng D, Connolly AJ, Tam C, Coughlin SR (1998) Antibodies to protease-activated receptor 3 inhibit activation of mouse platelets by thrombin. Blood 91:4152-4157.

Ishihara H, Connolly AJ, Zeng D, Kahn ML, Zheng YW, Timmons C, Tram T, Coughlin SR (1997) Protease-activated receptor 3 is a second thrombin receptor in humans. Nature 386:502-506.

Jenkins AL, Bootman MD, Taylor CW, Mackie EJ, Stone SR (1993) Characterization of the receptor responsible for thrombin-induced intracellular calcium responses in osteoblast-like cells. J Biol Chem 268:21432-21437.

Jenkins AL, Chinni C, De Niese MR, Blackhart B, Mackie EJ (2000) Expression of protease-activated receptor-2 during embryonic development. Dev Dyn 218:465-471.

Kahn ML, Hammes SR, Botka C, Coughlin SR (1998a) Gene and locus structure and chromosomal localization of the protease-activated receptor gene family. J Biol Chem 273:23290-23296.

Kahn ML, Nakanishi-Matsui M, Shapiro MJ, Ishihara H, Coughlin SR (1999) Protease-activated receptors 1 and 4 mediate activation of human platelets by thrombin. J Clin Invest 103:879-887.

Kahn ML, Zheng YW, Huang W, Bigornia V, Zeng D, Moff S, Farese RV, Jr., Tam C, Coughlin SR (1998b) A dual thrombin receptor system for platelet activation. Nature 394:690-694.

Kanke T, Macfarlane SR, Seatter MJ, Davenport E, Paul A, McKenzie RC, Plevin R (2001) Proteinase-activated receptor-2-mediated activation of stress-activated protein kinases and inhibitory kappa B kinases in NCTC 2544 keratinocytes. J Biol Chem 276:31657-31666.

Kanthou C, Kanse SM, Kakkar VV, Benzakour O (1996) Involvement of pertussis toxin-sensitive and -insensitive G proteins in alpha-thrombin signalling on cultured human vascular smooth muscle cells. Cell Signal 8:59-66.

Kantorow M, Piatigorsky J (1998) Phosphorylations of alpha A- and alpha B-crystallin. Int J Biol Macromol 22:307-314.

Kawabata A, Saifeddine M, Al-Ani B, Leblond L, Hollenberg MD (1999) Evaluation of proteinase-activated receptor-1 (PAR1) agonists and antagonists using a cultured cell receptor desensitization assay: activation of PAR2 by PAR1-targeted ligands. J Pharmacol Exp Ther 288:358-370.

Knight DA, Lim S, Scaffidi AK, Roche N, Chung KF, Stewart GA, Thompson PJ (2001) Protease-activated receptors in human airways: upregulation of PAR-2 in respiratory epithelium from patients with asthma. J Allergy Clin Immunol 108:797-803.

Kong W, McConalogue K, Khitin LM, Hollenberg MD, Payan DG, Bohm SK, Bunnett NW (1997) Luminal trypsin may regulate enterocytes through proteinase-activated receptor 2. Proc Natl Acad Sci U S A 94:8884-8889.

Kreutz MR, Bockers TM, Sabel BA, Hulser E, Stricker R, Reiser G (1997) Expression and subcellular localization of p42IP4/centaurin-alpha, a brain-specific, high-affinity receptor for inositol 1,3,4,5-tetrakisphosphate and phosphatidylinositol 3,4,5-trisphosphate in rat brain. Eur J Neurosci 9:2110-2124.

Krishnamoorthy RR, Agarwal P, Prasanna G, Vopat K, Lambert W, Sheedlo HJ, Pang IH, Shade D, Wordinger RJ, Yorio T, Clark AF, Agarwal N (2001) Characterization of a transformed rat retinal ganglion cell line. Brain Res Mol Brain Res 86:1-12.

Lam WL, Chow PH, Chik KP, Yew DT (1996) Bilateral biochemical and biophysical retinal changes after unilateral ocular trauma in the mouse. Neurosci Lett 218:1-4.

Lampl Y, Fleminger G, Gilad R, Galron R, Sarova-Pinhas I, Sokolovsky M (1997) Endothelin in cerebrospinal fluid and plasma of patients in the early stage of ischemic stroke. Stroke 28:1951-1955.

Lerner DJ, Chen M, Tram T, Coughlin SR (1996) Agonist recognition by proteinase-activated receptor 2 and thrombin receptor. Importance of extracellular loop interactions for receptor function. J Biol Chem 271:13943-13947.
Levin ER (1996) Endothelins as cardiovascular peptides. Am J Nephrol 16:246-251.
Liao SL, Chen WY, Raung SL, Kuo JS, Chen CJ (2001) Association of immune responses and ischemic brain infarction in rat. Neuroreport 12:1943-1947.
Macfarlane SR, Seatter MJ, Kanke T, Hunter GD, Plevin R (2001) Proteinase-activated receptors. Pharmacol Rev 53:245-282.
Maeda A, Ohguro H, Maeda T, Nakagawa T, Kuroki Y (1999) Low expression of alphaA-crystallins and rhodopsin kinase of photoreceptors in retinal dystrophy rat. Invest Ophthalmol Vis Sci 40:2788-2794.
Mahajan VB, Pai KS, Lau A, Cunningham DD (2000) Creatine kinase, an ATP-generating enzyme, is required for thrombin receptor signaling to the cytoskeleton. Proc Natl Acad Sci U S A 97:12062-12067.
McKerracher L, Essagian C, Aguayo AJ (1993a) Marked increase in beta-tubulin mRNA expression during regeneration of axotomized retinal ganglion cells in adult mammals. J Neurosci 13:5294-5300.
McKerracher L, Essagian C, Aguayo AJ (1993b) Temporal changes in beta-tubulin and neurofilament mRNA levels after transection of adult rat retinal ganglion cell axons in the optic nerve. J Neurosci 13:2617-2626.
Misantone LJ, Gershenbaum M, Murray M (1984) Viability of retinal ganglion cells after optic nerve crush in adult rats. J Neurocytol 13:449-465.
Molino M, Blanchard N, Belmonte E, Tarver AP, Abrams C, Hoxie JA, Cerletti C, Brass LF (1995) Proteolysis of the human platelet and endothelial cell thrombin receptor by neutrophil-derived cathepsin G. J Biol Chem 270:11168-11175.
Molino M, Barnathan ES, Numerof R, Clark J, Dreyer M, Cumashi A, Hoxie JA, Schechter N, Woolkalis M, Brass LF (1997) Interactions of mast cell tryptase with thrombin receptors and PAR-2. J Biol Chem 272:4043-4049.
Morris R, Winyard PG, Brass LF, Blake DR, Morris CJ (1996) Thrombin receptor expression in rheumatoid and osteoarthritic synovial tissue. Ann Rheum Dis 55:841-843.
Nakanishi-Matsui M, Zheng YW, Sulciner DJ, Weiss EJ, Ludeman MJ, Coughlin SR (2000) PAR3 is a cofactor for PAR4 activation by thrombin. Nature 404:609-613.
Napoli C, De Nigris F, Cicala C, Wallace JL, Caliendo G, Condorelli M, Santagada V, Cirino G (2002) Protease-activated receptor-2 activation improves efficiency of experimental ischemic preconditioning. Am J Physiol Heart Circ Physiol 282:H2004-2010.
Napoli C, Cicala C, Wallace JL, de Nigris F, Santagada V, Caliendo G, Franconi F, Ignarro LJ, Cirino G (2000) Protease-activated receptor-2 modulates myocardial ischemia-reperfusion injury in the rat heart. Proc Natl Acad Sci U S A 97:3678-3683.
Nelken NA, Soifer SJ, O'Keefe J, Vu TK, Charo IF, Coughlin SR (1992) Thrombin receptor expression in normal and atherosclerotic human arteries. J Clin Invest 90:1614-1621.
Nguyen KT, Eskin SG, Patterson C, Runge MS, McIntire LV (2001a) Shear stress reduces protease activated receptor-1 expression in human endothelial cells. Ann Biomed Eng 29:145-152.
Nguyen KT, Frye SR, Eskin SG, Patterson C, Runge MS, McIntire LV (2001b) Cyclic strain increases protease-activated receptor-1 expression in vascular smooth muscle cells. Hypertension 38:1038-1043.
Niclou SP, Suidan HS, Pavlik A, Vejsada R, Monard D (1998) Changes in the expression of protease-activated receptor 1 and protease nexin-1 mRNA during rat nervous system development and after nerve lesion. Eur J Neurosci 10:1590-1607.
Nystedt S, Emilsson K, Wahlestedt C, Sundelin J (1994) Molecular cloning of a potential proteinase activated receptor. Proc Natl Acad Sci U S A 91:9208-9212.

Nystedt S, Larsson AK, Aberg H, Sundelin J (1995) The mouse proteinase-activated receptor-2 cDNA and gene. Molecular cloning and functional expression. J Biol Chem 270:5950-5955.

O'Brien PJ, Molino M, Kahn M, Brass LF (2001) Protease activated receptors: theme and variations. Oncogene 20:1570-1581.

Overbeek PA, Chepelinsky AB, Khillan JS, Piatigorsky J, Westphal H (1985) Lens-specific expression and developmental regulation of the bacterial chloramphenicol acetyltransferase gene driven by the murine alpha A-crystallin promoter in transgenic mice. Proc Natl Acad Sci U S A 82:7815-7819.

Pai KS, Mahajan VB, Lau A, Cunningham DD (2001) Thrombin receptor signaling to cytoskeleton requires Hsp90. J Biol Chem 276:32642-32647.

Papadaki M, Ruef J, Nguyen KT, Li F, Patterson C, Eskin SG, McIntire LV, Runge MS (1998) Differential regulation of protease activated receptor-1 and tissue plasminogen activator expression by shear stress in vascular smooth muscle cells. Circ Res 83:1027-1034.

Parry MA, Myles T, Tschopp J, Stone SR (1996) Cleavage of the thrombin receptor: identification of potential activators and inactivators. Biochem J 320:335-341.

Pike CJ, Vaughan PJ, Cunningham DD, Cotman CW (1996) Thrombin attenuates neuronal cell death and modulates astrocyte reactivity induced by beta-amyloid in vitro. J Neurochem 66:1374-1382.

Rabacchi SA, Bonfanti L, Liu XH, Maffei L (1994) Apoptotic cell death induced by optic nerve lesion in the neonatal rat. J Neurosci 14:5292-5301.

Rasmussen UB, Vouret-Craviari V, Jallat S, Schlesinger Y, Pages G, Pavirani A, Lecocq JP, Pouyssegur J, Van Obberghen-Schilling E (1991) cDNA cloning and expression of a hamster alpha-thrombin receptor coupled to Ca2+ mobilization. FEBS Lett 288:123-128.

Reid JL, Dawson D, Macrae IM (1995) Endothelin, cerebral ischaemia and infarction. Clin Exp Hypertens 17:399-407.

Renesto P, Si-Tahar M, Moniatte M, Balloy V, Van Dorsselaer A, Pidard D, Chignard M (1997) Specific inhibition of thrombin-induced cell activation by the neutrophil proteinases elastase, cathepsin G, and proteinase 3: evidence for distinct cleavage sites within the aminoterminal domain of the thrombin receptor. Blood 89:1944-1953.

Riek-Burchardt M, Striggow F, Henrich-Noack P, Reiser G, Reymann K (2002) Increase of prothrombin-mRNA after global cerebral ischemia in rats, with constant expression of protease nexin-1 and protease-activated receptors. Neurosci Lett 329:181.

Rohatgi T, Sedehizade F, Sabel BA, Reiser G (2003) Protease-activated receptor subtype expression in developing eye and adult retina of the rat after optic nerve crush. J Neurosci Res 73:246-254.

Rousseau V, Engelmann R, Sabel BA (1999) Restoration of vision III: soma swelling dynamics predicts neuronal death or survival after optic nerve crush in vivo. Neuroreport 10:3387-3391.

Sabel BA, Kasten E, Kreutz MR (1997) Recovery of vision after partial visual system injury as a model of postlesion neuroplasticity. Adv Neurol 73:251-276.

Sabri A, Muske G, Zhang H, Pak E, Darrow A, Andrade-Gordon P, Steinberg SF (2000) Signaling properties and functions of two distinct cardiomyocyte protease-activated receptors. Circ Res 86:1054-1061.

Saifeddine M, al-Ani B, Cheng CH, Wang L, Hollenberg MD (1996) Rat proteinase-activated receptor-2 (PAR-2): cDNA sequence and activity of receptor-derived peptides in gastric and vascular tissue. Br J Pharmacol 118:521-530.

Sautter J, Sabel BA (1993) Recovery of brightness discrimination in adult rats despite progressive loss of retrogradely labelled retinal ganglion cells after controlled optic nerve crush. Eur J Neurosci 5:680-690.

Schmidt VA, Nierman WC, Maglott DR, Cupit LD, Moskowitz KA, Wainer JA, Bahou WF (1998) The human proteinase-activated receptor-3 (PAR-3) gene. Identification within a Par gene cluster and characterization in vascular endothelial cells and platelets. J Biol Chem 273:15061-15068.

Schultheiss M, Neumcke B, Richter HP (1997) Endogenous trypsin receptors in Xenopus oocytes: linkage to internal calcium stores. Cell Mol Life Sci 53:842-849.

Sharkey J, Butcher SP, Kelly JS (1994) Endothelin-1 induced middle cerebral artery occlusion: pathological consequences and neuroprotective effects of MK801. J Auton Nerv Syst 49:S177-185.

Shibuya K, Tajima M, Yamate J (1993) Unilateral atrophy of the optic nerve associated with retrograde and anterograde degenerations in the visual pathways in Slc: Wistar rats. J Vet Med Sci 55:905-912.

Shpacovitch VM, Brzoska T, Buddenkotte J, Stroh C, Sommerhoff CP, Ansel JC, Schulze-Osthoff K, Bunnett NW, Luger TA, Steinhoff M (2002) Agonists of proteinase-activated receptor 2 induce cytokine release and activation of nuclear transcription factor kappaB in human dermal microvascular endothelial cells. J Invest Dermatol 118:380-385.

Simon MI, Strathmann MP, Gautam N (1991) Diversity of G proteins in signal transduction. Science 252:802-808.

Smirnova IV, Zhang SX, Citron BA, Arnold PM, Festoff BW (1998) Thrombin is an extracellular signal that activates intracellular death protease pathways inducing apoptosis in model motor neurons. J Neurobiol 36:64-80.

Smirnova IV, Ma JY, Citron BA, Ratzlaff KT, Gregory EJ, Akaaboune M, Festoff BW (1996) Neural thrombin and protease nexin I kinetics after murine peripheral nerve injury. J Neurochem 67:2188-2199.

Srinivasan AN, Nagineni CN, Bhat SP (1992) alpha A-crystallin is expressed in non-ocular tissues. J Biol Chem 267:23337-23341.

Steinhoff M, Corvera CU, Thoma MS, Kong W, McAlpine BE, Caughey GH, Ansel JC, Bunnett NW (1999) Proteinase-activated receptor-2 in human skin: tissue distribution and activation of keratinocytes by mast cell tryptase. Exp Dermatol 8:282-294.

Steinhoff M, Vergnolle N, Young SH, Tognetto M, Amadesi S, Ennes HS, Trevisani M, Hollenberg MD, Wallace JL, Caughey GH, Mitchell SE, Williams LM, Geppetti P, Mayer EA, Bunnett NW (2000) Agonists of proteinase-activated receptor 2 induce inflammation by a neurogenic mechanism. Nat Med 6:151-158.

Striggow F, Riek M, Breder J, Henrich-Noack P, Reymann KG, Reiser G (2000) The protease thrombin is an endogenous mediator of hippocampal neuroprotection against ischemia at low concentrations but causes degeneration at high concentrations. Proc Natl Acad Sci U S A 97:2264-2269.

Striggow F, Riek-Burchardt M, Kiesel A, Schmidt W, Henrich-Noack P, Breder J, Krug M, Reymann KG, Reiser G (2001) Four different types of protease-activated receptors are widely expressed in the brain and are up-regulated in hippocampus by severe ischemia. Eur J Neurosci 14:595-608.

Suidan HS, Bouvier J, Schaerer E, Stone SR, Monard D, Tschopp J (1994) Granzyme A released upon stimulation of cytotoxic T lymphocytes activates the thrombin receptor on neuronal cells and astrocytes. Proc Natl Acad Sci U S A 91:8112-8116.

Suttnar J, Dyr JE, Doleckova L (2000) Determination of the putative binding sites for thrombin receptor activating peptide through a hydropathic complementary approach. Thromb Haemost 83:165-170.

Suzuki M, Kudo A, Otawara Y, Hirashima Y, Takaku A, Ogawa A (1999) Extrinsic pathway of blood coagulation and thrombin in the cerebrospinal fluid after subarachnoid hemorrhage. Neurosurgery 44:487-493; discussion 493-484.

Tesser P, Jones PS, Schechter N (1986) Elevated levels of retinal neurofilament mRNA accompany optic nerve regeneration. J Neurochem 47:1235-1243.

Trejo J, Chambard JC, Karin M, Brown JH (1992) Biphasic increase in c-jun mRNA is required for induction of AP-1-mediated gene transcription: differential effects of muscarinic and thrombin receptor activation. Mol Cell Biol 12:4742-4750.

Turgeon VL, Lloyd ED, Wang S, Festoff BW, Houenou LJ (1998) Thrombin perturbs neurite outgrowth and induces apoptotic cell death in enriched chick spinal motoneuron cultures through caspase activation. J Neurosci 18:6882-6891.

Ubl JJ, Reiser G (1997) Characteristics of thrombin-induced calcium signals in rat astrocytes. Glia 21:361-369.

Ubl JJ, Vohringer C, Reiser G (1998) Co-existence of two types of [Ca2+]i-inducing protease-activated receptors (PAR-1 and PAR-2) in rat astrocytes and C6 glioma cells. Neuroscience 86:597-609.

Vaughan PJ, Pike CJ, Cotman CW, Cunningham DD (1995) Thrombin receptor activation protects neurons and astrocytes from cell death produced by environmental insults. J Neurosci 15:5389-5401.

Vergnolle N, Wallace JL, Bunnett NW, Hollenberg MD (2001a) Protease-activated receptors in inflammation, neuronal signaling and pain. Trends Pharmacol Sci 22:146-152.

Vergnolle N, Derian CK, D'Andrea MR, Steinhoff M, Andrade-Gordon P (2002) Characterization of thrombin-induced leukocyte rolling and adherence: a potential proinflammatory role for proteinase-activated receptor-4. J Immunol 169:1467-1473.

Vergnolle N, Bunnett NW, Sharkey KA, Brussee V, Compton SJ, Grady EF, Cirino G, Gerard N, Basbaum AI, Andrade-Gordon P, Hollenberg MD, Wallace JL (2001b) Proteinase-activated receptor-2 and hyperalgesia: A novel pain pathway. Nat Med 7:821-826.

Vu TK, Hung DT, Wheaton VI, Coughlin SR (1991a) Molecular cloning of a functional thrombin receptor reveals a novel proteolytic mechanism of receptor activation. Cell 64:1057-1068.

Vu TK, Wheaton VI, Hung DT, Charo I, Coughlin SR (1991b) Domains specifying thrombin-receptor interaction. Nature 353:674-677.

Wang H, Reiser G (2003a) Thrombin signaling in the brain: the role of protease-activated receptors. Biol Chem 384:193-202.

Wang H, Reiser G (2003b) The role of the Ca2+-sensitive tyrosine kinase Pyk2 and Src in thrombin signalling in rat astrocytes. J Neurochem 84:1349-1357.

Wang H, Ubl JJ, Reiser G (2002a) Four subtypes of protease-activated receptors, co-expressed in rat astrocytes, evoke different physiological signaling. Glia 37:53-63.

Wang H, Ubl JJ, Stricker R, Reiser G (2002b) Thrombin (PAR-1)-induced proliferation in astrocytes via MAPK involves multiple signaling pathways. Am J Physiol Cell Physiol 283:C1351-1364.

Wang K, Spector A (1996) alpha-crystallin stabilizes actin filaments and prevents cytochalasin-induced depolymerization in a phosphorylation-dependent manner. Eur J Biochem 242:56-66.

Weinstein JR, Gold SJ, Cunningham DD, Gall CM (1995) Cellular localization of thrombin receptor mRNA in rat brain: expression by mesencephalic dopaminergic neurons and codistribution with prothrombin mRNA. J Neurosci 15:2906-2919.

Weinstein JR, Lau AL, Brass LF, Cunningham DD (1998) Injury-related factors and conditions down-regulate the thrombin receptor (PAR-1) in a human neuronal cell line. J Neurochem 71:1034-1050.

Xi G, Reiser G, Keep RF (2003) The role of thrombin and thrombin receptors in ischemic, hemorrhagic and traumatic brain injury: deleterious or protective? J Neurochem 84:3-9.

Xu WF, Andersen H, Whitmore TE, Presnell SR, Yee DP, Ching A, Gilbert T, Davie EW, Foster DC (1998) Cloning and characterization of human protease-activated receptor 4. Proc Natl Acad Sci U S A 95:6642-6646.

Yan SJ, Blomme EA (2003) In situ zymography: a molecular pathology technique to localize endogenous protease activity in tissue sections. Vet Pathol 40:227-236.

Yew DT, Yang QD, Mak NY, Au CY, Li WW, Liu WK (1990) Bilateral retinal responses after traumatic injury of one eye in mice. A histopathologic and immunohistochemical study. Ophthalmic Res 22:67-72.

Yu Z, Ahmad S, Schwartz JL, Banville D, Shen SH (1997) Protein-tyrosine phosphatase SHP2 is positively linked to proteinase-activated receptor 2-mediated mitogenic pathway. J Biol Chem 272:7519-7524.

Zhong C, Hayzer DJ, Corson MA, Runge MS (1992) Molecular cloning of the rat vascular smooth muscle thrombin receptor. Evidence for in vitro regulation by basic fibroblast growth factor. J Biol Chem 267:16975-16979.

Zimmermann M, Seifert V (1998) Endothelin and subarachnoid hemorrhage: an overview. Neurosurgery 43:863-875; discussion 875-866.

8. Abbreviations

Ab	Antibody
AD	Activation domain
Ade	Adenine
AP	Activating peptide
AT	Adenine thymine
3-AT	3-amino-1,2,4-triazole
A.U	Arbitary units
bp	Base pair
cDNA	Complementary deoxyribonucleic acid
CNS	Central nervous system
cAMP	Cyclic adenosine monophosphate
CAPS	3-(Cyclohexylamino)-1-propansulfonic acid
Cl	Cytoplasmic loop
DMEM	Dulbecco's Modified Eagle's Medium
DNA	Deoxyribonucleic acid
dNTP	Deoxyribonucleoside triphosphate
DNA-BD	Deoxyribonucleic acid binding domain
DEPC	Diethyl pyrocarbonate
DMSO	Dimethyl sulfoxide
DMF	N,N-dimethylformamide
ds	double stranded
DMSO	Dimethyl sulfoxide
DO	Dropout
EGF	Epidermal growth factor
e-MCAO	endothelin-Middle Cerebral Artery Occlusion
EST	Expressed Sequence TAG
ERK	Extracellular regulated kinase
FCS	Fetal calf serum
FTP	FCS-Triton-X100-PBS
GAL	Galactose
GC	Guanine cytosine
GFAP	Glial fibrillary acidic protein
GAPDH	Glyceraldehyde phosphate dehydrogenase

GFP	Green fluorescent protein
GPCR	G-protein coupled receptor
GDP	Guanosine diphosphate
GTP	Guanosine triphosphate
HA	Hemagglutinin
HAT	Hypoxanthine aminopterine thymidine
HBSS	Hank's balanced salt solution
Hsp	Heat shock protein
hTRAP	Human thrombin receptor activating peptide
HEK	Human embryonic kidney
His	Histidine
HW	Histidine-tryptophan
H_2O	Hydrogen dioxide
H_2O_2	Hydrogen peroxide
$InsP_3$	Inositol 1,4,5-trisphosphate
ICON	in vivo confocal neuroimaging technique
JNK	c-jun related kinase
Kana	Kanamycin
KCM	KCl- $CaCl_2$- $MgCl_2$
Leu	Leucine
LB	Luria bertini
LH	Leucine-Histidine
LD-PCR	Long distance polymerase chain reaction
LW	Leucine-tryptophan
MMPs	Matrix Metalloproteinases
MCA	Middle Cerebral Artery
MAPK	Mitogen-activated protein kinase
MCS	Multiple cloning site
MES	(2-[N-Morpholino] ethanesulfonic acid) Hydrate
mRNA	Messenger ribonucleic acid
MOPS	N-Morpholino-3-propansulphonic acid
MCS	Multiple cloning site
ONC	Optic nerve crush
OD	Optical density

OGD	Oxygen glucose deprivation
p38 MAP	p38 mitogen activated protein
PFA	Paraformaldehyde
PNS	Peripheral nervous system
PTX	Pertussis toxin
PBS	Phosphate buffered saline
PLC	Phospholipase C
PAR	Protease-activated receptor
PKC	Protein kinase C
PCR	Polymerase Chain Reaction
PVDF	Polyvinyliden difluorid
QDO	Quadruplet dropout medium
RGC	Retinal ganglion cells
RT	Reverse Transcription
SD	Synthetic dropout
SDS-PAGE	Sodium dodecyl sulphate-polyacrylamide gel electrophoresis
ss	Single stranded
TCM	Tris/HCl- $CaCl_2$- $MgCl_2$
Trp	Trptophan
TDO	Triple dropout medium
TSR	Template Suppression Reagent
TM	Transmembrane
Tm	Melting temperature
TRag	Thrombin receptor agonist
TBE	Tris-boric acid-EDTA
TE	Tris-EDTA
UAS	Upstream activating sequence
UV	Ultraviolet
X-gal	5-bromo-4-chloro-3-indolyl-β-D-galactopyranoside
YPDA	Yeast-peptone-dextrose-adenine

List of articles and conference abstracts contributed to during Ph.D studies:

Articles:

1) Protease-activated receptor (PAR) subtype expression in developing rat eye and in adult retina, following optic nerve crush

T. Rohatgi, F. Sedehizade, B.A. Sabel and G. Reiser -J. Neuroscience Research (2003) Jul 15;73(2):246-54

2) Differential regulation of mRNA expression of protease-activated receptors (PAR-1-4) in rat brain after transient focal ischemia

T. Rohatgi, P. Henrich-Noack, F. Sedehizade, Goertler M., Wallesch CW., K.G. Reymann and G. Reiser- J. Neuroscience Research (2004) Jan 15; 75(2): 273-9

Conference Abstracts:

1) Adaptive vs lethal calcium activity rise in retinal ganglion cells after optic nerve crush in adult rat.

V. Rousseau, H. Tietgans, **T. Rohatgi**, J. Hanke and B. A. Sabel
At International conference: Neuroprotection and Neurorepair 2000, Magdeburg, Germany.

2) Structural reorganization of the retinal ganglion cells and superior colliculus following optic nerve crush in adult rat.

T. Rohatgi, M. Arndt, J. Hanke, U. Lendeckel, S. Ansorge and B. A. Sabel
At 5th International Neurotrauma symposium 2000, Munich, Germany

3) Intrinsic axon repair following traumatic optic nerve injury in adult rats.

T. Rohatgi, M. Arndt, J. Hanke, U. Lendeckel, S. Ansorge and B. A. Sabel
At SFN Annual meeting 2001, San Diego, USA

4) Protease-activated receptors (PARs) mRNA expression in the retina after optic nerve crush in developing and adult rat

T. Rohatgi, F. Sedehizade, B. A. Sabel and G. Reiser
At FENS 2002, Paris, France and SFN Annual meeting 2002, Orlando, USA

5) Expression of protease-activated receptors after CNS injury (nerve crush and ischemia)

T. Rohatgi, F. Sedehizade, P. Henrich-Noack, K.G. Reymann and G. Reiser
At EMBO conference 2003, Ascona, Switzerland

6) Identification of a Protease-activated receptor-2 (PAR-2) interacting protein as a 20 kDa structural protein

G. Reiser, **T. Rohatgi**, R. Stricker, T. Hanck and F. Sedehizade
At SFN Annual meeting 2003, New Orleans, USA

Curriculum Vitae

Name:	Tanuja Rohatgi
Birthday:	1 September 1973
Place of Birth:	Delhi, India

Education & Experience:

7/ 1991- 4/ 1994	University of Delhi, Delhi, India Bachelor of Science majored in Zoology
7/1994- 4/1996	University of Delhi, Delhi, India Master of Science majored in Zoology. Specialisation: Cellular and molecular biology
10/ 1996- 3/ 1999	Junior research fellow, Institute of Genomics and Integrative Biology (formerly, Centre for Biochemical Technology), Delhi, India Research project: Studies on Palm Oil Mill Effluent Treatment
4/ 1999- 7/ 1999	Senior research fellow, Department of Zoology, University of Delhi, Delhi, India Research project: Cloning and characterization og ligninase/ Laccase gene from white rot fungus
8/ 1999-12/ 2000	Graduate student , Institut für Medizinische Psychologie, Magdeburg, Germany. Supported by Deutsche Forschungsgemeinschaft (Graduiertenkolleg für 'Biologische Grundlagen von Erkrankungen des Nervensystems') Research project: Expression studies on cytoskeletal changes after optic nerve crush in the adult rat
1/ 2001- 3/ 2004	Ph.D student, Institut für Neurobiochemie, Otto-von-Guericke-Universität, Magdeburg, Germany. Supported by Deutsche Forschungsgemeinschaft (Graduiertenkolleg für 'Biologische Grundlagen von Erkrankungen des Nervensystems')